INL/EXT-22-67587
Revision 0

AGR-5/6/7 Final Release-to-Birth Ratio Data Analysis

Binh T. Pham
Dawn M. Scates

June 2022

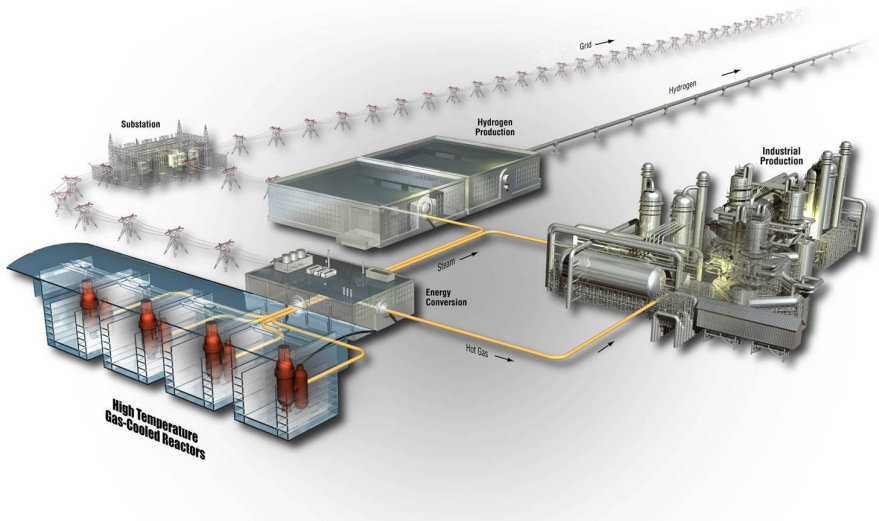

Idaho National Laboratory

INL is a U.S. Department of Energy National Laboratory operated by Batelle Energy Alliance, LLC

DISCLAIMER

This information was prepared as an account of work sponsored by an agency of the U.S. Government. Neither the U.S. Government nor any agency thereof, nor any of their employees, makes any warranty, expressed or implied, or assumes any legal liability or responsibility for the accuracy, completeness, or usefulness, of any information, apparatus, product, or process disclosed, or represents that its use would not infringe privately owned rights. References herein to any specific commercial product, process, or service by trade name, trade mark, manufacturer, or otherwise, does not necessarily constitute or imply its endorsement, recommendation, or favoring by the U.S. Government or any agency thereof. The views and opinions of authors expressed herein do not necessarily state or reflect those of the U.S. Government or any agency thereof.

INL/EXT-22-67587
Revision 0

AGR-5/6/7 Final Release-to-Birth Ratio Data Analysis

Binh T. Pham
Dawn M. Scates

June 2022

Idaho National Laboratory
INL Advanced Reactor Technologies Program
Idaho Falls, Idaho 83415

http://www.inl.gov

Prepared for the
U.S. Department of Energy
Office of Nuclear Energy
Under DOE Idaho Operations Office
Contract DE-AC07-05ID14517

INL ART Program

AGR-5/6/7 Final Release-to-Birth Ratio Data Analysis

INL/EXT-22-67587
Revision 0

June 2022

Technical Reviewer: (Confirmation of mathematical accuracy, and correctness of data and appropriateness of assumptions.)

Mitchell A. Plummer — 6/23/2022
Mitchell A. Plummer — Date
NDMAS Technical Lead

Approved by:

Paul Demkowicz — 6/23/2022
Paul A. Demkowicz — Date
AGR Program Technical Director

Travis Mitchell — 6/23/2022
Travis R. Mitchell — Date
INL ART Program Manager

Michelle Sharp — 6/23/2022
Michelle T. Sharp — Date
INL Quality Assurance

ACKNOWLEDGEMENTS

This work is supported by the DOE Advanced Reactor Technologies Program at Idaho National Laboratory under the U.S. Department of Energy Contract DE-AC07-05ID14517.

SUMMARY

AGR-5/6/7 is the last of a series of Advanced Gas Reactor (AGR) experiments conducted in the Advanced Test Reactor (ATR) at Idaho National Laboratory (INL) in support of development and qualification of tristructural isotropic (TRISO) low-enriched fuel for use in the high-temperature gas cooled reactor (HTGR). AGR configuration and irradiation conditions are based on prismatic HTGR technology that is distinguished primarily through the use of helium coolant, a low-power-density ceramic core capable of withstanding very high temperatures, and TRISO-coated particle fuel. The AGR tests provide valuable irradiation-performance data to support fuel process development, qualify fuel for normal operation and accident conditions, and support development and validation of fuel performance and fission-product (FP) transport models and codes.

Each AGR test consists of multiple independently controlled and monitored capsules containing fuel compacts placed in a graphite cylinder shrouded by a steel shell. Release-to-birth ratios (R/B) for fission-gas (FG) isotopes released from each capsule are calculated from release rates, measured by germanium detectors in the Fission Product Monitoring System (FPMS) installed downstream from each capsule, and birth rates calculated using numerical models of FG generation. The R/Bs are a critical measure of the ability of the fuel kernel, the particle coating layers, and the compact matrix to retain fission-gas atoms, preventing their release into the sweep-gas flow, and the impact of initially defective particles and/or particle-coating failures that occur during irradiation. For fission-gas isotopes, particle failure is defined as failure of all coating layers, allowing gaseous fission atoms to escape from a particle.

R/B data analysis for the first three irradiation experiments—AGR-1, AGR-2, and AGR-3/4—was reported in INL/EXT-14-32970, "AGR-1, AGR-2, and AGR-3/4 Release-to-Birth Ratio Data Analysis" (Pham et al 2019). Data from those experiments have been used to establish an empirical model for the TRISO fuel design for the R/B of FG from both exposed particles and dispersed uranium as a function of krypton or xenon isotope-decay constant and fuel temperature.

As-fabricated or in-pile particle failures were not identified during the AGR-1 irradiation experiment, thus FG releases from the AGR-1 capsules originated mainly from dispersed uranium (DU) in the fuel compacts. Therefore, the AGR-1 release data were used to estimate the DU release factor, defined as the ratio between release from DU and release from an exposed kernel (EK) with the same uranium mass. The DU release factor determined from comparison between AGR-1 and AGR-3/4 data is 5.1 ±3.1 for all isotopes: 6.1 ±3.5 for krypton and 4.0 ±2.4 for xenon.

The AGR-3/4 experiment contained a fixed number of designed-to-fail particles, and the particle failures were counted during irradiation. The AGR-3/4 R/B data were therefore used to establish the empirical relationship between R/B per-exposed-kernel, decay constant and temperature. This R/B per-exposed-kernel relationship can be used to assess fission product release from TRISO particle failures.

The AGR-5/6/7 fuel compacts, fabricated at pilot scale at BWX Technologies, Inc., had higher fractions of EK defects and dispersed uranium contamination relative to compacts used in the AGR-1 and AGR-2 experiments. The AGR-5/6/7 irradiation began on February 16, 2018 and ended on July 22, 2020, spanning nine ATR cycles (162B–168A) over two and a half years, totaling approximately 360.9 effective full-power days.

During the first five cycles (162B – 165A), R/Bs were stable in the 10^{-8}–10^{-6} range and - based on the gross gamma counts - no in-pile particle failures were observed. The maximum R/B value of around 2×10^{-6} for Kr-85m resulted from the presence of as-fabricated exposed kernels (based on the high exposed kernel fraction), the dispersed uranium, and high fuel particle temperatures in Capsule 1. Comparison of capsule-measured R/Bs from these early cycles to predictions using the previously developed AGR R/B model demonstrated FG release from the AGR-5/6/7 TRISO fuel was comparable to that of previous experiments. In addition, the Kr-85m R/B per-exposed-kernel values are comparable to R/B values obtained in AGR-3/4 irradiation experiment and four irradiation experiments performed during 1980s: : (1) HRB-17/18 (General Atomics 1987); (2) COMEDIE-BD1 (Richards 1994); (3) HFR-B1 (ORNL 1994); and (4) HRB-21 (DOE 1995). In contrast, all measured R/B values are lower than predictions by the commonly used Richards and German models, which are intentionally conservative.

A large number of in-pile particle failures occurred in Capsule 1 by the end of Cycle 166A. During the final four cycles (166A – 168A), apparent damage to the Capsule 1 gas line appeared to cause FG leakage from that capsule into the other four capsules, resulting in an increase in FG detected in the effluent for all capsules. Isolation of the Capsule 1 gas line during the last three cycles also prevented measurement of its FG release. Thus, R/Bs in all capsules after Cycle 166A are highly uncertain because of undefined amount of leakage from Capsule 1, especially for long-lived isotopes.

A few hundred in-pile particle failures were estimated for Capsule 1 before the end of Cycle 166A, but the total number of failures is unknown due to the lack of FG release data in the later cycles. Based primarily on evidence from the gross gamma counts during Cycle 168A, approximately 15 particles failed in Capsule 3 and four particles failed in Capsule 2. In-pile failures in Capsule 3 were anticipated because this capsule was designed to operate beyond the HTGR normal operating temperature range. In contrast, no in-pile failures were identified in the top two capsules (4 and 5) based on the absence of the typical spikes in gross gamma counts and low failure estimates using the AGR model, developed in INL/EXT-14-32970 (Pham et l 2019), for R/B of the short-lived isotopes (Kr-89 and Xe-137) with minimal leakage from Capsule 1.

CONTENTS

FIGURES

TABLES

ACRONYMS

AGR	Advanced Gas Reactor
ATR	Advanced Test Reactor
BOI	beginning of irradiation
BWXT-NOG	BWX Technologies Nuclear Operations Group
DLBL	deconsolidation and leach burn leach
DTF	designed to fail
DU	dispersed uranium
DUF	dispersed uranium fraction
EFPD	effective full-power day
EK	exposed kernel
EKF	exposed kernel defect fraction
FG	fission gas
FPMS	Fission Production Monitoring System
GG	Gross gamma
HTGR	high-temperature gas-cooled reactor
INL	Idaho National Laboratory
IPyC	inner pyrolytic carbon
OPyC	outer pyrolytic carbon
ORNL	Oak Ridge National Laboratory
PALM	powered axial locator mechanism
PF	packing fraction
PIE	post-irradiation examination
R/B	release-to-birth ratio
SiC	silicon carbide
TC	thermocouple
TRISO	tristructural isotropic
U.S.	United States
UCO	uranium carbide/oxide
UO_2	uranium dioxide
VHTR	very high-temperature reactor

AGR-5/6/7 Final Release-to-Birth Ratio Data Analysis

1. INTRODUCTION

AGR-5/6/7 is the last of a series of Advanced Gas Reactor (AGR) experiments sponsored by Advanced Reactor Technologies (ART) and conducted in the Advanced Test Reactor (ATR) at Idaho National Laboratory (INL) in support of development and qualification of tristructural isotropic (TRISO) low-enriched fuel for use in the high-temperature gas cooled reactor (HTGR). The configuration and irradiation conditions of the AGR experiments are based on prismatic HTGR technology, a technology involving the use of helium coolant, a low-power-density ceramic core capable of withstanding very high temperatures, and coated particle fuel as described in PLN-3636 (Mitchell 2020). The tests are designed to provide irradiation performance data to support fuel process development, qualification of fuel for a variety of irradiation conditions, and development and validation of fuel performance and fission product transport models and codes.

The FG release rate of TRISO-coated fuel is a key factor for performance assessment of very high-temperature reactors (VHTRs) (General Atomics 2009). Under normal operating conditions, the kernels of the TRISO particles should retain more than 95% of the radiologically important, short-lived fission gas (FG) isotopes (IAEA 1997). Fabrication defects or in-pile particle failures, however, may result in compromised coatings, or 'exposed kernels,' from which the noble gases produced by fission may escape into the surrounding materials. The fractional release of these FGs, defined as the ratio of the release rate of a gaseous fission isotope (measured) to its instantaneous birth rate (calculated), is a licensing-relevant measure described in this report as the release-to-birth ratio (R/B). The capsule-average R/B at the beginning of irradiation (BOI) can be used to assess the quality of the fuel manufacturing process in terms of exposed kernel (EK) defect and dispersed uranium fractions. The R/B per-exposed-kernel is a property of the TRISO fuel design and can be used to assess FG releases from the fuel and assess the presence of particle failures in the reactor.

A few irradiation studies executed in the 1980s were designed to study fission-gas releases from low enriched uranium carbide/oxide (UCO) TRISO fuels. Those studies included either designed-to-fail (DTF) particles or identified in-pile failures (General Atomics 1987; Richards 1994; ORNL 1994; and DOE 1995). Since 2006, four AGR irradiation tests (AGR-1, AGR-2, AGR-3/4, and AGR-5/6/7) have been conducted in the ATR at INL. Each AGR test included multiple independent capsules, each containing cylindrical fuel compacts housed within a graphite cylinder shrouded by a steel shell. Thermocouples (TCs) were embedded in the graphite to monitor temperature and facilitate its control. FGs that were released from the fuel were carried by a purge gas to a Fission Product Monitoring System (FPMS) to quantify the release rate for each capsule.

The main sources of FG release are from heavy-metal contamination in the fuel coatings and graphite matrix material and from defective or failed particles (IAEA 1997). FG transport is frequently modeled as a diffusion process with a rate described with an effective diffusivity that encompasses several mechanisms. This effective diffusivity is determined by material properties of the kernel, particle coatings, and compact matrix. The activity of radioactive species reaching the FPMS depends on both the diffusive transport rate and the decay constant of the species. Species with relatively large decay constants (i.e., short half-lives) might not reach the detector if the transport time is long enough that most of the gas decays in transit. There are a few commonly used mechanistic models derived from R/B data from historical irradiations where the number of failed particles could be accurately determined. These models have been used to predict the R/B per-exposed-kernel for the fuel.

The AGR-5/6/7 fuel compacts, fabricated at pilot scale at BWX Technologies, Inc., had higher fractions of EK defects and dispersed uranium contamination relative to compacts used in the AGR-1 and AGR-2 experiments. The AGR-5/6/7 irradiation began on February 16, 2018 and ended on July 22, 2020, spanning nine ATR cycles (162B–168A) over two and a half years, totaling approximately 360.9 effective

full-power days. The measured R/Bs from the five AGR-5/6/7 capsules were analyzed to assess irradiation performance of the reference TRISO fuel.

R/B data analysis for the first three irradiation experiments—AGR-1, AGR-2, and AGR-3/4—was reported in INL/EXT-14-32970, "AGR-1, AGR-2, and AGR-3/4 Release-to-Birth Ratio Data Analysis" (Pham et al. 2019). Data from those experiments have been used to establish an empirical model for UCO TRISO fuel for the R/B of FG from both exposed particles and dispersed uranium as a function of krypton or xenon isotope-decay constant and fuel temperature.

As-fabricated or in-pile particle failures were not identified during the AGR-1 irradiation experiment based on the extremely low R/B values, thus FG releases from the AGR-1 capsules originated mainly from dispersed uranium (DU) in the fuel compacts. Therefore, the AGR-1 release data were used to estimate the DU release factor, defined as the ratio between release from DU and release from an exposed kernel (EK) with the same uranium mass. The DU release factor determined from comparison between AGR-1 and AGR-3/4 data is 5.1 ±3.1 for all isotopes: 6.1 ±3.5 for krypton and 4.0 ±2.4 for xenon (Pham et al. 2019).

The AGR-3/4 experiment contained a fixed number of designed-to-fail particles, and the particle failures were counted during irradiation. The AGR-3/4 R/B data were therefore used to establish the empirical relationship between R/B per-exposed-kernel, decay constant and temperature. This R/B per-exposed-kernel relationship can be used to assess fission product release from similar particle failures. The AGR-5/6/7 daily average R/B values for four krypton isotopes (i.e., Kr 85m, Kr-87, Kr-88, and Kr-89) and three xenon isotopes (i.e., Xe-135, Xe-137, and Xe-138) were used for this analysis. The resulting R/B values per-exposed-kernel were compared with data from previous irradiations and with predictions using AGR-3/4-based and commonly used mechanistic models. Historic R/B values per-exposed-kernel for Kr-85m were extracted from four irradiation experiments performed during the 1980s: (1) HRB-17/18 (General Atomics 1987); (2) COMEDIE-BD1 (Richards 1994); (3) HFR-B1 (ORNL 1994); and (4) HRB-21 (DOE 1995). Also, R/Bs for two short-lived isotopes, Kr-89 and Xe-137, were used to roughly estimate number of particle failures in Capsules 2-5 as described in the AGR-5/6/7 as-run report (Pham et al. 2021) and summarized here for completeness.

2. ADVANCED GAS REACTOR-5/6/7 IRRADIATION

2.1 Experimental Description

AGR-5/6/7 was aimed at testing low-enriched UCO TRISO-coated fuel. The AGR 5/6 portion of the experiment was intended to provide fuel performance data under conditions of burnup, fast fluence, and temperature expected during normal operation of a high-temperature gas-cooled reactor. The AGR-7 portion served as a high-temperature performance margin test of the same fuel type used in AGR-5/6, irradiating the fuel beyond normal operating conditions, to explore the level of performance margin that exists for this fuel design. A detailed description of the experiment is provided in the test plan (Collin 2018). The experimental test train consisted of five independently controlled and monitored capsules, stacked on top of each other, as shown in Figure 1. Capsules 1, 2, 4, and 5 comprised the AGR-5/6 experiment, while Capsule 3 was the AGR-7 experiment.

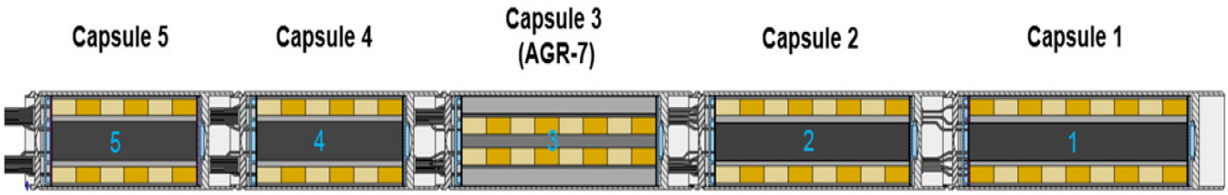

Figure 1. Schematic view of the AGR-5/6/7 test train (Note: Capsule 5 is at the top of the test train).

Capsule 1 contained the greatest number of compacts, consisting of ten stacks with nine compacts each, totaling 90 compacts. Capsule 2 contained 32 compacts; and Capsules 3, 4, and 5 each contained 24 compacts. A leadout tube, that extended from the test train to the reactor penetration, contained and the gas lines and TC wiring. To control fuel temperatures during irradiation, a variable mixture of helium and neon gases was delivered to each capsule by capsule-specific mass-flow controllers, in response to variations in fuel fission power.

The AGR-5/6/7 irradiation began on February 16, 2018 and ended on July 22, 2020, spanning nine ATR cycles (162B–168A) over two and a half years, and comprising approximately 360.9 effective full-power days (EFPDs) (Pham et al. 2021). The capsule-average R/B, calculated from the measured release rates in the five capsules and calculated fuel temperatures during the nine cycles, was used in this analysis.

2.1.1 Tristructural Isotropic Coated Fuel Particles

Each TRISO fuel particle, as shown in Figure 2 (A), consists of the fissile fuel kernel, buffer layer, and three coating layers (i.e., the inner pyrolytic carbon [IPyC], silicon carbide [SiC], and outer pyrolytic carbon [OPyC]). The coating system constitutes a miniature pressure vessel that has been engineered to provide containment of the radionuclides and gases generated by fission of the nuclear material in the kernel. Thousands of these TRISO-coated particles, as seen in Figure 2 (B) and (C), are bonded in a carbonaceous material inside a cylindrical fuel compact designed for use in a prismatic HTGR. The particles can endure fuel temperatures up to 1,800°C for several hundred hours without loss of particle-coating integrity (INL 2010). This high-temperature radionuclide retention capability of TRISO fuel is the key element in the design and licensing of modular HTGRs.

Lessons learned from the comparison of process attributes and irradiation conditions (e.g., burnup, fast neutron fluence, temperature, degree of acceleration) between German fuel tests (Nickel et al. 2002) and previous U.S irradiation tests of TRISO-coated particle fuel were used as a basis for improvement of the manufacturing process of the modern United States (U.S.) TRISO-coated fuel (Petti et al. 2003). Fuel particles used in AGR-5/6/7 capsules were fabricated by application of coatings to low-enriched (15.5% U-235) UCO kernels. The TRISO particle lot J52R-16-98005 was selected as the parent material for all fuel compacts fabricated at the BWX Technologies Nuclear Operations Group (BWXT-NOG) facilities in

Lynchburg, Virginia. These particles were fabricated based on the selected reference fuel design; details on particle fabrication are documented in INL/EXT-19-53720, "AGR-5/6/7 Fuel Fabrication Report" (Marshall D.W. 2019). The AGR-5/6/7 experiment included a larger population of particles than previous irradiation campaigns (approximately 570,000).

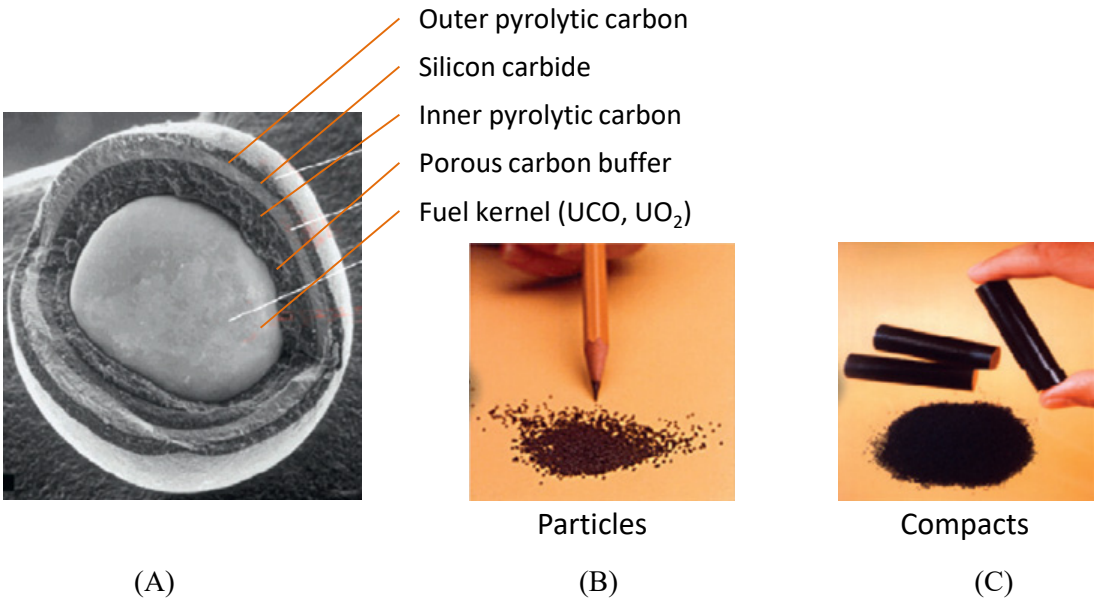

Figure 2. TRISO-coated particle fuel and compacts used in AGR experiments. (A) Micrograph image showing the coating layers and fissile kernel of a single particle; (B) image showing particle size; and (C) image illustrating compact size.

2.1.2 Fuel Compacts

The AGR-5/6/7 compacts were fabricated using near-production-scale equipment at BWXT-NOG in accordance with "AGR-5/6/7 Fuel Specification" (Marshall 2017). Four aliquots of the TRISO particle lot were individually over-coated with a resinated graphite 'matrix' powder, targeting a nominal TRISO particle volumetric packing fraction (PF) of either 25% or 40%. Each of four over-coated TRISO particle batches was pressed into multiple cylindrical fuel compacts, creating four compact lots (i.e., J52R-16-14154, J52R-16-14155, J52R-16-14156, and J52R-16-14157). The 40% volumetric PF compacts occupy the bottom and top capsules (e.g., Capsules 1 and 5, respectively), while the 25% PF compacts occupy the three middle capsules (e.g., Capsules 2, 3, and 4) of the AGR-5/6/7 test train (Table 1). The bottom Capsule 1 contains 90 out of the 194 AGR-5/6/7 compacts, which came from two 40%-PF compact lots. Number of particles per compact was an average value for each compact lot.

Table 1. Compacts used in AGR-5/6/7 capsules.

Capsule	Experiment	Compact Lot	Packing Fraction	N Compacts	N Particles per Compact
Capsule 1	AGR-5/6	J52R-16-14154	40%	55	3434
Capsule 1	AGR-5/6	J52R-16-14155	40%	35	3393
Capsule 2	AGR-5/6	J52R-16-14156	25%	32	2265
Capsule 3	AGR-7	J52R-16-14156	25%	24	2265
Capsule 4	AGR-5/6	J52R-16-14157	25%	24	2197
Capsule 5	AGR-5/6	J52R-16-14155	40%	24	3393

DU contamination and EK fabrication defects are the primary sources of fission-gas release in the AGR capsules when no in-pile particle failures occur (Pham et al 2019). The dispersed uranium fraction (DUF) represents the mass of uranium contamination trapped in the OPyC layer of the TRISO particle and matrix, normalized to the total mass of uranium in the fuel compact. The EK fraction (EKF) describes the number of physically damaged particles, with cracked or broken coating layers, normalized to the total particle count in the compact. These two fuel fabrication defect metrics are important inputs to the analysis of FG release from AGR capsules. They were initially characterized by BWXT-NOG and Oak Ridge National Laboratory (ORNL) using the deconsolidation-leach-burn-leach (DLBL) method. Those values were subsequently revised, lower than in the AGR-5/6/7 preliminary R/B report (Pham and Scates 2019), based on results from an ORNL fuel defect analysis. DUF and EKF values presented in Table 2 are the ORNL values, believed to be more accurate due to much fewer anomalies observed (Marshall 2019). The measured defect fractions exceed the AGR-5/6/7 fuel specification for the EKF, for the 40% PF compact lots: J52R-16-14154 and J52R-16-14155. It is also worth mentioning that the uncertainty of measured DUF and EKF are quite high due to inconsistency of results measured by ORNL and BWXT-NOG, as well as the small number of compacts used in the defect analysis.

Table 2. Dispersed uranium fractions and exposed kernel defect fractions with specifications including one-tailed confidence interval upper limit.

Compact Lot	DUF	DUF 95%	DUF Spec.	EKF	EKF 95%	EKF Spec.
J52R-16-14154, J52R-16-14155	4.95×10^{-6}	$\leq 5.7\times10^{-6}$	$\leq 1.0\times10^{-5}$	5.39×10^{-5}	$\leq 8.3\times10^{-5}$	$\leq 5.0\times10^{-5}$
J52R-16-14156, J52R-16-14157	5.02×10^{-6}	$\leq 5.6\times10^{-6}$	$\leq 1.0\times10^{-5}$	7.27×10^{-6}	$\leq 3.5\times10^{-5}$	$\leq 5.0\times10^{-5}$

(Red type indicates lot was outside specification)

2.2 Thermal and Physics Analyses

The as-run physics and thermal analyses were performed immediately following completion of each ATR cycle. Based on as-run ATR operating parameters, the physics analysis predicts daily heating rates, fast fluence, and burnup for fuel compacts in the five capsules. The heating rate and fast fluence, combined with neon fraction in the gas flow to each capsule, are used in the thermal model to calculate daily fuel compact temperature. As for previous AGR experiments, detailed model description and results for the AGR-5/6/7 as-run thermal analysis and physics analysis are reported in ECAR-5633 (Hawkes 2021) and ECAR-5321 (Sterbentz 2020), respectively.

2.2.1 Fuel Compact Temperature Distribution

Fuel temperature is one of the most influential factors in FG release rate. Fuel temperatures in AGR capsules cannot be directly measured because contact with the TC heads could lead to unwanted particle failures. Therefore, ABAQUS-based (Version 6.14-2), three-dimensional, finite-element thermal models were created for each capsule of the AGR-5/6/7 experiment to calculate daily averages of temperatures at the fuel compacts and at TC locations during irradiation. The TC temperatures are used for calibration of this thermal model, which uses an eight-node hexahedral-brick finite-element mesh to estimate capsule temperature profiles. Figure 3 shows a temperature contour plot cut-away view of capsule 1 fuel during cycle 162B day 20, which was reported in ECAR-5633, “AGR-5/6/7 Daily As-Run Thermal Analyses” (Hawkes 2021).

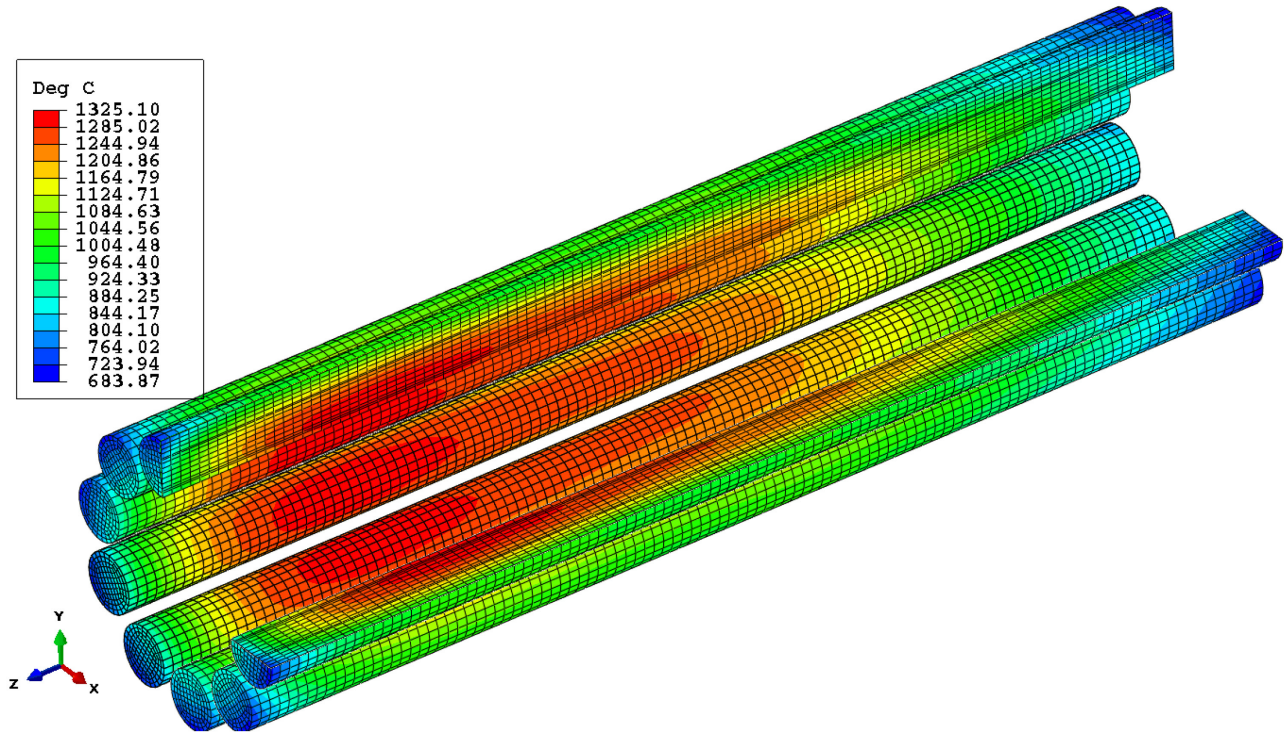

Figure 3. Temperature contour plot (°C) cut-away view of capsule 1 fuel during cycle 162B day 20. (Hawkes 2021).

Sufficient data were available for calculation of fuel temperatures for all capsules, except Capsule 1 during the last cycle, 168A, when neon fraction could not be estimated due to gas leaking from the leadout while its gas line was isolated. Figure 4 depicts the minimum, maximum, and volume-averaged fuel temperatures as a function of irradiation time for each of the five capsules. Fuel temperatures in the capsules were maintained at target temperature range except for the beginning of Cycle 162B and two low-power powered axial locator mechanism (PALM) Cycles, 163A and 167A, when fuel temperatures were significantly below target temperatures because the capsules ran on pure helium.

Temperature variation was greatest in Capsule 1 compacts due to the taller fuel stacks in that capsule and its location at the bottom of the test train in a region with a relatively high neutron flux gradient. Daily fuel temperatures in Capsule 1 vary by more than 600°C (in the ~700ºC to ~1300°C range, as shown in Figure 3 and Figure 4). Capsule 1 contained the greatest number of fuel compacts (90) and was designed to ensure achievement of the highest temperature range targets for the AGR-5/6 experiment: 30% of fuel in the 1050ºC to 1250ºC range and 10% of the fuel > 1250ºC range. Fuel temperatures in the other three AGR-5/6 capsules (i.e., 2, 4, and 5) were significantly lower, and consisted of significant fuel portions in the two lowest target temperature ranges: 30% of fuel < 900ºC and 30% of fuel in 900ºC to 1050ºC range. Finally, the AGR-7 Capsule 3 had the highest fuel temperature (up to 1500°C) because its compacts are designed to test the fuel beyond normal operating conditions.

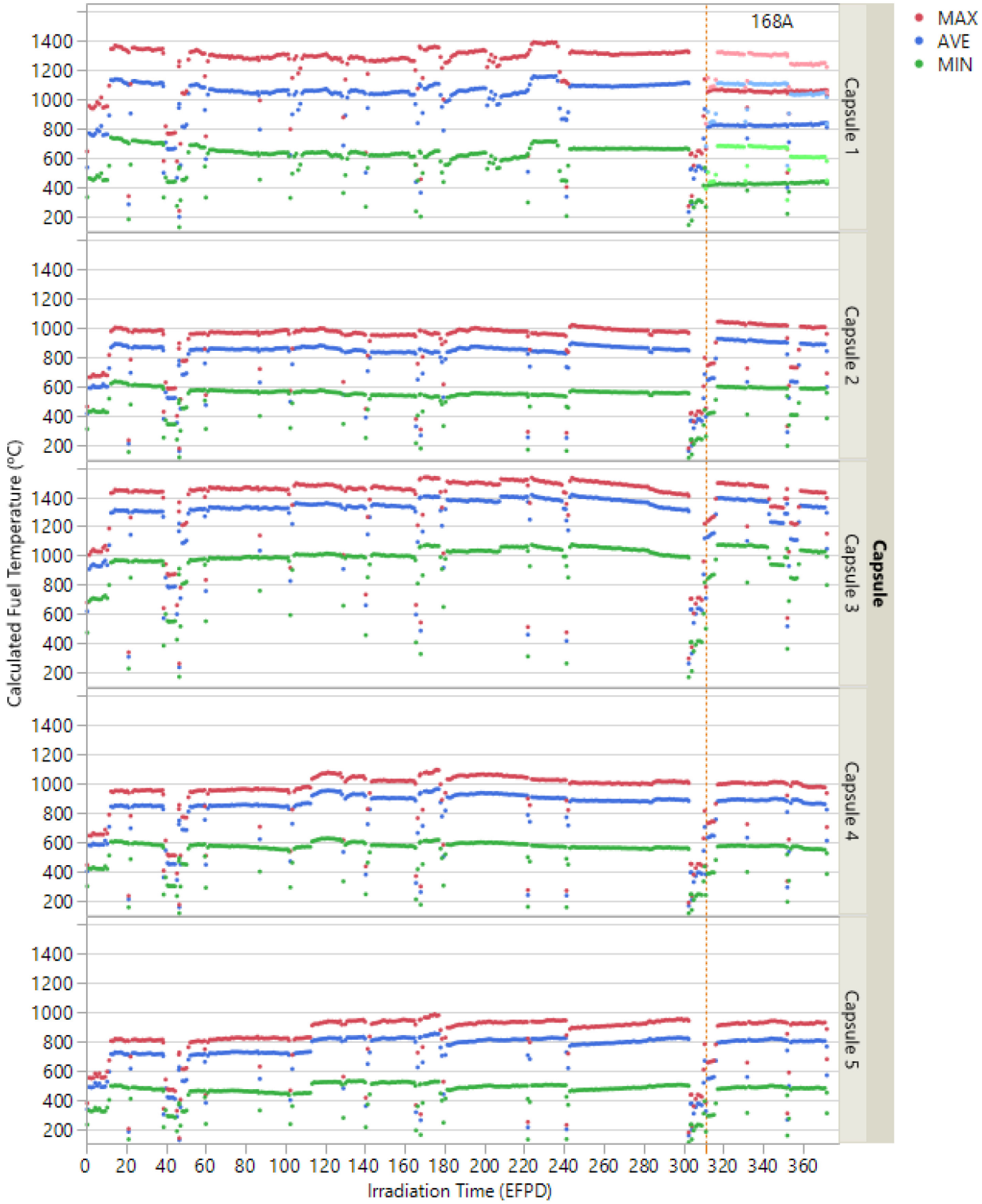

Figure 4. Calculated daily minimum, maximum, and volume-averaged fuel temperatures as a function of irradiation time (light color dots for Capsule 1 are for the assumed leadout neon fraction instead of zero and vertical dot line is at the start of Cycle 168A). (Pham et al 2021)

For calculations of the R/B as a function of temperature, the relevant temperature is that of the particles releasing fission gas or the particles releasing those gases. Because the locations of those particles are unknown, we use the daily volume-averaged fuel temperature for each capsule, as calculated via heat transport simulation, as the best estimate of the relevant particle temperature. As an estimate of its one-sigma uncertainty, we assume that the mean particle temperature is a normally distributed random variable, centered on the daily volume-averaged temperature, with upper and lower standard deviations equal to half the distance to the capsule maximum and minimum temperatures, respectively. Table 3 shows the mean temperature and associated uncertainty, in terms of one standard deviation, for each capsule (Pham et al 2021). Because the minima and maxima are not equidistant from the mean, the upper and lower standard deviations are unequal and a confidence interval based on those values is asymmetric. The impacts of uncertainties in fuel temperature in predicting R/Bs is discussed in Section 3.2.

Table 3. Average and standard deviations of fuel temperature during Cycles 162B, 164A, and 164B.

Capsule	Average Fuel Temperature, ℃	Upper Uncertainty, ℃	Lower Uncertainty, ℃
Capsule 1	1030	76	135
Capsule 2	827	37	92
Capsule 3	1290	43	111
Capsule 4	842	36	94
Capsule 5	726	33	87

2.2.2 Fuel Compact Physical Parameters at the End of Irradiation

The fuel temperature, heat rate, and power per particle presented in Figure 5 are time-averaged values for each compact, while fast fluence and burnup are cumulative values calculated at the end of the last cycle (168A). As can be seen in the plots, the physical parameters in the five capsules varied widely, both within and across the capsules. Fuel heat rate and power per particle are restricted by the limit of peak kernel temperature to minimize FG diffusion and the need to maintain fuel temperature within a specified range.

In general, the daily-average power values for AGR-5/6/7 compacts are lower in the bottom capsule (1) and top capsule (5) relative to the middle capsules (2, 3, and 4). The overall range is 50 to 160 mW per particle, typical power levels for TRISO particles in an HTGR. The instantaneous peak power per particle was well below the specification of 400 mW per particle to limit particle failures. On compact average, by the end of irradiation, the peak fast fluence was 5.55×10^{25} n/m^2 for compacts in the middle Capsule 3 (3-3-2 and 3-3-3) and the highest burnup level was 15.26% for compacts in Capsule 2 (2-7-4 and 2-8-4) (Pham et al. 2021).

Time-average volume-average fuel temperatures, on a compact basis, in the four AGR-5/6 capsules (e.g., 1, 2, 4, and 5) ranged from ~750ºC to ~1100ºC by the end of irradiation (a typical temperature range for gas reactors). As designed, fuel compacts in the AGR-7 Capsule 3 had the highest fuel temperature, ranging from 970ºC to 1400ºC on time-average by the end of irradiation, testing the fuel beyond normal operating condition (Pham et al 2021).

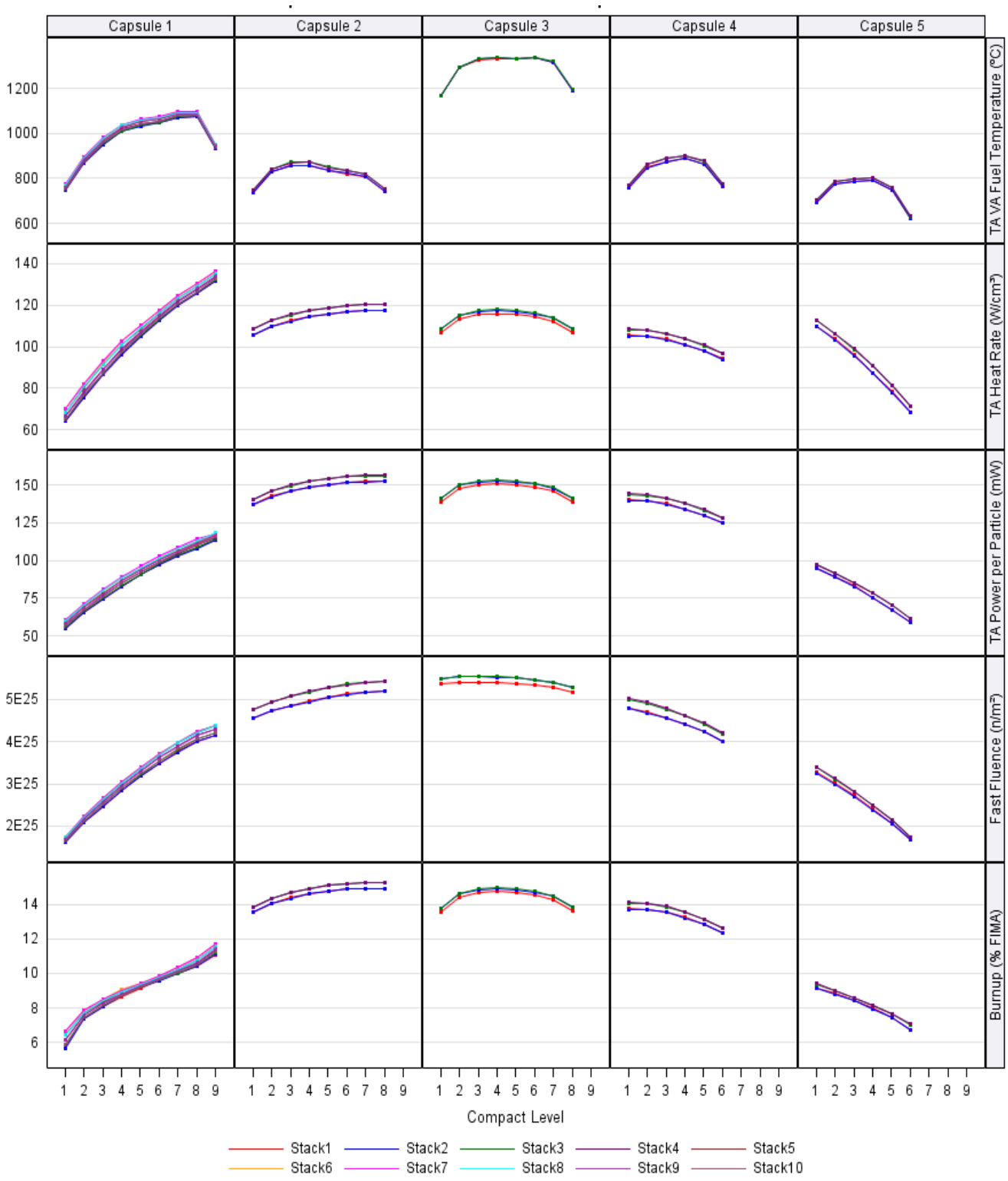

Figure 5. Summary of physical parameters for fuel compacts at the end of Cycle 168A.

2.3 Fission-Gas Release

One measure of the performance of a nuclear fuel test is the R/B ratio, which is, again, the ratio of the released activity of an isotope from the fuel to the calculated production rate (or birthrate) of the isotope during irradiation. For all AGR experiments, the following 12 isotopes were monitored: Kr-85m, Kr-87, Kr-88, Kr-89, Kr-90, Xe-131m, Xe-133, Xe-135, Xe-135m, Xe-137, Xe-138, and Xe-139. These nuclides were selected because they are chemically inert fission gases with relatively short half-lives, allowing each isotope to reach equilibrium concentration in the fuel during each cycle. The as-run FG release analysis results for AGR-5/6/7 experiment are documented in ECAR-5352 (Scates, 2021). This ECAR is used as a basis for the qualification of the FG release data.

2.3.1 Fission-Gas Release Monitoring

Each capsule had an independent gas line to route its helium/neon gas mixture and any released FGs from the capsule to the corresponding FPMS detector, which could detect individual fuel particle failures and provide release rates for 12 gaseous radionuclides, as specified in the document "AGR-5/6/7 Irradiation Experiment Test Plan" (Collin 2018). Each AGR capsule was continuously and independently monitored by a gross radiation detector and a spectrometer detector in the FPMS installed downstream from the capsule sweep-gas line. Figure 6 shows a simplified flow path for the AGR-5/6/7 capsules from the gas control system to the FPMS detector. The mass flow controllers blended the necessary mixture of neon and helium to maintain temperature of the control TC in each capsule within a specified band.

This mixture of inert gases, flowing through a capsule, carried FGs released from the capsule to the detector system, with a transit time of about 150 seconds under normal conditions. Gas flow passed through a high-purity-germanium detector, gamma-ray spectrometer system. The continuous gamma-ray spectrum measurements from the high-purity-germanium detectors were used to compute the release activities of several isotopes of krypton and xenon. These measured activities were converted to per-capsule FG release rates by correcting for decay that occurred during transport from the capsules to the detectors. Transport times were calculated from outlet-gas flow rates and the capsule-specific volumes through which samples flow to reach the respective monitoring detector. This conversion formula was derived under the assumption that equilibrium release conditions were established (Scates 2010). Fission-gas release rates for each capsule were provided as averages at 8-hour intervals, except during the leadout gas testing, when the release rates were provided at a much higher frequency (i.e., 20-minute intervals).

The gross-radiation detectors also had the capacity to detect each fuel-particle failure, up to and including the first 250 failures from each capsule. A particle failure would cause a rapid rise and drop (or spike) in the temporal profile of the measured gross gamma-count rate and raise the baseline gramma count afterward. The increase is the result of a sudden release of stored fission-product inventory inside a just-failed particle while the subsequent decrease reflects the exhaustion of that stored inventory and return to production-related release rate.

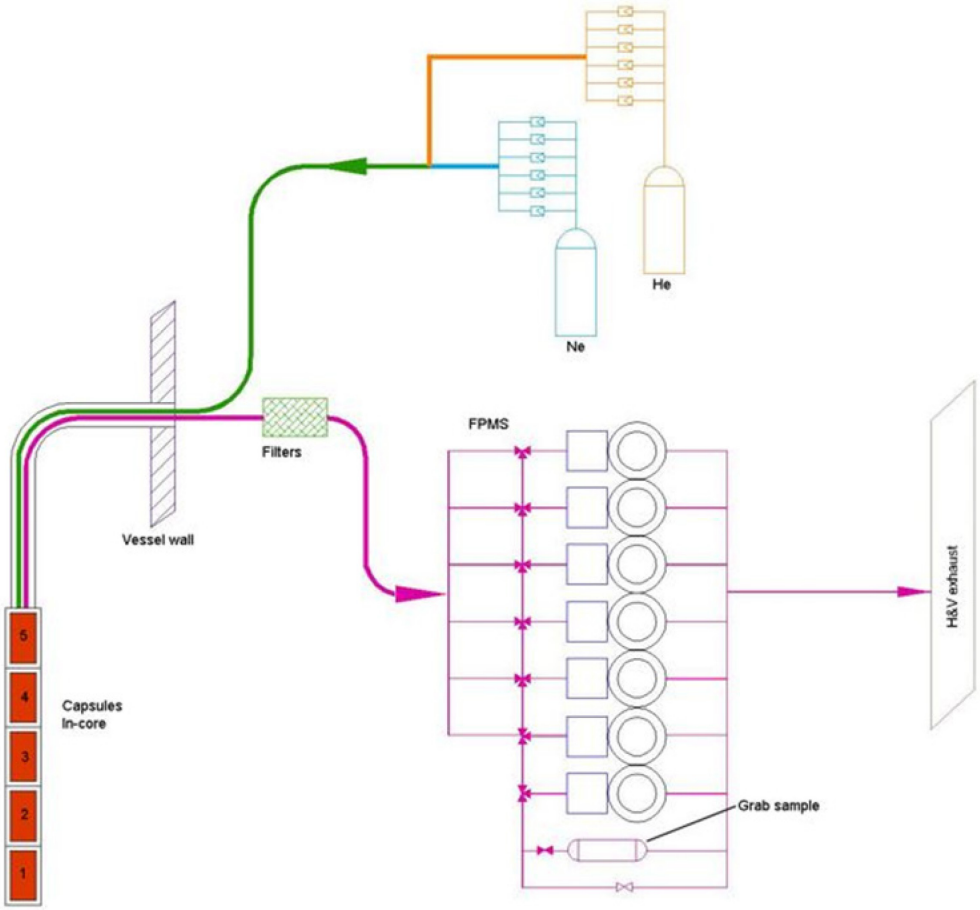

Figure 6. Simplified flow path for AGR-5/6/7 sweep gas (top) and a gross radiation monitor and spectrometer detector for each capsule (bottom).

2.3.2 Measured Fission-Gas Release Rate

Measurement-based R/Bs (Figure 7 and Figure 8) were based on released activities that were generally reported as an average for the eight-hour interval during normal irradiation conditions to reduce measurement uncertainty. However, during the initial test of the leadout flow system, release rates were recorded at a much higher frequency (i.e., every 20 minutes), so those measurements usually had higher measurement uncertainty. To preclude the use of data with high-measurement uncertainty in the analysis of fission-gas release, values where uncertainties are greater than 50% are omitted. Negative values are also excluded. These data filters remove data from the 'short' leadout flow runs or incomplete measurements, while leaving other runs unaffected.

Gas flow issues in Capsule 1 occurred beginning in the fourth cycle (Cycle 164B) as an obstruction apparently formed somewhere downstream of the capsule outlet. This issue was managed to minimize crosstalk between capsule gas lines until the end of the fifth cycle (Cycle 165A), as indicated by the stable R/B in all capsules during Cycles 164A and 165A relative to the three earlier cycles (Figure 7 and Figure 8). Since no in-pile particle failures were detected based on the gross gamma (GG) counts during the first five cycles, FG releases during these cycles (162B–165A) were releases from as-manufactured EK defects and DU contamination. During this time, R/B ratios were stable in the 10^{-8}–10^{-6} range on average for most isotopes (Table 4). The exception is Xe-131m with significantly higher R/Bs, 10^{-3} on average, which is associated with high measurement uncertainty of 42%, on average. A higher EK

fraction (EKF) and high fuel temperatures in Capsule 1 led to the maximum R/B value of around 2×10^{-6} for Kr-85m.

Table 4. AGR-5/6/7 measured R/B per capsule and uncertainty statistics for krypton and xenon isotopes for the first five cycles (162B-165A).

Isotope	Half-Life (min)	Measured R/B			Uncertainty [a] (%)		
		Average	Minimum	Maximum	Average	Minimum	Maximum
Kr-85m	268.7	3.53E-07	2.15E-10	1.95E-06	6.8	5.8	49.5
Kr-88	170.4	2.35E-07	1.16E-09	8.26E-07	6.4	5.8	24.5
Kr-87	76.0	2.88E-07	7.35E-11	1.11E-06	6.9	5.8	42.3
Kr-89	3.2	6.36E-08	5.74E-10	5.11E-07	9.7	5.8	36.2
Kr-90	0.5	1.40E-06	3.02E-09	3.44E-05	33.6	13.9	49.6
Xe-131m	17,162.0	2.60E-03	3.74E-05	3.03E-02	42.0	27.5	50.0
Xe-133	7,558.9	6.10E-07	4.28E-09	7.87E-05	17.8	6.0	50.0
Xe-135	545.8	1.47E-07	1.12E-09	9.09E-07	6.8	5.8	48.5
Xe-135m	15.3	9.89E-08	6.10E-10	6.07E-07	6.5	5.8	27.6
Xe-138	14.1	3.24E-08	5.34E-10	3.16E-07	8.8	5.8	33.8
Xe-137	3.8	5.31E-08	6.51E-11	2.71E-07	6.2	5.8	37.0
Xe-139	0.7	1.89E-08	3.72E-10	1.18E-06	33.0	9.5	50.0

[a] Only R/B values with an uncertainty under 50% and a standard 8-hour interval are used.

Green rows are the shortest-lived isotopes with uncertainty under 10% on average.

Red rows are either short- or long-lived isotopes with high uncertainty (more than 30% on average).

By the end of the sixth cycle (Cycle 166A), a significant number of in-pile failures appeared to have occurred in Capsule 1, causing a substantial increase in FG activities, saturation of the FPMS HPGe detector, and increased activity in the 1A primary cubicle that housed the FPMS that was picked up by the GG NaI(Tl) detectors. As a result, gas flow was suspended for Capsule 1, which prevented measurement of FG release during the last three cycles (Cycles 166B, 167A, and 168A), except for a short attempt to flow gas through Capsule 1 during the PALM Cycle 167A.

After the start of Cycle 166A, Capsule 1 gas line issues deteriorated and caused FG leakage into Capsules 2–5 to various degrees. R/Bs for all capsules from Cycle 166A are therefore considered highly uncertain because of undefined contamination from Capsule 1 (Scates 2021). However, they can still be used when the leakage rate from Capsule 1 can be estimated or deemed negligible. For example, FG leakage from Capsule 1 for short-lived isotopes (i.e., Kr-89 (pink dots in Figure 7) and Xe-137 (red dots in Figure 8) with a 3.2 and 3.8-min half-life, respectively) is expected to be considerably lower due to decay before reaching Capsule 5 at the top of the test train. Therefore, R/Bs of these isotopes can be used to assess possible particle failures in Capsules 2–5 in conjunction with GG counts: if no evidence of in-pile particle failures is seen for any capsule in the GG data, an increase in R/Bs can be contributed to FG leakage.

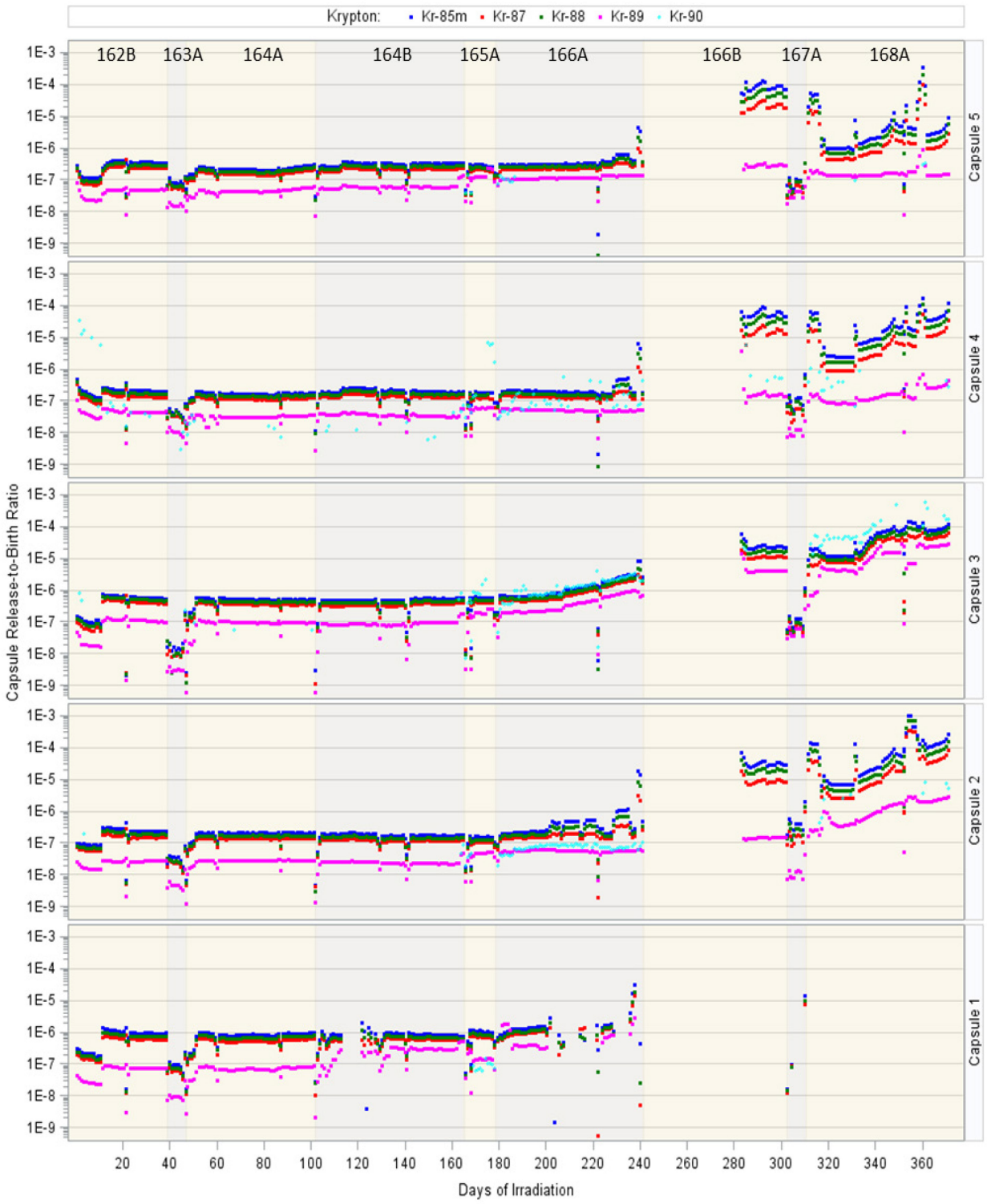

Figure 7. Measured R/B in AGR-5/6/7 capsules for krypton isotopes.

Figure 8. Measured R/B in AGR-5/6/7 capsules for xenon isotopes.

3. CYCLES 162B–165A RELEASE-TO-BIRTH RATIO: WITHOUT IN-PILE PARTICLE FAILURE

Throughout the first five cycles (162B – 165A), the R/Bs in all AGR-5/6/7 capsules were stable in the 10^{-8}–10^{-6} range, and no in-pile particle failures were observed, based on the gross gamma counts (Pham et al 2021). Additionally, Capsule 1 gas line damage started during Cycle 164B but was successfully managed, so that impact to FG release in all capsules was minimal by the end of Cycle 165A. Therefore, the R/Bs during these cycles can be compared to those from four previous fuel irradiation tests (i.e., AGR-1, -2, and -3/4) as a measure of the quality of test fuels manufactured at different scales. Then, the R/B per-exposed-kernel values, estimated based on the as-fabricated DU and EK fractions, are compared to data and models obtained from AGR-3/4 capsules and historical irradiations to demonstrate similarity in term of FG release from an EK defect of the AGR-5/6/7 TRISO fuel.

3.1 Comparison of Measured R/B per Capsule with AGR-1, AGR-2, and AGR-3/4 Experiments

Table 5 presents selected fabrication data for fuel compacts used in all AGR capsules. Fuel kernels were fabricated at BWXT for all AGR experiments. AGR-1 and AGR-3/4 particles were coated at ORNL. AGR-2 and AGR-5/6/7 particles were coated at BWXT in the larger coater. The AGR-5/6/7 EKF and DUF values in this table represent revisions of prior values, based on results from the ORNL fuel defect analysis (Marshall 2019). EK defect and DU fractions for AGR-5/6/7 are generally higher than in previous experiments. The fuel temperature is included in Table 5 to show that AGR fuels were irradiated under typical VHTR conditions.

Table 5. Selected fuel property and irradiation data for AGR-1, AGR-2, AGR-3/4, and AGR-5/6/7 capsules.

Property	AGR-1[a]	U.S. AGR-2[a]	AGR-3/4[a]	AGR-5/6/7
Particle manufacturing	Baseline + Variants 1, 2, 3	Large coater	Baseline	Near commercial
Fuel temperature[b] (°C)	600–1,400	700–1,410	820–1,500	400–1,500
Number of compacts/capsules	72 / 6	48 / 4	48 / 12	194 / 5
Number of particles per capsule	49,140–49,848	38,112 / 18,516	7,488	52,728–307,625
Number of DTF particles	0	0	80	0
Kernel diameter (μm)	349.7	426.7	357.3	425.8
EK fraction	0	9.4×10^{-6} / 8.1×10^{-6}	$< 3.5 \times 10^{-5}$	7.27×10^{-6} / 5.39×10^{-5}
DU fraction	1.62×10^{-7} / 3.85×10^{-7}	3.94×10^{-6} / 9.66×10^{-7}	—	4.95×10^{-6} / 5.02×10^{-6}
^{85m}Kr R/B at BOI	1.1×10^{-8}	5.8×10^{-7}	1.3×10^{-4}	4.5×10^{-7}

a. Data for AGR-1, AGR-2, and AGR-3/4 were extracted from (Pham et al 2019).
b. Fuel temperatures are the range of minimum to maximum daily temperatures for AGR-1, AGR-2, and AGR-5/6/7; and centerline temperatures for AGR-3/4.

Table 5 includes the BOI R/B for Kr-85m (average for all capsules), which is often used as a metric of as-manufactured fuel quality. For AGR-1, the first cycle is excluded from analysis because fuel temperatures were excessively low during that shakedown period. Cycle 1 was also excluded for AGR-

3/4 because most of the DTF particles failed during that cycle, which caused a significant increase in R/B over the course of the cycle. Therefore, AGR-1 and AGR-3/4 BOI R/B values are the average for Cycle 2. On the other hand, AGR-2 and AGR-5/6/7 R/B values were stable during Cycle 1, so the BOI R/B is the average R/B for Cycle 1 excluding the first few days, when fuel temperatures were still low. Low BOI R/B in AGR-1 capsules indicates high-quality and very low-defect fuel with low levels of dispersed uranium, while high BOI R/B in AGR-3/4 capsules reflects the high number of particle failures due to the embedded DTF particles.

The capsule-average R/B can be used to demonstrate differences in the defect fractions of fuel compacts in different AGR capsules, especially when no in-pile failures occurred. Thus, measured Kr-85m and Xe-135 R/B data in AGR-5/6/7, -3/4, -2, and -1 experiments during the first 160 EFPDs of irradiation are plotted side-by-side as a function of irradiation time , as shown in Figure 9 and Figure 10. This irradiation period corresponded to the first four cycles of the AGR-5/6/7 experiment. For AGR-2, due to gas flow issues, only data during the first three cycles and the four U.S capsules (2, 3, 5, and 6) were included; thus, the AGR-2 plots end earlier. The difference in as-manufactured fuel quality between AGR experiments is reflected on the capsule R/B values as summarized below.

1. AGR-1 capsules (Panel 4): the laboratory-scale manufactured fuel had very low DU fraction and evidence of EK defects or in-pile failures were not identified in any of the capsules (Demkowicz et al 2015), which resulted in the lowest R/B values (more than one order of magnitude lower) among all experiments.
2. AGR-2 capsules (Panel 3): The coated particles were manufactured in a pilot scale coater at BWXT, with the compacts fabricated at the laboratory scale at ORNL. The fuel had higher DU and EK defect fractions and, therefore, higher R/B values than AGR-1, especially the three UCO capsules (e.g., 2, 4, and 5). The R/Bs in AGR-2 Capsule 3, the only AGR capsule that contained UO_2 fuel, are the lowest among the AGR-2 capsules. Based on the as-fabricated fuel qualification characterization data, the number of EKs in each UCO capsule is expected to be less than 1 at 95% confidence. However, because the AGR-2 compacts have only slightly higher DU fractions than AGR-1 compacts, but significantly higher R/B values, one or more EK defects may have existed in the AGR-2 capsules (Stempien et al 2021, Pham et al 2019).
3. AGR-3/4 capsules (Panel 2): this laboratory-scale manufactured baseline fuel should have similar DU and EK defect fractions as for AGR-1 and AGR-2, but they are not characterized because the expected number of as-fabricated equivalent EKs is negligible compared to the large amount of expected in-pile failures from the 80 DTF particles included in each capsule. Most of the DTF failures occurred during the first cycle, leading to increasing R/B values during this cycle (Pham et al 2019). In subsequent cycles, R/B values in AGR-3/4 capsules are a few orders of magnitudes higher than R/B in AGR-1 capsule, where no EKs existed.
4. AGR-5/6/7 capsules (Panel 1): This near-commercial-scale manufactured fuel had similar DU and EK defect fractions as AGR-2, which resulted in the same order of magnitude R/Bs as in AGR-2 capsules, but about two orders of magnitude lower than the AGR-3/4 capsules where up to 80 in-pile DTF failures occurred. Given high fuel temperature in Capsule 1, this capsule had the highest capsule R/B values (blue dots) because of the high EKF and lager number of particles resulting in high number of as-fabricated equivalent EKs (i.e., 16 EKs as shown in Table 7) while in Capsule 5, the same fuel compacts were used but with much lower temperature, and therefore had lower R/B values. Although, Capsule 3 experienced the highest fuel temperatures (~200ºC higher than in other capsules), R/B values in Capsule 3 were lower than Capsule 1 because of lower EKF relative to Capsule 1. The two remaining capsules, 2 and 4, have the lowest R/Bs due to lower fuel temperatures and relatively small fraction of equivalent EKs.

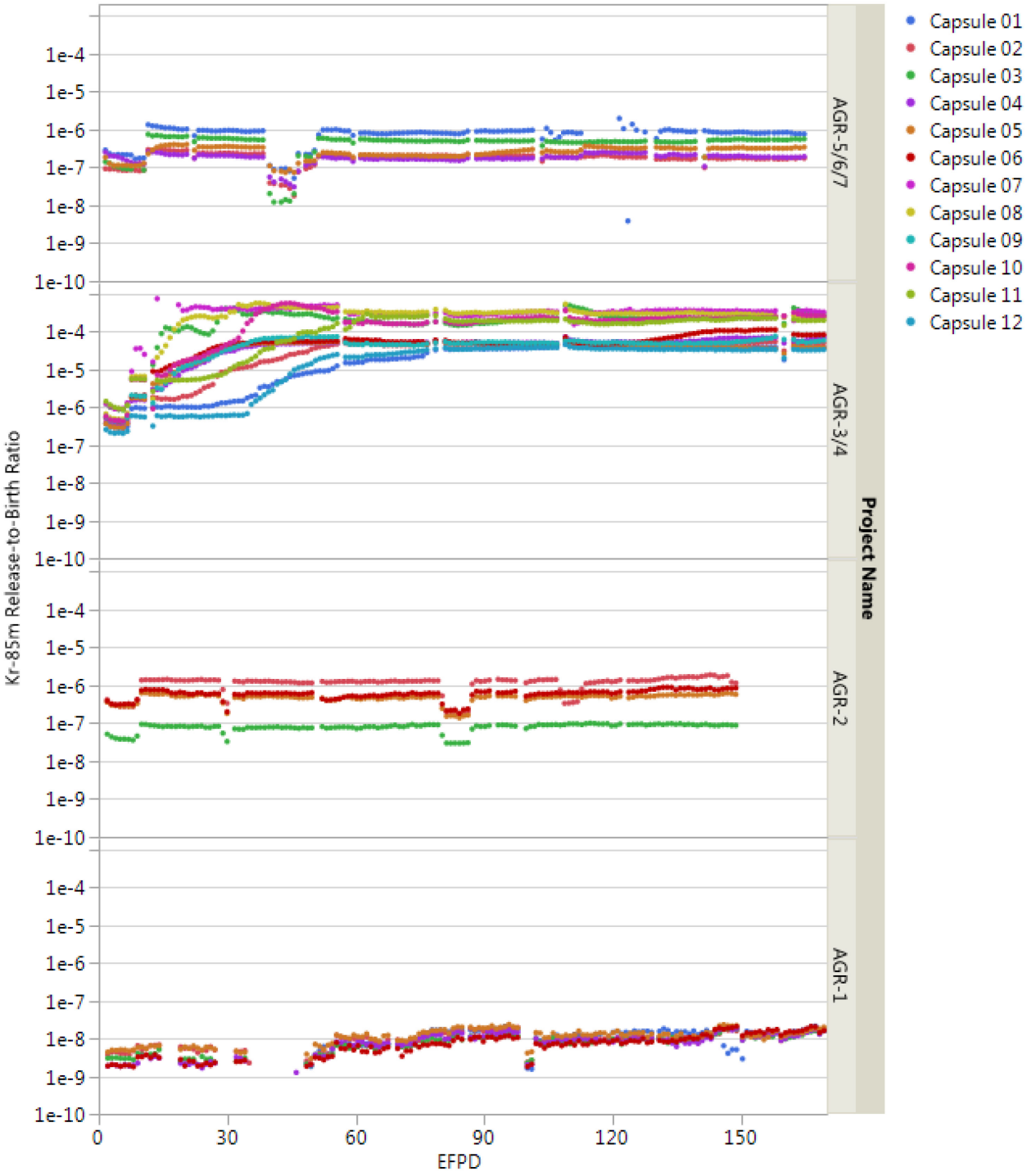

Figure 9. Kr-85m measured R/B per capsule from AGR-5/6/7, AGR-3/4, AGR-2, and AGR-1 capsules.

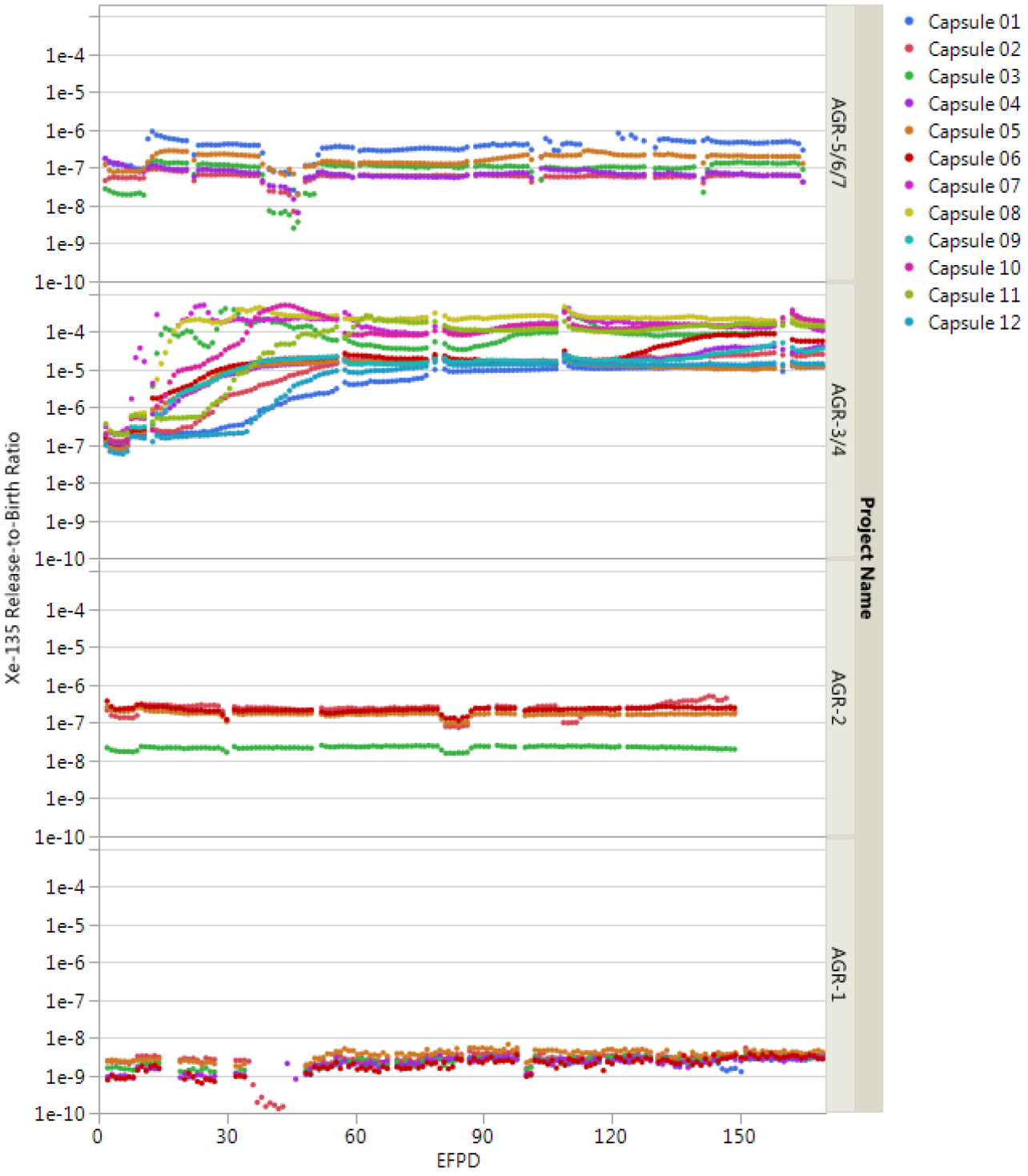

Figure 10. Xe-135 measured R/B per capsule from AGR-5/6/7, AGR-3/4, AGR-2, and AGR-1 capsules.

3.2 Comparison of Measured R/B to PARFUME-German Model Predictions

A model accounting for release of short-lived fission product gases from EKs and from DU contamination in the fuel matrix material is incorporated into PARFUME. This model is referred to as the PARFUME-German model, which is based upon the Booth equivalent sphere gas release model. This model used different reduced diffusion coefficients for release from EKs (D_2') and from DU contamination (D_1'). The total R/B is calculated by (INL 2018):

$$R/B_{Total} = R/B_{DU} + R/B_{EK} \quad (1)$$

The DU release portion （R/B_{DU}）is expressed as:

$$R/B_{DU} = DUF \cdot \frac{3}{X_1} \cdot \left[\coth X_1 - \frac{1}{X_1}\right] \quad (2)$$

where $X_1 = \sqrt{\frac{\lambda}{D_1'}}$

$D_1' = 3 \times 10^{-5} e^{-1.06\times10^5/rT}$ for krypton

$D_1' = 1 \times 10^{-7} e^{-7.86\times10^4/rT}$ for xenon

r is the gas constant (8.314 J/(mol-K))

T is the matrix temperature (K)

Similarly, the EK release portion (R/B_{EK}) is expressed as:

$$R/B_{EK} = EKF \cdot \frac{3}{X_2} \cdot \left[\coth X_2 - \frac{1}{X_2}\right] \quad (3)$$

where $X_2 = \sqrt{\frac{\lambda}{D_2'}}$

$$D_2' = \left(\frac{500}{d_k}\right)^2 \times 10^p$$

d_k is the kernel diameter (= 425.8 μm for AGR-5/6/7 kernels);

p is a function of kernel temperature in (K), which was derived experimentally as:

$p = -7.97 - \frac{1920}{T}$ if T < 1137K

$p = -2.6 - \frac{8220}{T}$ if T > 1137K

A DU release factor for this PARFUME-German model can be derived as the ratio between R/B_{DU} and R/B_{EK} when the EK and DU fractions are equal as:

$$F_{DU\_release} = \frac{R/B_{DU}}{R/B_{EK}} = \sqrt{\frac{D_2'}{D_1'}} \cdot \frac{\coth X_1 - \frac{1}{X_1}}{\coth X_2 - \frac{1}{X_2}} \quad (4)$$

According to Eq. 4, the DU release factor is a function of kernel diameter and temperature. The DU release factors are different for krypton and xenon elements, but not for individual isotopes. In general, the PARFUME-German DU release factors in Figure 11 are significantly less than the AGR-1/AGR-4 based DU factor (6.1 ±3.5 for krypton and 4.0 ±2.4 for xenon). The PARFUME-German DU release factors are mostly < 1 (average of 0.86 for krypton and 0.23 for xenon for temperature range of 800 to

1500 °C). This contradicts the conventional understanding that DU releases a higher fraction of fission products compared to a solid spherical kernel with the same amount of uranium.

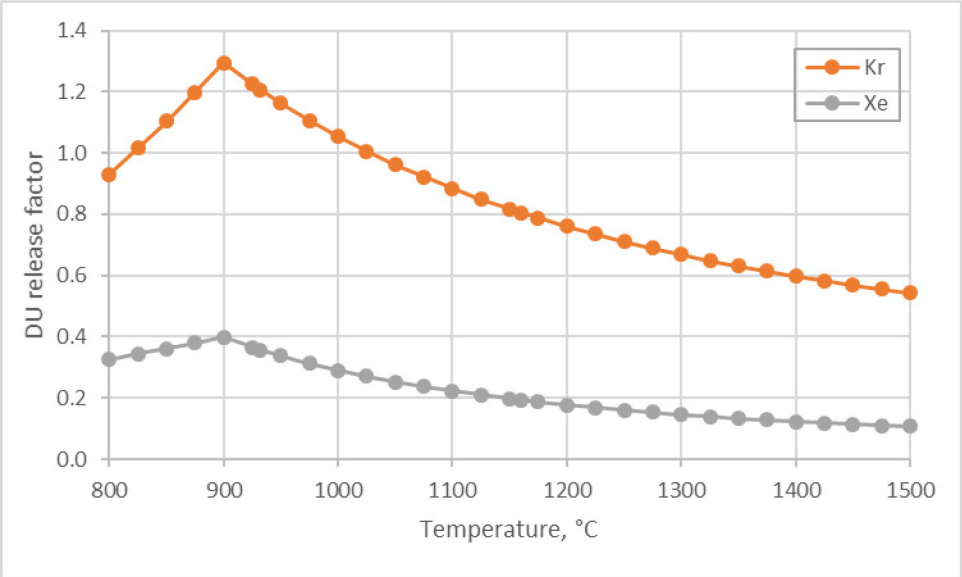

Figure 11. DU release factors based on the PARFUME-German model and kernel diameter of AGR-5/6/7 fuel.

For krypton isotopes, the PARFUME-German model predicted quite well the AGR-5/6/7 R/B values: slightly underpredicted Capsules 2 and 4 R/Bs, and slightly over-predicted Capsules 1, 3, and 5 R/Bs (Figure 12). However, this model overpredicted R/B per capsule values for xenon isotopes in all capsules (Figure 13).

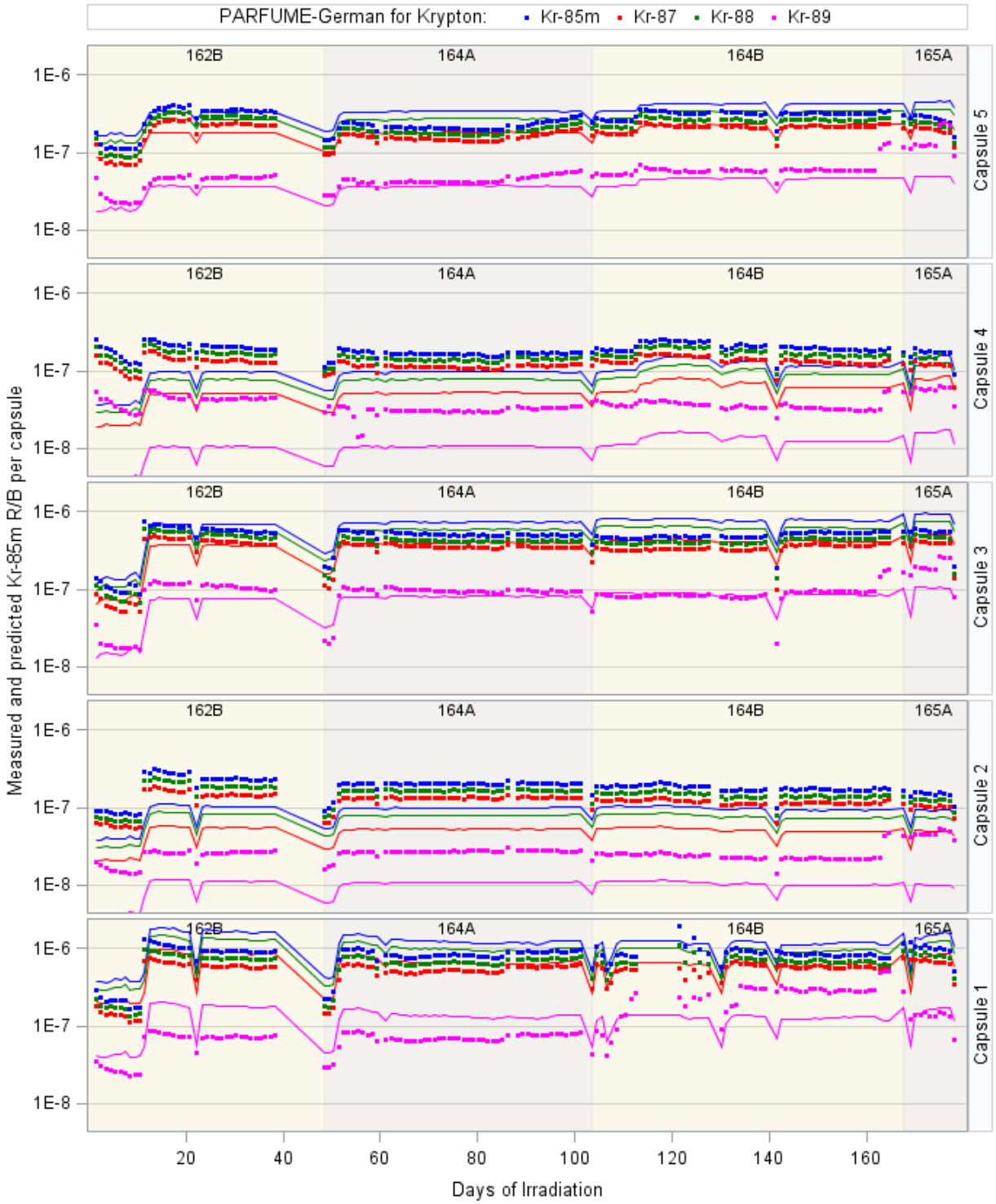

Figure 12. AGR-5/6/7 measured (dots) and PARFUME-German-model predicted (lines) R/B per capsules for krypton during the first five cycles excluding the short low-temperature PALM Cycle 163A.

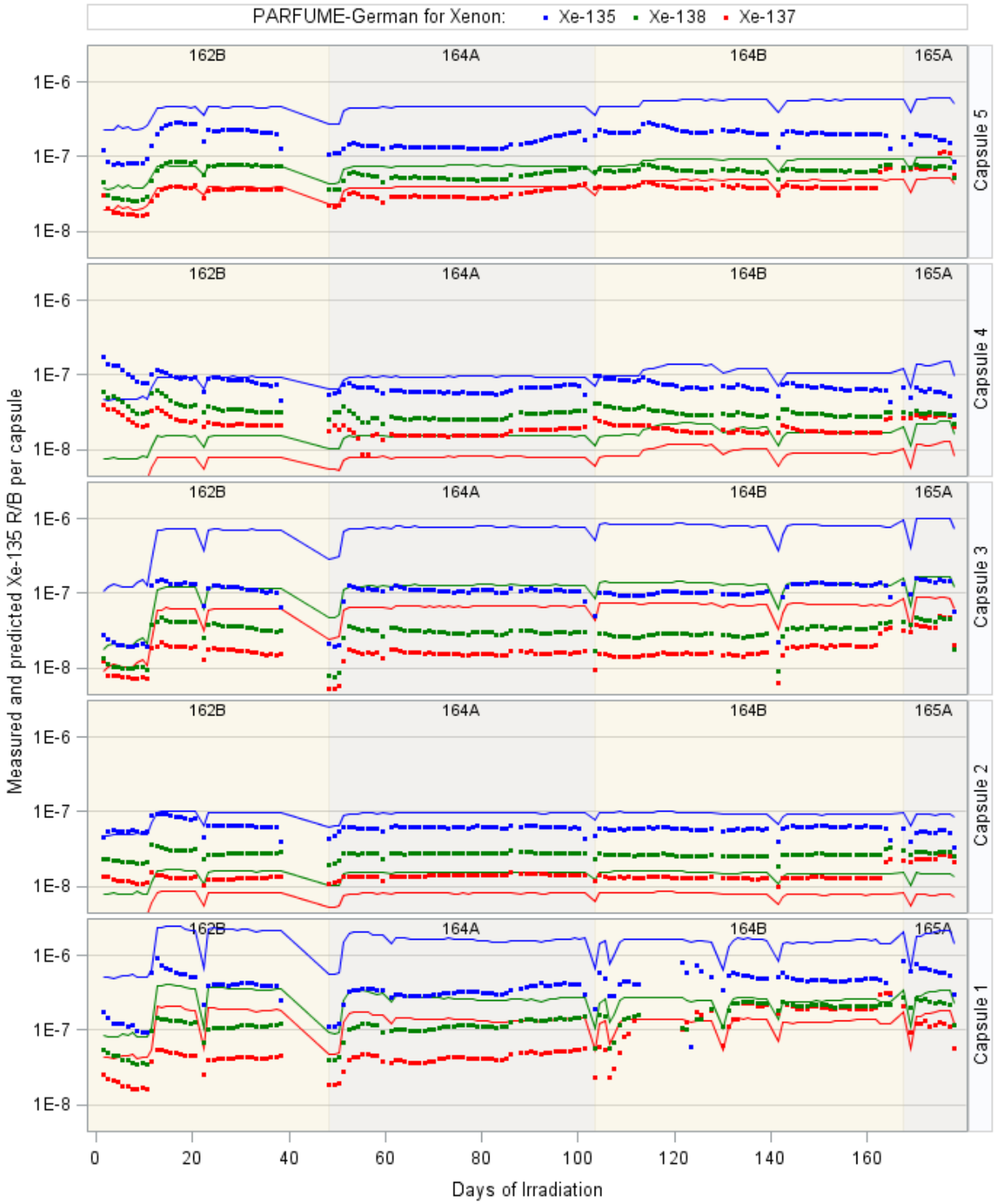

Figure 13. AGR-5/6/7 measured (dots) and PARFUME-German-model predicted (lines) R/B per capsules for krypton during the first five cycles excluding the short low-temperature PALM Cycle 163A.

3.3 Comparison of Measured R/B to AGR Model Predictions

The AGR model, comprised of the R/B per-exposed-kernel model established using the AGR-3/4 R/B data and the DU release factors based on AGR-1 R/B data, have been used to predict FG release from particle failures and DU contamination. The model is described below, followed by its application to data from AGR-5/6/7.

3.3.1 R/B per-exposed-kernel Model

The R/B per-exposed-kernel is a property of the TRISO fuel design and can be used to assess FG releases from postulated particle failures in the reactor. The R/B per-exposed-kernel is also commonly used to compare release rates between different irradiation tests to eliminate differences in number of particle failures. A fission-gas release model for R/B per-exposed-kernel can be derived from decay correlations for transport of fission-produced atoms of noble gases born in the kernel of fuel particles through the surrounding materials—the fuel kernel, coating layers, and compact matrix. The form of the regression model of R/B per-exposed-kernel for krypton and xenon isotopes as a function of decay constant and temperature is (Pham et al 2019):

$$\ln R_p = n \ln \frac{1}{\lambda} + \frac{B}{T} + C \quad (5)$$

where n is a coefficient ranging between 0.1 and 0.5, depending on the effect of the particle coatings on release; λ is the isotope-specific decay constant; B is a fuel-particle-specific constant representing diffusion coefficient dependence on temperature, and C is an irradiation-specific constant. The parameter n reflects the impact of the decay constant term and can be estimated for each day from the R_P of different isotopes to test whether it is similar for different experiments. The average values of n for krypton and xenon isotopes for the five AGR-5/6/7 capsules during the first fine cycles (Figure 14) are 0.318 for krypton and 0.312 for xenon isotopes. These values are very close to the AGR-3/4 average values of 0.325 and 0.302, respectively, indicating consistency of the effect of the particle coatings for AGR-3/4 and AGR-5/6/7 fuel. Also, the n values are steady over time, indicating no significant burnup influence on FG release. The exception was for Capsule 1 stating from Cycle 164B when n-values were notably lower, coinciding with the low gas flow implemented due to the inlet gas pressure issue.

For AGR-3/4 capsules, particle failures (in the form of EKs) were expected due to the inclusion of DTF particles; these particle failures were counted during irradiation. Thus, R/B data measured from each capsule were used to establish the relationship of R/B per-exposed-kernel as a function of the isotope-decay constant and fuel temperature for krypton and for xenon isotopes. A regression analysis was performed using R/B data from the AGR-3/4 irradiation to optimally estimate the parameters n, B, and C in Eq. 5 for the krypton and xenon isotopes. These regression results, obtained using reciprocal fuel temperature in degrees Kelvin and decay constants in s^{-1}, are presented in Table 6.

Table 6. Parameter estimates using AGR-3/4 R/B per-exposed-kernel.

Isotope	n	B	C
Kr-85m Kr-87 Kr-88	0.325	−8,572	−1.41
Xe-135 Xe-137 Xe-138	0.302	−7,793	−2.73

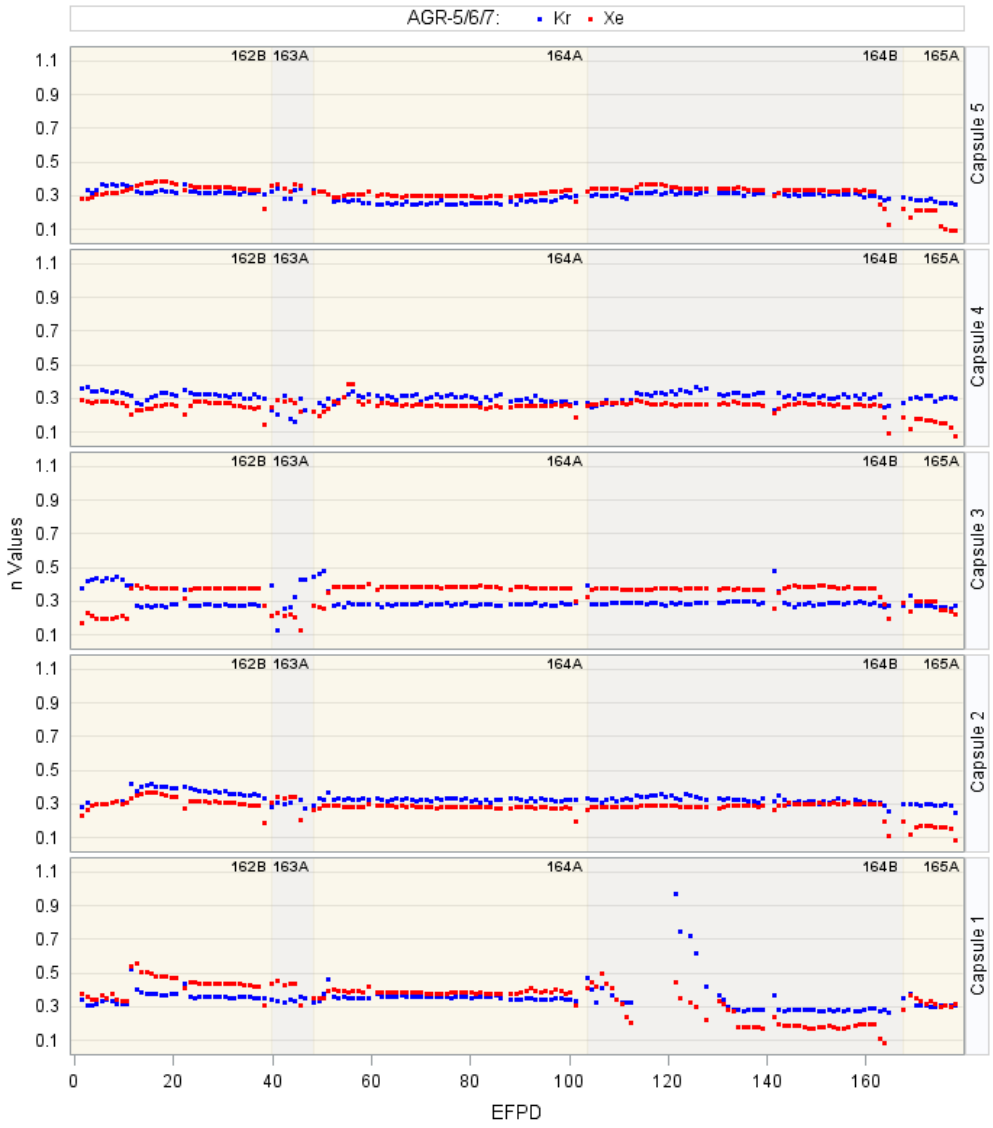

Figure 14. Krypton and xenon *n* values as function of EFPD for AGR-5/6/7 capsules.

3.3.2 Number of Equivalent Exposed Kernels

The number of EK defects and mass of DU in the AGR-5/6/7 capsules was estimated based on the average EK defect number and DU fractions measured during fuel quality control measurements. These values are presented in Table 7, and include prediction intervals at the 68% confidence level, as a measure of the uncertainty of those values. Because the DU and EK amounts represent different statistical distributions with different release rate behavior, they are calculated differently and combined for an effective total number of EK release equivalents.

For EK defects, the mean number of EK defects in each capsule and prediction bounds on that number were calculated assuming a binomial distribution with a defect fraction measured in a sample obtained during fabrication and number of trials equal to the number of particles per capsule (Table 7). The mean is simply the observed defect fraction multiplied by the number of particles in each capsule. Upper and lower prediction bounds on the number of EK defects represent the minimum and maximum number of EKs expected in each capsule, at specified confidence. A 68% confidence lower prediction bound, for example, implies that we can be 68% certain that in a sample size equivalent to the number of

particles in a capsule there will be at least that many defects. The 68% confidence level was used because it is equivalent to confidence level of one standard deviation used for DUF and fuel temperature.

The release rate from DU contamination is several times greater than the release from an EK, on a mass basis. The DU release factor ($F_{DU\_release}$) defines the ratio of release from DU to the release from an EK with the same uranium mass. Based on data from AGR-1, these factors have been estimated as 6.1 for krypton isotopes and 4.0 for xenon isotopes (Pham et al, 2019). Different DU release factors used for krypton and xenon lead to different numbers of release equivalent EKs (Table 7). Assuming the AGR-1 DU is representative of the DU in AGR-5/6/7 fuel in terms of its physical form and behavior, the mean DU, expressed as release equivalent kernels, is the product of the DU fraction (*DUF*), the number of particles in a capsule, and the DU release factor ($F_{DU\_release}$):

$$N_{DU\_EKequivalents} = N_{particle} * DUF * F_{DU\_release} \quad (6)$$

As the DUF is a continuous variable, assumed to have a normal distribution, the standard deviation used for calculation of a DU prediction interval was estimated as one fourth of the range of the provided 95% confidence interval on that parameter (Marshall 2019).

The sum of EK defects and DU in release equivalent kernels is the number of "equivalent EKs" contributing to FG release at the beginning of the experiment, which can be expressed as:

$$N_{EKequivalents} = N_{EK} + N_{DU\_EKequivalents} \quad (7)$$

The 40%-PF fuel compacts had a higher EKF than the 25%-PF compacts. Capsule 1, which contained the 40%-PF compacts and had the most compacts of all the capsules, has the highest number of expected EK defects. Capsule 5, which also contains the 40%-PF compacts, has the second highest expected EKFs. Capsules 2, 3, and 4 – which contain the 25%-PF fuel compacts – are not expected to have any EK defects.

Table 7. Numbers of equivalent EKs calculated from DU and EK fractions.

Capsule	Total Particles	Kernels of Dispersed Uranium [a]	Exposed Kernel Defects [a]	Equivalent Exposed Kernels for Krypton [a]	Equivalent Exposed Kernels for Xenon [a]
Capsule 1	307625	1.52 [± 0.11]	16 [13–21]	25.3 [21.6–31.0]	22.1 [18.6–27.5]
Capsule 2	72480	0.36 [± 0.02]	0 [0–1]	2.2 [2.1–3.3]	1.5 [1.4–2.5]
Capsule 3	54360	0.27 [± 0.02]	0 [0–1]	1.7 [1.6–2.8]	1.1 [1.0–2.2]
Capsule 4	52728	0.26 [± 0.02]	0 [0–1]	1.6 [1.5–2.7]	1.1 [1.0–2.1]
Capsule 5	81432	0.40 [± 0.03]	4 [2–6]	6.5 [4.3–8.6]	5.6 [3.5–7.7]

[a] Estimated mean and 68% prediction interval for number of equivalent EKs due to EK defects and DU.

3.3.3 AGR Model Predictions

Since the number of equivalent EKs in each of the AGR-5/6/7 capsules can be estimated as described in previous section (Table 7), the R/B per capsule contributed from both EK defects and DU contamination can be expressed as:

$$R/B = R_p \cdot \frac{N_{EKequivalents}}{N_{particles}} \quad (8)$$

In general, the AGR model slightly underpredicted the AGR-5/6/7 R/B per capsule values for capsules with lower fuel temperatures (i.e., 2, 4, and 5) but fit quite well with higher temperature Capsule 1 R/Bs and overpredicted R/Bs in the highest temperature Capsule 3 for both krypton and xenon isotopes (Figure 15 and Figure 16, respectively). Although the estimated number of EK defects was zero for the three middle capsules (2, 3, and 4) as shown in Table 7, excessive overprediction of Capsule 3 R/Bs strongly suggested that no EK defects existed in Capsule 3 while underprediction of Capsules 2 and 4 R/Bs would increase the possibility of one EK defect in these capsules. Also, the AGR over-predictions might indicate that the AGR-1 DU factor could be too high for the high fuel temperatures in Capsule 3.

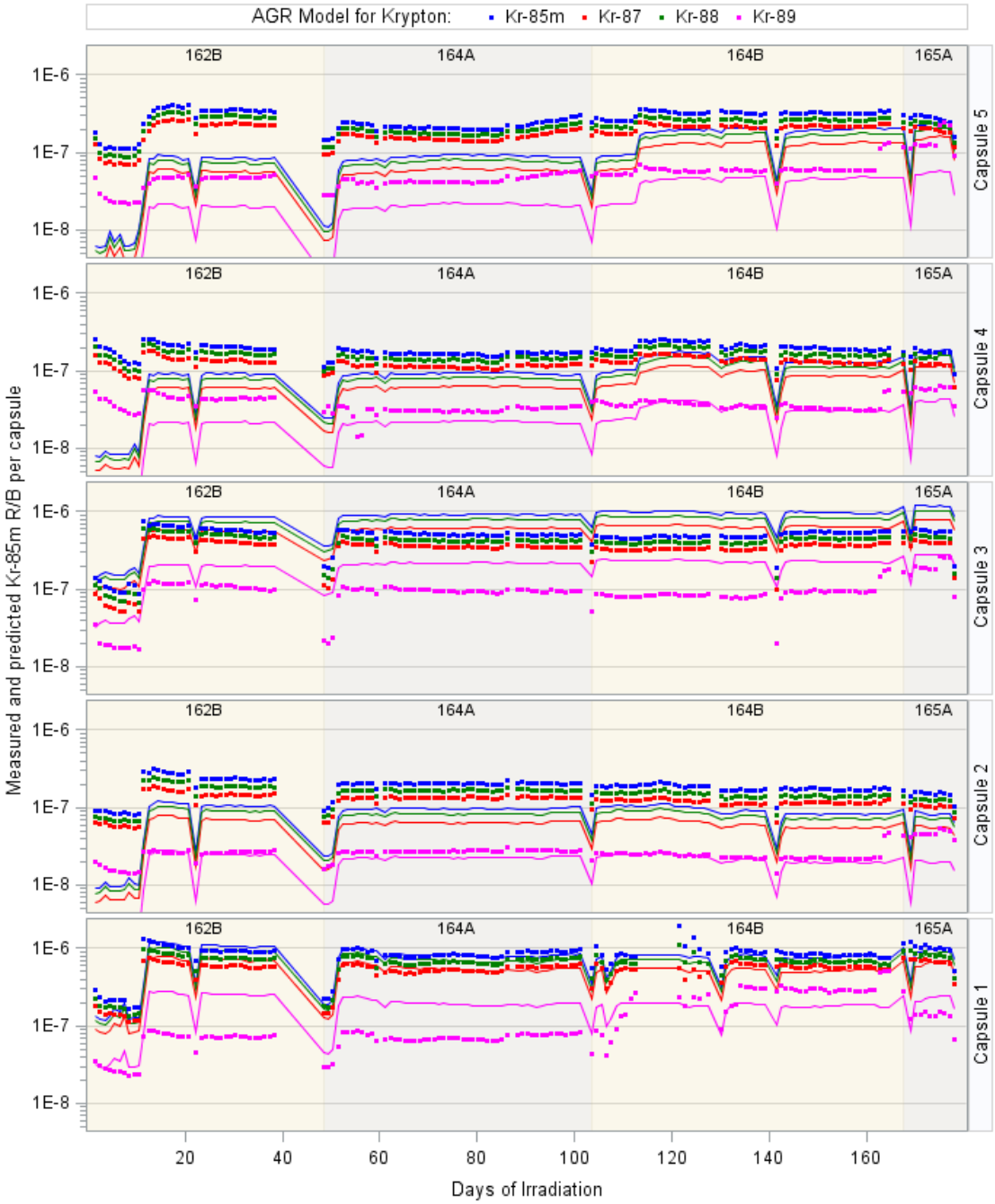

Figure 15. AGR-5/6/7 Measured (dots) and AGR-model predicted (lines) R/B per capsules values for krypton during the first five cycles excluding the short low-temperature PALM Cycle 163A.

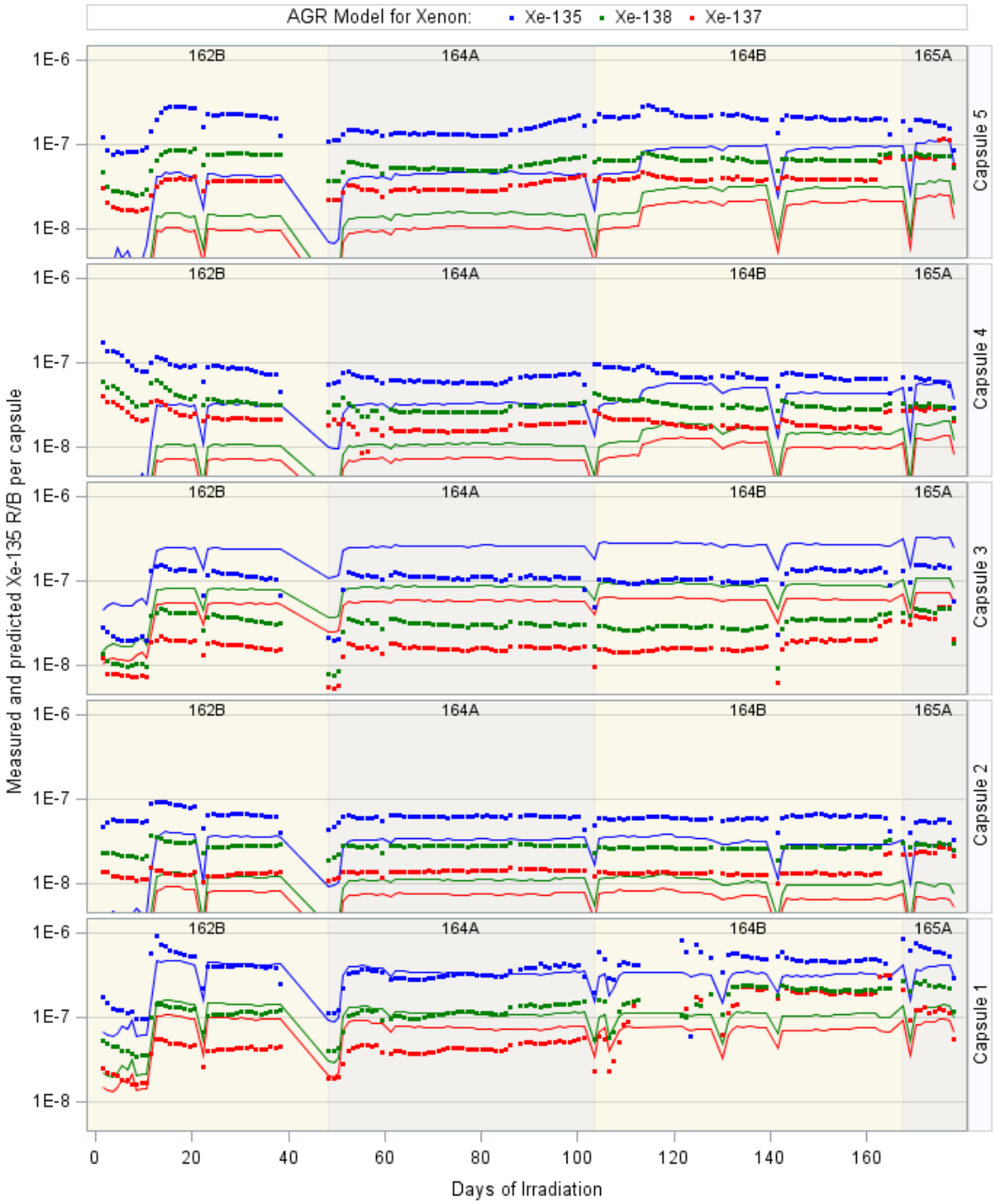

Figure 16. AGR-5/6/7 Measured (dots) and AGR-model predicted (lines) R/B per capsules values for xenon during the first five cycles excluding the short low-temperature PALM Cycle 163A.

3.4 PARFUME-German Model versus AGR Model in Predicting AGR-5/6/7 Release-to-Birth Ratios

The model-predicted R/B per capsule are compared with the measured R/B from AGR-5/6/7 capsules for Kr-85m and for Xe-135 in Figure 17 and Figure 18, respectively. To provide a measure of the uncertainty of those model-based calculations, due to the uncertainty of the EKF and DUF (heretofore referred to as defect fraction uncertainty), the effect of 68% prediction bounds on those values in the models are shown as shaded bands around the curve representing their mean. Note that these uncertainty bands are primarily intended to illustrate the sensitivity of the model values to uncertainties in EK fractions; they do not represent the total uncertainty of the model predictions, which is quite large for the AGR-3/4 model (Pham et al. 2019). Comparisons of model-predicted R/Bs, including the effects of defect fraction uncertainties, with measured R/Bs for each capsule suggests the following:

- For all capsules, uncertainty bands of predictions due to EKF and DUF uncertainties are smaller for the AGR model than for the PARFUME-German model. Capsules 2, 3, and 4, where numbers of EK defects from the EKF mean and lower 90% confidence were rounded to zero for AGR model while the PARFUME-German model uses the actual mean EKF and zero lower 90% confidence, which leads to much larger lower bound for PARFUME-German model.
- The PARFUME-German model uses different equations for the reduced diffusion coefficients for krypton vs xenon for release from DU contamination, which might lead to larger uncertainty bands for xenon than for krypton, as seen in values for the middle capsules (2, 3, and 4).
- Capsules 1 and 5 (40%-PF fuel) have smaller uncertainty bands than the three capsules containing 25%-PF fuel. This could be explained by the smaller relative EKF uncertainty of the 40%-PF fuel compacts.

In general, the AGR-model predictions are lower than the PARFUME-German model predictions, especially for capsules with lower fuel temperatures. Specifically:

- For Capsule 1, with the widest range of temperatures, the measured R/B per capsule are matched well with the AGR predictions (they are close to the predicted values and stayed within the defect fraction uncertainty bands) and are lower than the PARFUME-German predictions (they are on the bottom half of the defect fraction uncertainty bands) for both Kr-85m and Xe-135. The PARFUME-German model produces relatively high R/B for EKs – relative to the AGR model, and this may explain its overprediction of R/B per capsule, especially for Xe-135 isotope.
- For the low-temperature Capsules 2 and 4, each with zero EK defects (Table 7), the AGR-model and PARFUME-German models provide virtually identical results for Kr-85m, and are lower than the measured R/Bs for that isotope (Figure 17). However, the AGR model underpredicted and the PARFUME-German model overpredicted measured R/B per capsule for Xe-135 (Figure 18) with measured R/Bs laid in between the two models' predictions and stayed inside the uncertainty bounds. For the low-temperature Capsule 5, the measured R/B per capsule data are also right in the middle between the PARFUME-German-model predictions (red lines) and the AGR-model predictions (green lines) for both krypton and xenon isotopes.
- For the high-temperature Capsule 3, the measured R/B per capsule are significantly lower than both the PARFUME-German and AGR predictions for both Kr-85m and Xe-135. However, Capsule 3 R/B data are still within the large defect fraction uncertainty bands of the PARFUME-German predictions, but well outside of narrower uncertainty bands of the AGR model.

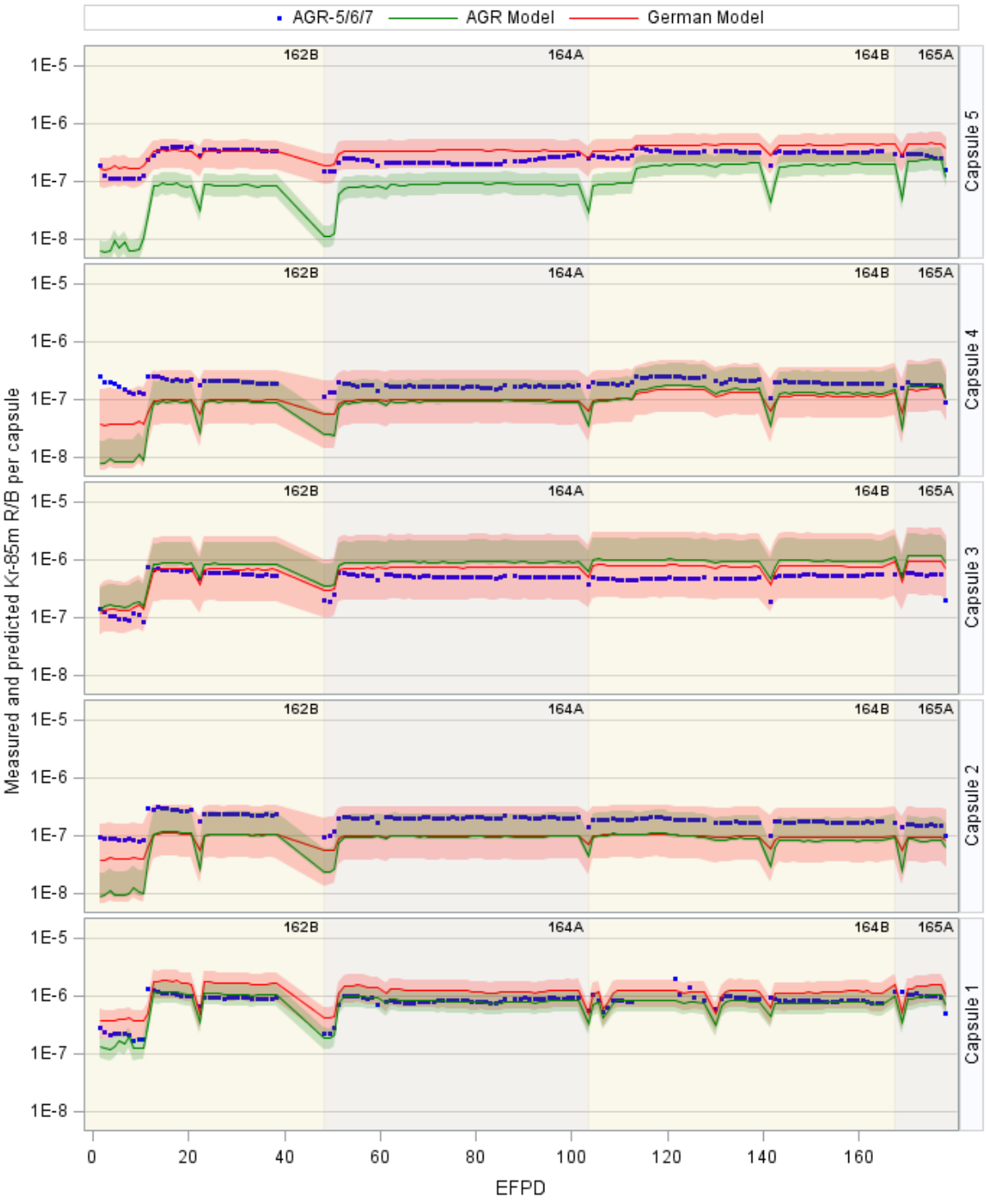

Figure 17. AGR-5/6/7 measured (blue dots), PARFUME-German-model predicted (red lines), and AGR-model predicted (green lines) R/B per capsule for Kr-85m. The shaded areas represent uncertainty band of model predictions due to the 90% lower and upper confidence limits for EKF and DUF.

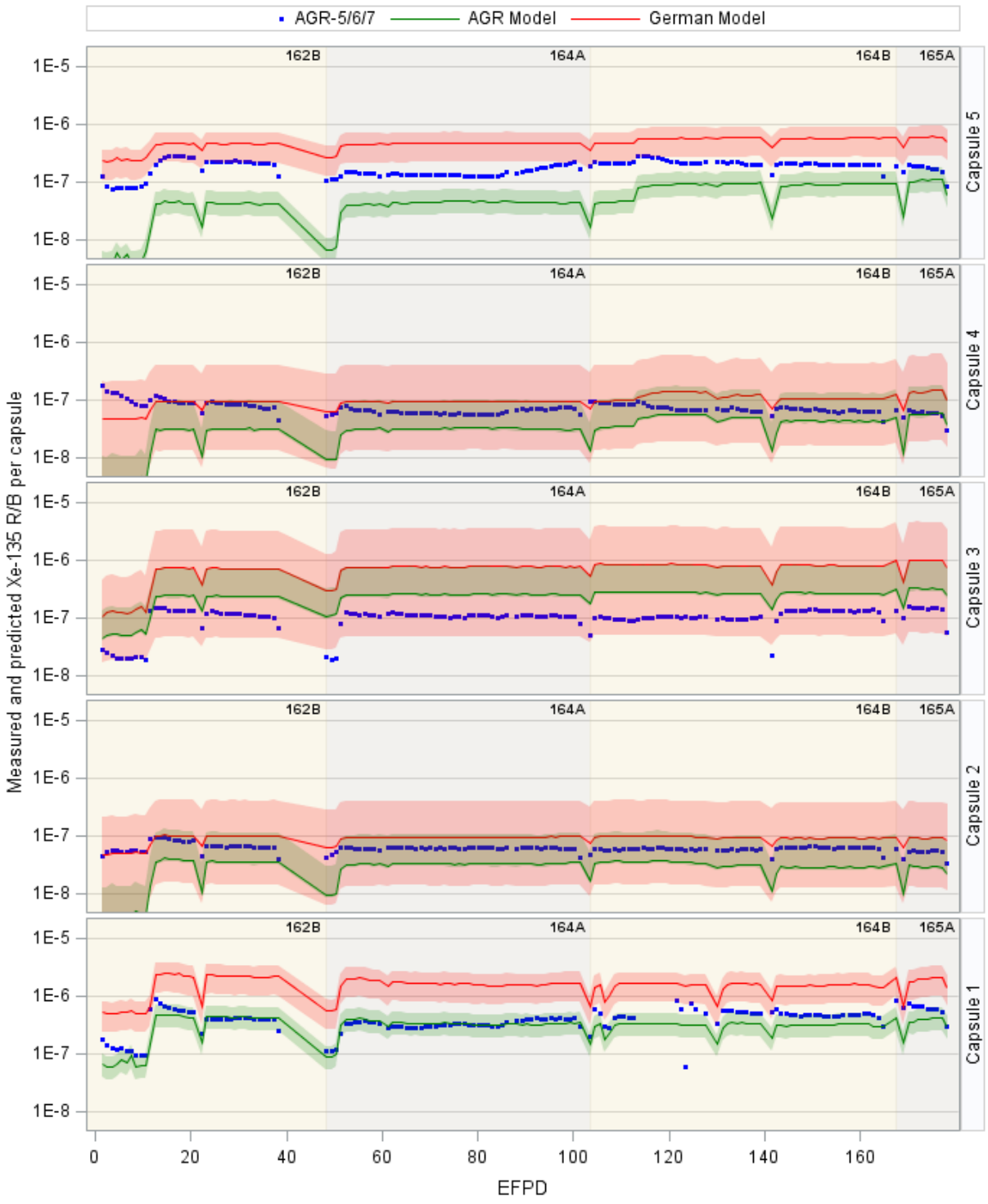

Figure 18. AGR-5/6/7 measured (blue dots), PARFUME-German-model predicted (red lines), and AGR-model predicted (green lines) R/B per capsule for Xe-135. The shaded areas represent uncertainty band of model predictions due to the 90% lower and upper confidence limits for EKF and DUF.

3.5 AGR-5/6/7 R/B per-Exposed-Kernel

3.5.1 Release-to-Birth Ratio per Exposed Kernel Calculation

The performance of a nuclear fuel test is typically evaluated using R/Bs that compare the released activity (R) of a certain isotope from the fuel to the predicted activity of the isotope in the fuel due to irradiation conditions (i.e., birth activity [B]). The R/B per-exposed-kernel (R_p) is the ratio between release rate (R_1) and birth rate (B_1) from one EK as:

$$R_p = R_1/B_1 \tag{9}$$

For each AGR capsule, the activity of the outflow gas stream, measured by the FPMS, was corrected for decay during transport, and converted to isotope atoms per second. The measured R/B values used in this analysis are the capsule-average R/Bs (Scates 2021) and calculated as:

$$R/B = R/[N_{particle} * B_1] \tag{10}$$

Then, the capsule release rate can be expressed as:

$$R = [R/B] * N_{particle} * B_1. \tag{11}$$

Without in-pile particle failures, the FG release from a capsule originated exclusively from EK defects and DU contamination as number of equivalent EKs (Table 7). Thus, R/B per-exposed-kernel can be estimated as the ratio of the capsule release rate and the birth rate from the number of equivalent EKs. That formula is expressed as follows:

$$R_p = \frac{R}{N_{EKequivalents} * B_1} \tag{12}$$

Applying Eq. 5 to Eq. 6, the formula for the R/B per-exposed-kernel can be rewritten as:

$$R_p = \frac{[R/B] \times N_{particle}}{N_{EKequivalents}} \tag{13}$$

The R/B per-exposed-kernel values for each of the AGR-5/6/7 capsules during the first five cycles are presented in Figure 19 for the krypton isotopes (e.g., Kr-85m, Kr-87, Kr-88, and Kr-89) and Figure 20 for the xenon isotopes (e.g., Xe-133, Xe-135, Xe-135m, Xe-137, and Xe-138). Three isotopes, Kr-90, Xe-131m, and Xe-139, were excluded because of data scatter due to high measurement uncertainty, and the low-power short PALM Cycle 163A data were excluded due to significantly lower fuel temperatures. Notably, R/B per-exposed-kernel values are a few orders of magnitude higher than the measured capsule R/Bs (Figure 7 and Figure 8) because the number of equivalent EKs contributing to capsule release are only a very small fraction of total number of fuel particles. The R/B per-exposed-kernel values are highest for the two high-temperature Capsules 1 and 3, which were higher than 10^{-2} or 1% for several isotopes.

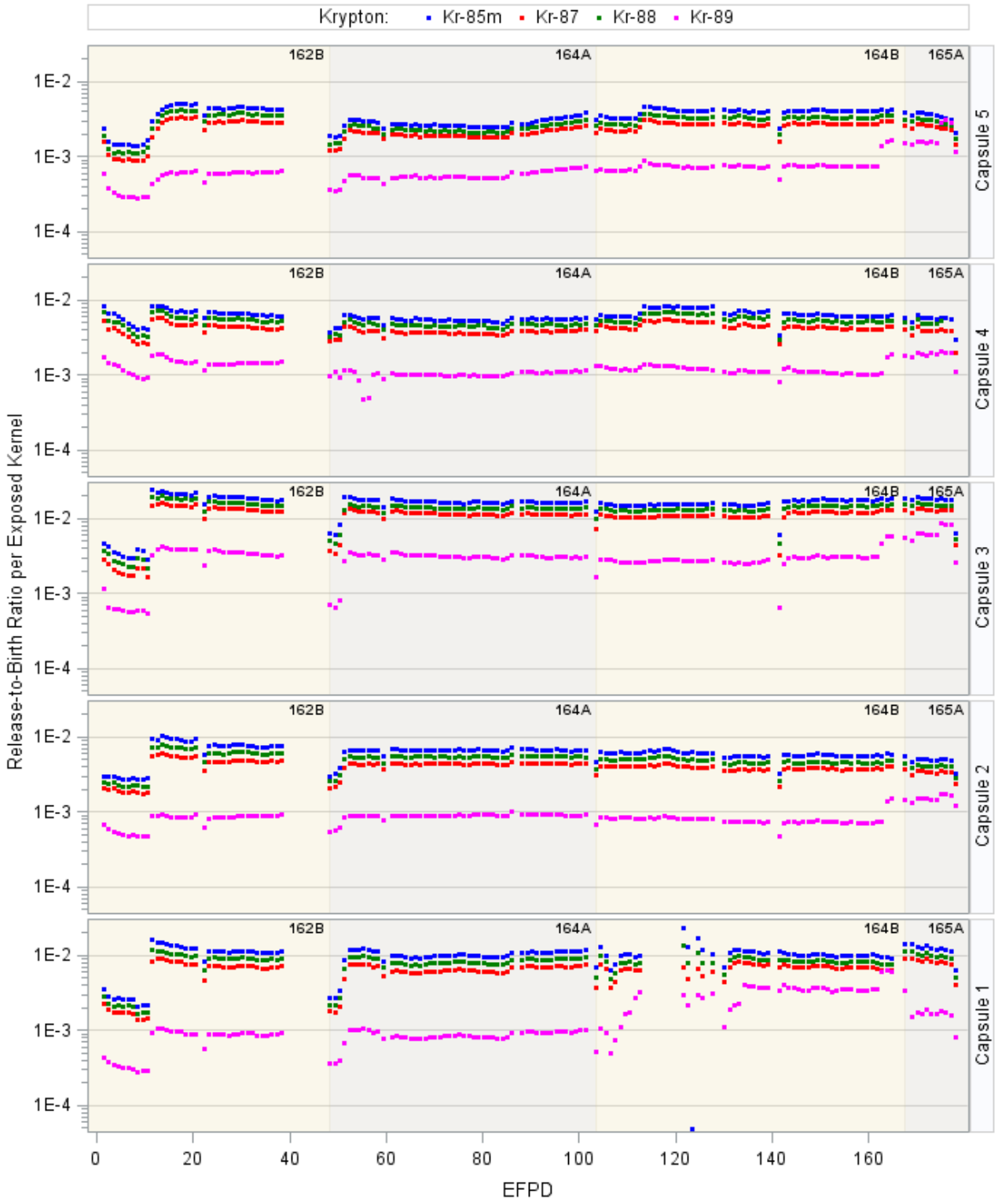

Figure 19. Daily average R/B per-exposed-kernel for krypton isotopes in AGR-5/6/7 capsules.

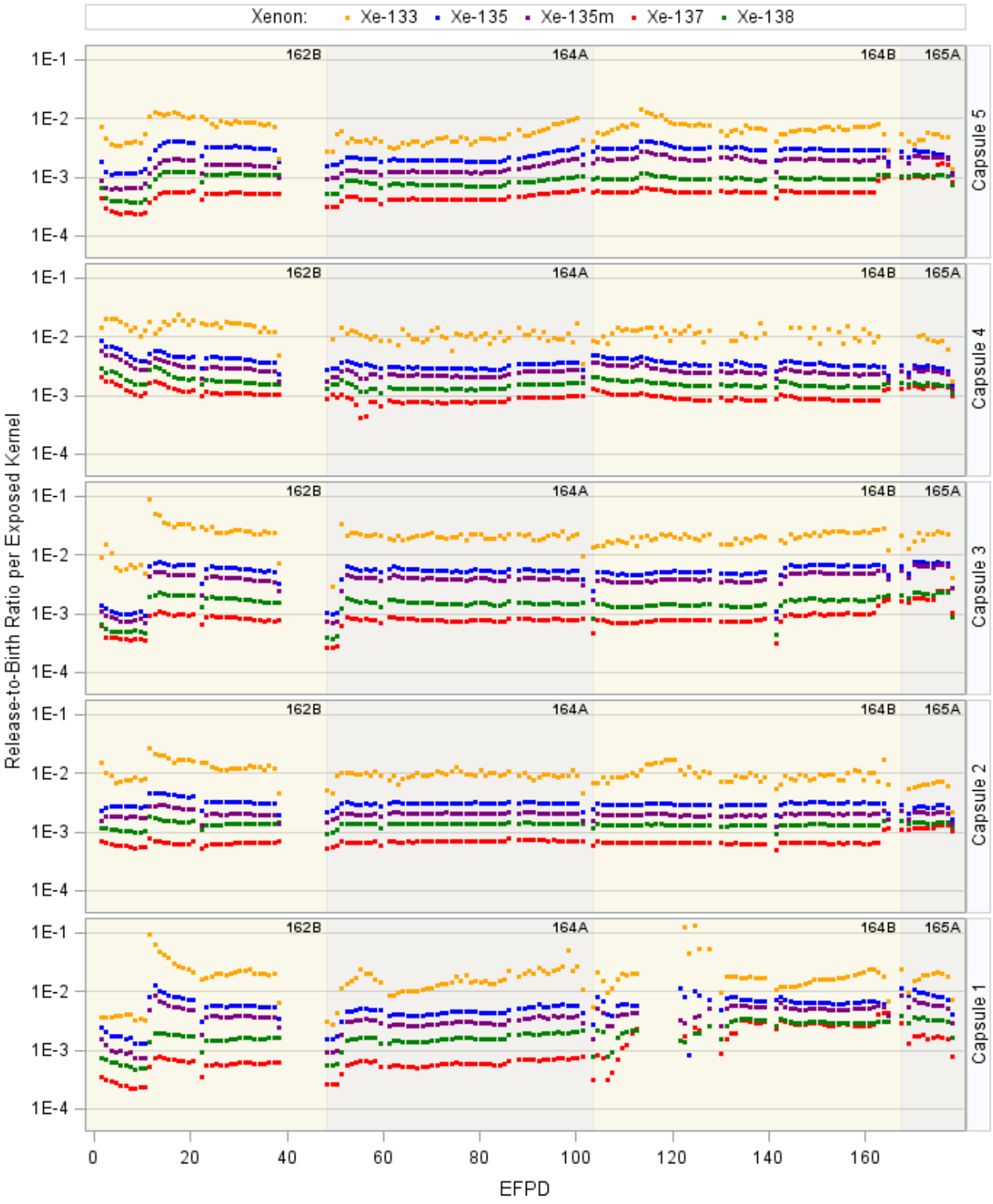

Figure 20. Daily average R/B per-exposed-kernel for xenon isotopes in AGR-5/6/7 capsules.

3.5.2 Comparison of R/B per-Exposed-Kernel with AGR-3/4 Experiment

The R/B per-exposed-kernel can be compared with release rates from the previous irradiation tests and model predictions as a function of fuel temperature and isotope. R/B per-exposed-kernel in the five AGR-5/6/7 capsules are calculated by applying Eq. 5 to daily calculated volume-average fuel temperatures. The constants of Eq. 5, estimated using the AGR-3/4 R/B data, are presented in Table 6. Table 8 contains measured R/B per-exposed-kernel for the selected isotopes values for AGR-5/6/7 as well as values predicted using the AGR-3/4 model. R/B data during partial days of ATR power and low-power Cycle 163A are excluded. For Capsule 1, R/B data during the first 3 weeks of ATR Cycle 164B are also excluded because of issues with flow to the FPMS. Close to 1,0 for the ratio of predicted to measured R/B per-exposed-kernel indicate good model agreement, on average, as shown in detail in Figure 17 and Figure 18.

Table 8. Average measured and predicted R/B per-exposed-kernel for selected krypton and xenon isotopes for four cycles, 162A, 164A, 164B, and 165A.

Isotope	Measured in AGR-5/6/7 Capsules	Predicted by AGR-3/4 Model	Measured to Predicted Ratio
Kr-85m	8.37E-03	9.13E-03	0.92
Kr-87	5.58E-03	6.05E-03	0.92
Kr-88	6.88E-03	7.87E-03	0.87
Xe-135	4.02E-03	4.14E-03	0.97
Xe-137	8.62E-04	9.27E-04	0.93
Xe-138	1.45E-03	1.37E-03	1.06

To assess the influence of temperature on FG release rates obtained from the AGR-5/6/7 test, the measured R/B per-exposed-kernel in the five AGR-5/6/7 capsules are plotted as a function of the reciprocal of temperature side-by-side with the AGR-3/4 data and fitted lines for each isotope (see Figure 21 and Figure 22). The y-axis of R/B per-exposed-kernel is plotted using a natural logarithm of the capsule daily R/B per-exposed-kernel values during most of cycles (excluded the first cycle) for AGR-3/4 and four specified cycles for AGR-5/6/7. Thus, the relationship between R/B and the reciprocal of temperature will be linear for clearer visual presentation of the data trend. The following conclusions can be drawn:

1. On average, the measured R/B per-exposed-kernel are close to the predicted values as the measured to predicted ratios were close to 1 (Table 8).
2. The lower EKF and DUF (Table 5), relative to the data used in the preliminary AGR-5/6/7 R/B report, led to an increase in measured R/B per-exposed-kernel and better match with the model prediction, especially for the highest temperatures in Capsule 3 (reciprocal temperature in the range of 6-6.5, corresponding to temperatures of 1250-1400°C). Notably, there were likely no EK defects in Capsule 3, so all releases are caused by DU; the AGR-1 based DU release factors may be too high for high fuel temperatures as in Capsule 3.
3. The AGR-3/4 model fits best those R/Bs in the middle temperature range seen by Capsule 1 (7.0-8.5 reciprocal temperature range or 900-1150ºC), where measured data lies on both sides of the predicted line.
4. For the lower temperatures seen by Capsules 2, 4, and 5 (> 8.5 reciprocal temperature or less than 900ºC), AGR-5/6/7 R/B per-exposed-kernel values are higher than AGR-3/4 model predictions for

both krypton and xenon isotopes, which is consistent with AGR-3/4 measured R/Bs for this temperature range.

5. The AGR-3/4 capsules did not have any R/B data for reciprocal temperature >9.2 (below 850°C), but the trend of the AGR-5/6/7 R/B data is parallel to that of the AGR-3/4 regression model for R/B per-exposed-kernel in this region.

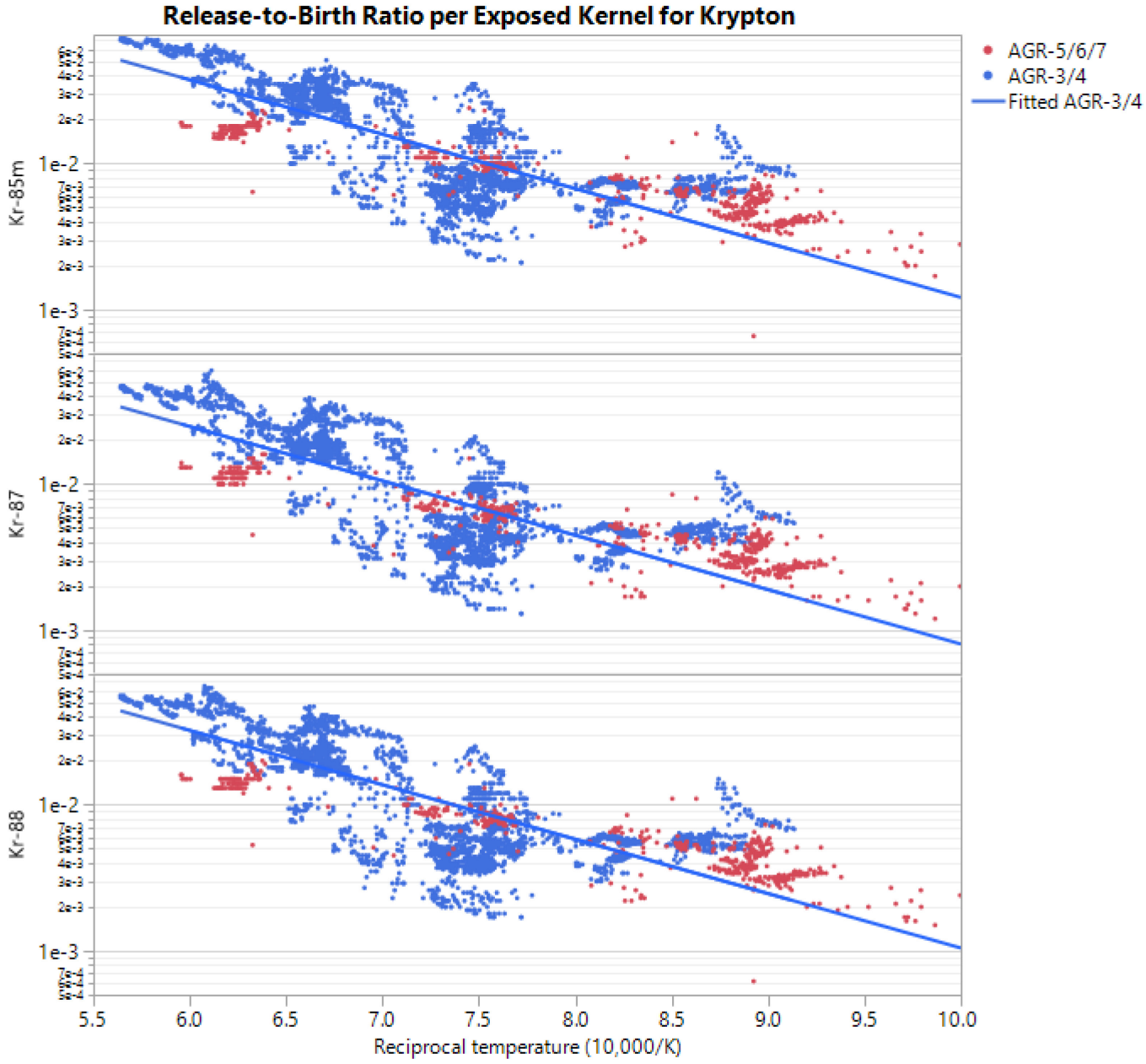

Figure 21. Measured krypton R/B per-exposed-kernel in log scale for the five AGR-5/6/7 capsules during Cycles 162A, 164A, 164B, and 165A in comparison with AGR-3/4 data and the fitted functions of reciprocal temperature.

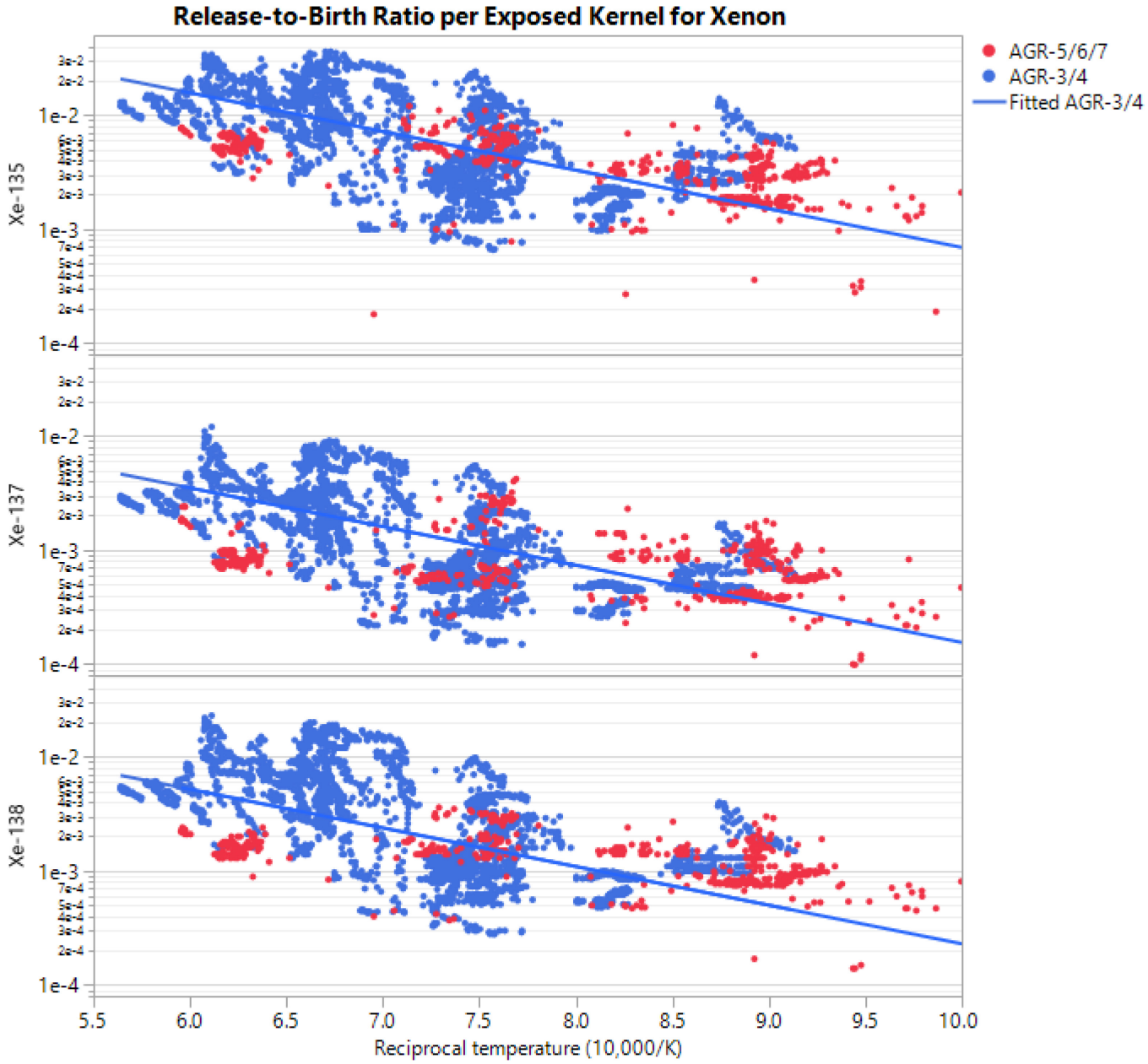

Figure 22. Measured xenon R/B per-exposed-kernel in log scale for the five AGR-5/6/7 capsules during Cycles 162A, 164A, 164B, and 165A in comparison with AGR-3/4 data and the fitted functions of reciprocal temperature.

3.5.3 Comparison of Kr-85m R/B per-Exposed-Kernel with Previous Experiments

As seen in Section 3.3, R/B per-exposed-kernel for the krypton and xenon isotopes behave similarly relative to fuel temperature. For the historical irradiation campaigns, R/B for the Kr-85m isotope is the most commonly available data. For that reason, the detailed comparisons in this section are presented using only R/B for Kr-85m.

In addition to the AGR-3/4 R/B data, several historical irradiation experiments provide R/B per-exposed-kernel data that can be compared with the AGR-5/6/7 R/B per-exposed-kernel data. These

experiments used low-enriched UCO TRISO fuel and either included DTF particles or experienced in-pile failures. The R/B per-exposed-kernel can be calculated only when the number of EKs can be accurately estimated. In many cases, these experiments were injected with moisture at some point during irradiation to study hydrolysis effects on fission-gas release from the UCO kernels. Those perturbations altered R/B, so only the R/B data prior to moisture injection are valuable for comparison here. Table 9 summarizes the R/B per-exposed-kernel data for Kr-85m from four key irradiation campaigns: (1) HRB-17/18 (General Atomics 1987); (2) COMEDIE-BD1 (Richards 1994); (3) HFR-B1 (ORNL 1994); and (4) HRB-21 (DOE 1995). In this table, the corresponding fuel temperatures are the average fuel temperature unless noted otherwise.

Table 9. R/B per-exposed-kernel for Kr-85m from four key historic irradiations.

Experiment	Fuel Temperature (°C)	R/B per-exposed-kernel
HRB-17 and18[a]	840	4.0E-4
COMEDIE	1,160	1.0E-2
HFR-B1 Capsule B[b]	1,140	8.0E-3
	1,015	3.0E-3
	912	2.0E-3
HRB-21[c]	950 (max)/932	9.0E-3
		7.0E-3

[a] Results were identical for two independent capsules run at the same time in different locations in the reactor (General Atomics 1987).

[b] 125°C added to TC temperatures to get fuel temperatures as recommended in the report (see Table 6.4.33 in ORNL 1994).

[c] The first R/B value represents the value for first particle failure (assumed to be at the maximum temperature), and the second value is an average based on the total number of estimated failures (DOE 1995).

AGR-2 R/B per-exposed-kernel data were also included for comparison purposes only. These R/B data come from the four U.S. capsules (i.e., 2, 3, 5, and 6) and during the two cycles, 148A and 148B, before valve failures that made subsequent R/B data unusable. Even though the number of EKs in AGR-2 capsules were not precisely known, based on gross gamma monitoring during irradiation and the initial post-irradiation examination activity, R/B data from AGR-2 capsules were significantly higher than data from the AGR-1 capsules (see Figure 9 and Figure 10), which indicates a possible EK on top of the high DU fraction. Therefore, assuming one equivalent EK for the uranium dioxide (UO_2) Capsule 3 (due to DU) and 2.5 equivalent EKs (one EK defect and 1.5 equivalent EK due to DU) for the three UCO capsules (i.e., 2, 5, and 6), AGR-2 R/B per-exposed-kernel can be estimated for comparison purposes.

For comparison, R/B per-exposed-kernel data from AGR-5/6/7 capsules are plotted together with data from previous experiments (see Figure 23). The 95% confident limits of the AGR-3/4 regression model predictions (blue-shaded area) are included to illustrate the wide variation of the release rate at a given fuel temperature. The following observations are made:

1. *Comparison with AGR-3/4 data (blue dots)*: In general, AGR-5/6/7 R/B per-exposed-kernel data are comparable with AGR-3/4 data as shown in the previous section because R/B per-exposed-kernel data lie inside the 95% prediction bounds for the AGR-3/4 regression model. For the high-temperature AGR-7 Capsule 3 (brown dots), R/B per-exposed-kernel is slightly lower than AGR-3/4 data. These low R/B per-exposed-kernel in Capsule 3 support fabrication data indicating that as-fabricated EK defects did not exist in this capsule. Since FG release in this capsule is, therefore, from DU, this suggests that the AGR-1 based DU release factor could be used for the AGR-5/6/7 fuel.

2. *Comparison with AGR-2 data (orange dots):* AGR-5/6/7 R/B per-exposed-kernel data are also consistent with AGR-2 data (assuming one EK defect in each of AGR-2 capsules) since the data points blend in seamlessly with AGR-3/4 data.
3. *Comparison with historical data (large symbols)*: R/B per-exposed-kernel in the four lower-temperature capsules, AGR-5/6 Capsules 1, 2, 4, and 5 (red dots), are consistent with R/Bs from the three HRB capsules (e.g., 17, 18, and 21) but higher than the COMEDIE and HFR-B1 data. The AGR-5/6 and historical R/B data exhibit similar slopes with respect to the reciprocal temperature, indicating the consistent and strong influence of temperature. In contrast, AGR-7 Capsule 3 had much higher fuel temperatures (i.e., 1200 to 1400ºC) relative to temperatures in historical capsules. Nevertheless, R/B per-exposed-kernel in this capsule (brown dots) were still comparable with the projected R/B level based on historical data.

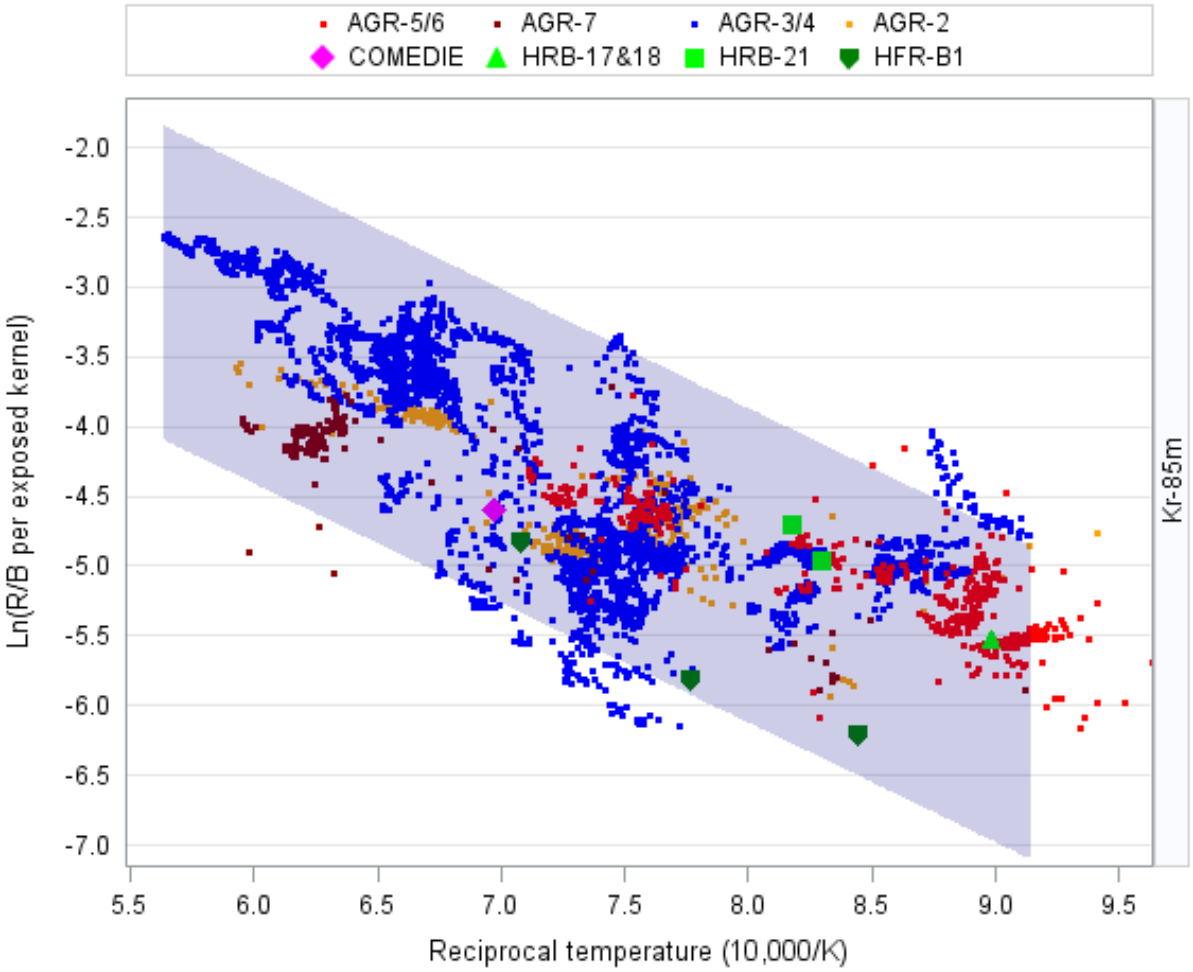

Figure 23. AGR-5/6/7 Kr-85m R/B per-exposed-kernel during Cycles 162B, 164A, 164B, and 165A in comparison with data from previous experiments as functions of reciprocal temperature. The blue shaded area delineates the 95% prediction bounds of the AGR-3/4 regression model.

3.5.4 Comparison of Kr-85m R/B per-Exposed-Kernel to Mechanistic Model Predictions

In addition to the AGR-3/4 regression model (see Eq. 5), there are two commonly used mechanistic models based on the historical irradiations that are used to compare with AGR-5/6/7 R/B data.

Specifically, the German model is discussed in IAEA TECDOC-978 (IAEA 1997) and the model developed by General Atomics (GA) is discussed by Richards (1994). The German model is discussed in Section 3.2, so R/B per-exposed-kernel for the German model is calculated using Eq. 3 as:

$$R_p = R/B_{EK} \qquad \text{where} \quad f_{EK} = 1 \tag{14}$$

The reference GA gas release model (also referred to as the Richards model) is expressed as (EPRI 2003):

$$R_p = \sqrt[3]{\left(\frac{\xi_0}{\lambda}\right)} \cdot \left[A + (1-A) \cdot \exp\left\langle -\frac{E}{R}\left(\frac{1}{T}\right) - \left(\frac{1}{T_0}\right)\right\rangle\right] \cdot [1 + \sigma * Bu^n] \tag{15}$$

where:

ξ_0 is the diffusion parameter for FG element (i.e., krypton or xenon)

Bu is the burnup (%FIMA)

E is the diffusion process activation energy [J/mol]

R is the universal gas constant [8.3143 J/(mol K)]

T is the kernel temperature [K]

A, T_0, σ, n are constants.

The values of the constants must be determined experimentally for each gaseous FG element and for each fuel kernel composition. Eq. 15 is a model for fractional release from UCO microspheres for non-hydrolyzed fuel with model parameters derived for capsule HFR-B1 containing DTF particles. It was concluded that FG release from low-enriched UCO fuel kernel is largely independent of burnup to at least 20% FIMA (General Atomic 2009), which is confirmed by stable R/B during the first four cycles of the AGR-5/6/7 irradiation. This means the last term of burnup in Eq. 15 can be omitted.

The predictions using the Richards model were taken from the previous R/B data analysis report (Pham et al 2019). The German model predictions were calculated for the actual kernel diameter of AGR-5/6/7 fuel particles. The release rates predicted by the German model for the larger diameter kernels from AGR-5/6/7 are lower than the predictions for the smaller diameter kernels from AGR-3/4, as anticipated.

For comparison, measured AGR-5/6/7 R/B per-exposed-kernel are plotted with predictions by the AGR-3/4 regression model and the two mechanistic models (see Figure 24). The 95% prediction bounds for the AGR-3/4 regression model predictions (blue-shaded area) are also included for discussion. The following observations can be made for AGR-5/6/7 R/B data:

1. In general, *AGR-5/6 R/B per-exposed-kernel data* (red dots) are comparable with predictions by AGR-3/4 model for the middle temperature range (1150-950°C) but lie between the AGR-3/4 model and the two historical models for the low temperature range (< 900°C) while AGR-7 R/B data (brown dots) with temperature above 1250°C are lower than all model predictions. However, AGR-5/6/7 R/Bs still stayed within the 95% prediction bounds for the AGR-3/4 model.
2. *For the AGR-3/4 regression model* (blue line): AGR-5/6 R/B per-exposed-kernel data are mostly higher than the AGR-3/4 model predictions for lower temperature range but lower for higher temperature range.
3. *For the Richards model* (green line): R/B per-exposed-kernel predictions by the Richards model lie above the AGR-3/4 model predictions, and the AGR-3/4 regression line is noticeably steeper. The AGR-5/6/7 FG release rates are lower than the model predictions, especially at higher fuel temperatures.

4. *For the German model* (orange piecewise line): R/B per-exposed-kernel predictions by the German model are the highest among the three models. AGR-5/6/7 R/B data are well below the German model predictions.

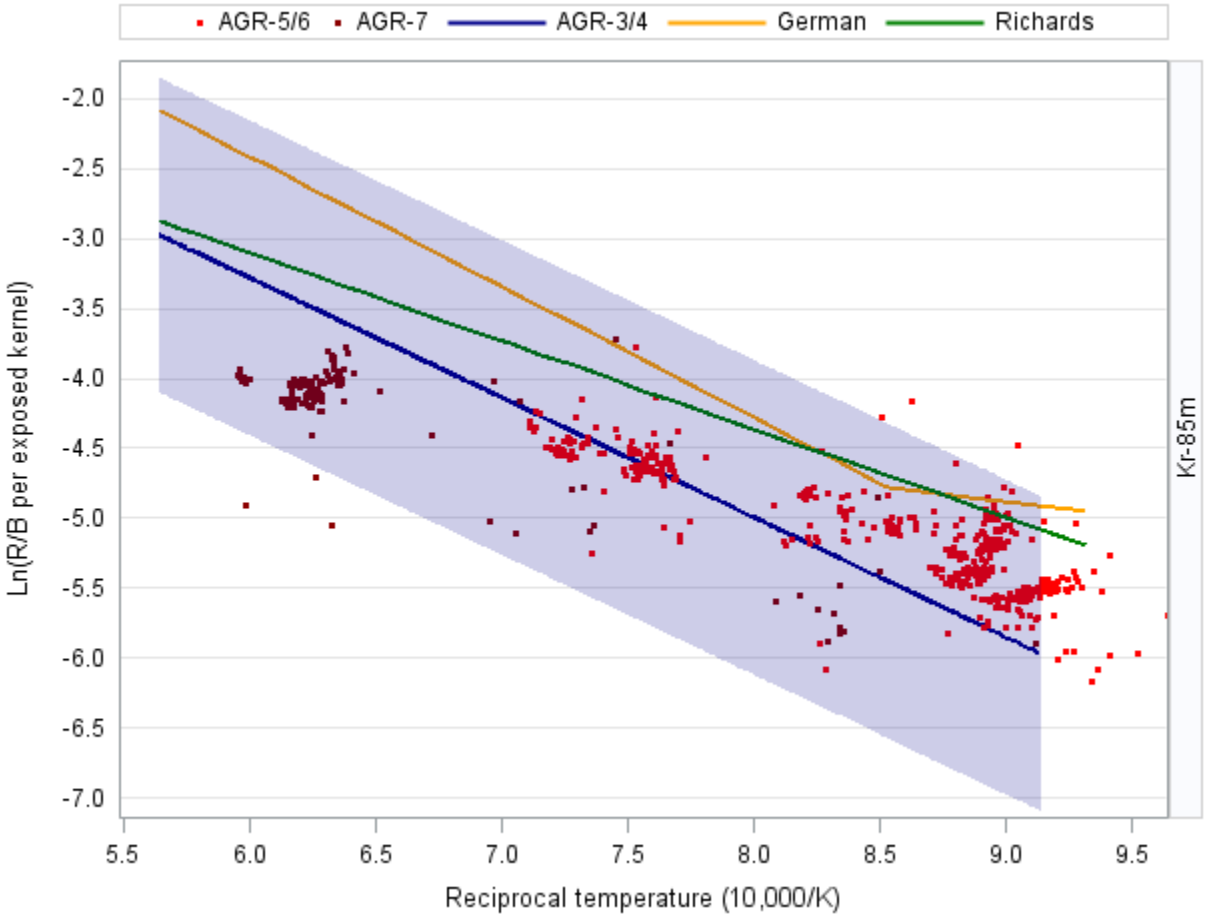

Figure 24. AGR-5/6/7 data comparison to model predictions as function of natural logarithm of Kr-85m R/B per-exposed-kernel versus reciprocal fuel temperature (the blue shaded area denotes the 95% prediction bounds of the AGR-3/4 model).

3.5.5 Combined Kr-85m R/B per-exposed-kernel Data and Model Predictions

The Kr-85m R/B per-exposed-kernel from AGR-5/6/7, AGR-3/4, the four historical irradiations, and predictions by AGR-3/4-based, German, and Richards models are combined in Figure 25. The fact that most of R/B per-exposed-kernel from these irradiation campaigns and the model predictions stay within the 95% prediction bounds (blue shaded area) of the AGR-3/4 fitted line indicates good consistency between the FG release rates from an EK of the TRISO particles.

The extensive variation of the measured release rates at a given fuel temperature indicates several other influential factors on FG release besides decay constant and temperature, which are not captured by these simplified transport models. This could be the reason that the German and Richards models are intentionally conservative, as they tend to predict higher FG release rates.

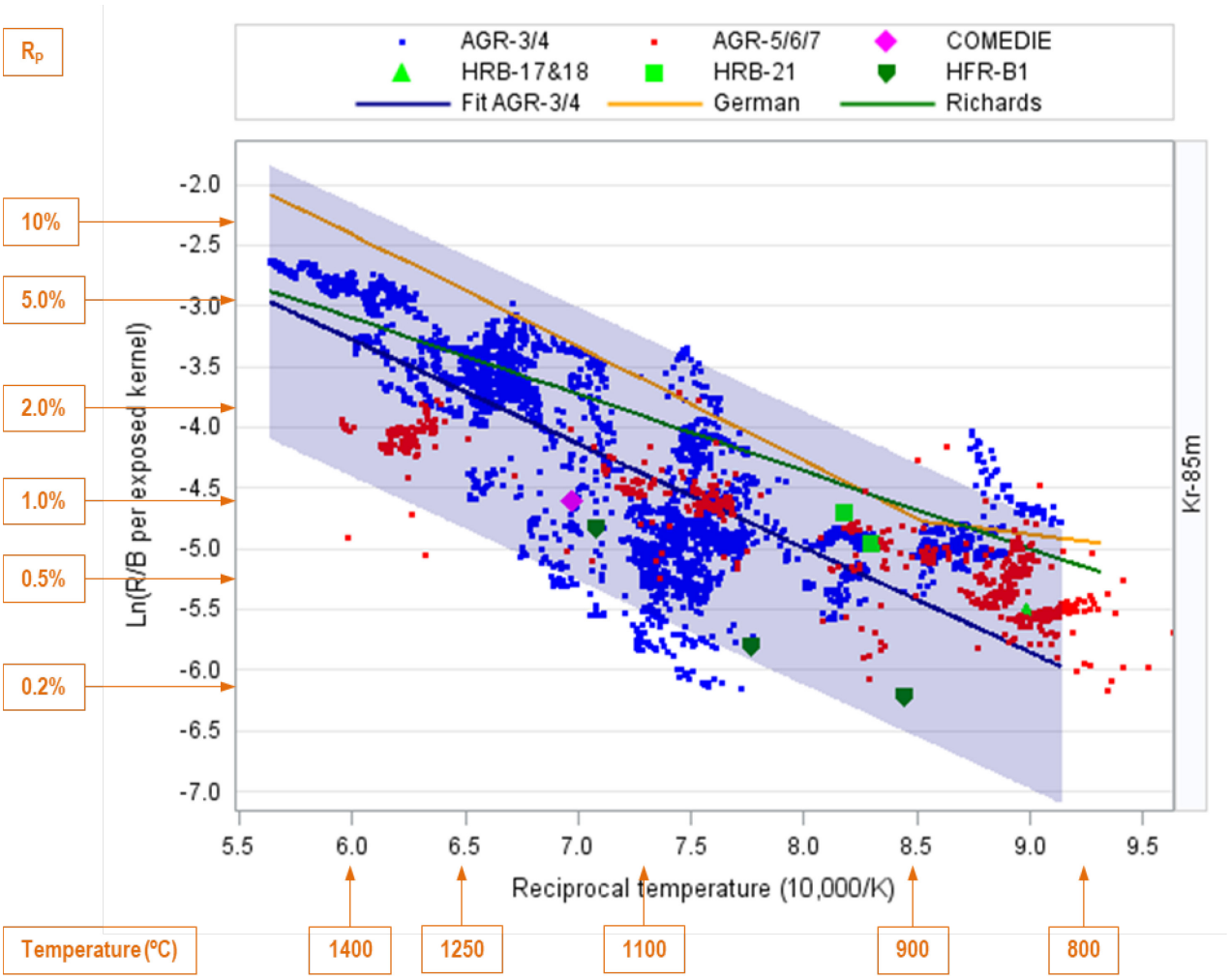

Figure 25. Kr-85m R/B per-exposed-kernel from AGR-5/6/7, AGR-3/4, and historical irradiations plotted together with AGR-3/4-based, German, and Richards's models (the blue shaded area is 95% bounds of the AGR-3/4 fitted line).

4. PARTICLE FAILURE ASSESSMENT FOR AGR-5/6/7 CAPSULES

Particle failure during irradiation is an important metric of fuel irradiation performance. Assessment of failures is founded on the combined evidence based on GG counts from the GG detectors and FG release rates from isotopic measurements made with HPGe spectrometers.

During the first five cycles (162B – 165A), the R/Bs and GG counts were low and stable, which were consistent with the conclusion that there were likely no in-pile particle failures, as detailed in the previous chapter.

Near the end of the sixth cycle (166A), a large number of particle failures occurred in Capsule 1 as indicated by numerous GG spikes accompanied by a consistent increase in GG averages and FG releases. For the other four capsules, minor spikes were synchronized across capsules, which suggests their GG detectors picked up the increased activities in the 1A primary cubicle caused by the substantial increase in FG activities in the Capsule 1 gas line. In addition, FG leakage from Capsule 1 into the leadout gas, and subsequently, into Capsules 2–5 and the through tube slip joints, could also have resulted in increased GG counts for these capsules (Pham et al 2021).

During the last three cycles (166B, 167A, and 168A), the R/Bs and GG count averages increased in all capsules relative to previous cycles, and numerous significant peaks were evident in several capsules while the Capsule 1 gas line was insolated, preventing GG count and FG release measurements for this capsule. Therefore, a more detailed look at the 5-minute GG plots was performed to identify particle failures in Capsules 2–5 (Pham et al 2021). In addition, The R/B data for the short-lived isotopes (Kr-89 and Xe-137), which had acceptable measurement uncertainty and the least impact from Capsule 1 leakage, can still be used for rough estimation of particle failures that can help articulate failure evidence based on GG counts.

4.1 In-pile Failure Evidence Based on Gross Gamma Counts

GG counts were recorded every 3.5 seconds. Daily peak and average GG counts in five capsules and two spare detectors were plotted and used to spot possible in-pile failures manifesting in prominent peaks and a subsequent increase in daily averages that cannot otherwise be explained. In-pile failures were not apparent during the first five cycles (Cycles 162B–165A) and short low-power PALM Cycle 167A based on the low and stable GG counts during these cycles (Figure 26).

Detailed discussion of in-pile particle failure evidence based on GG counts in capsules, reported in the AGR-5/6/7 as-run report (Pham et al 2021), indicated no particle failures likely occurred in Capsules 2–5 during Cycles 166A and 166B, while a large number of in-pile failures occurred in Capsule 1 by the end of Cycle 166A. However, based on typical peak values caused by particle failure apparent in the 5-min peaks and average GG data plots during the last Cycle 168A (Figure 27), several failures likely occurred in Capsules 2 and 3. At the same time, there is no strong evidence that in-pile particle failures occurred in Capsules 4 and 5.

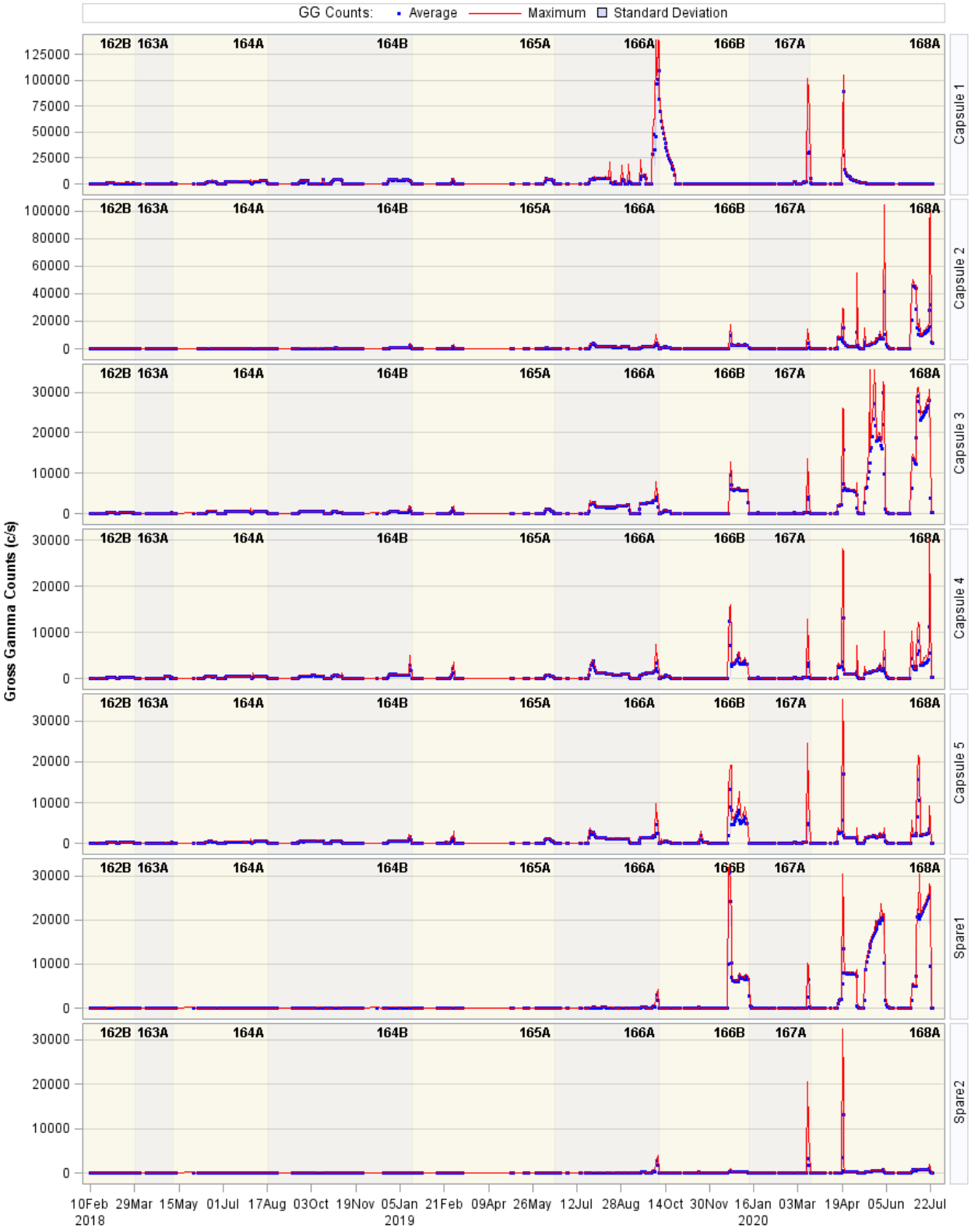

Figure 26. AGR-5/6/7 daily average and maximum GG counts for five capsules and two spare detectors.

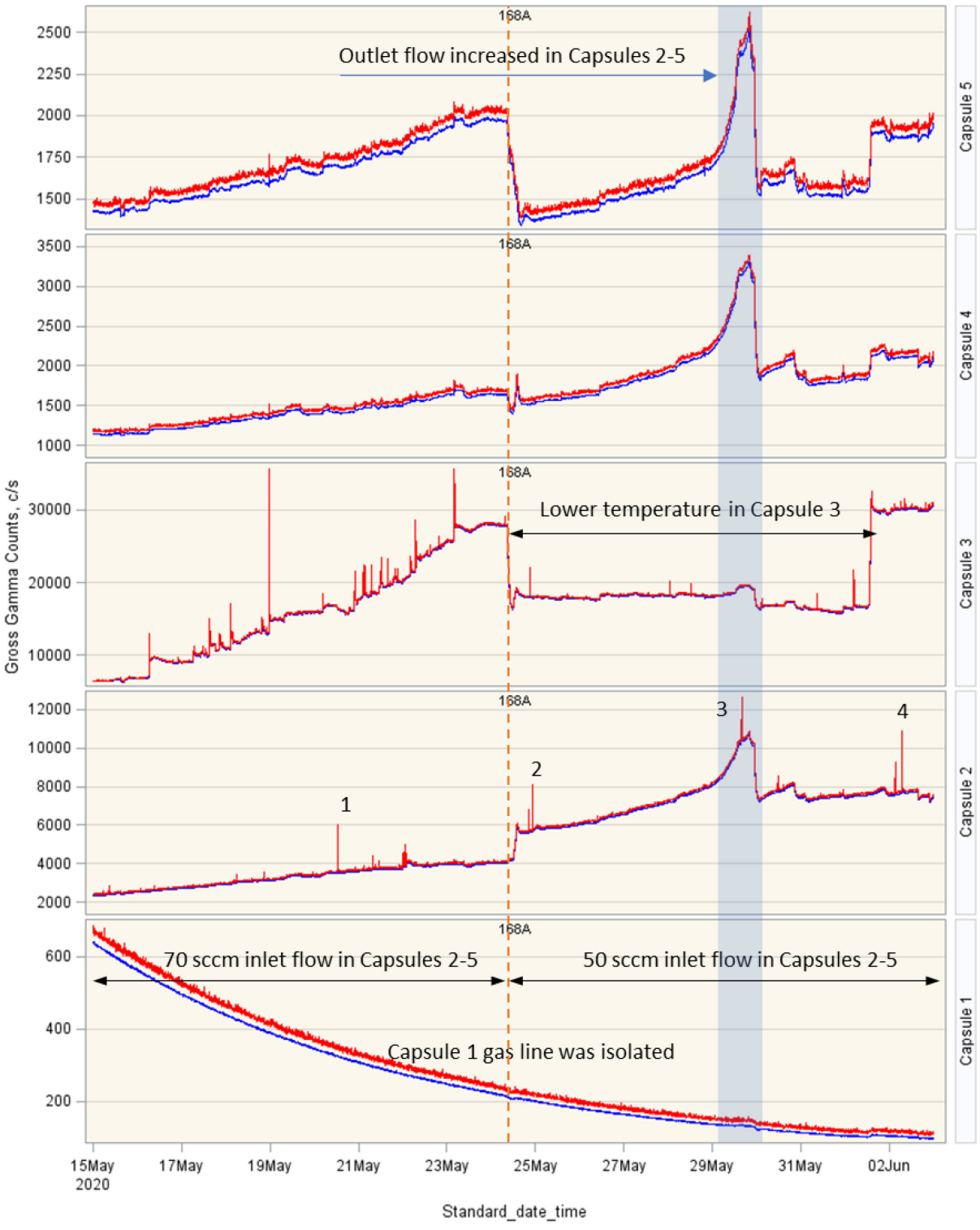

Figure 27. Spikes typically associated with particle failures are observable in Capsules 2 and 3 based on 5-minute peak and average GG counts between May 15 and June 4, 2020 during Cycle 168A.

4.2 In-Pile Particle Failures Based on Release-to-Birth Ratios

Substantial increase in measured R/Bs for certain isotopes in Capsules 2 – 5 during the last three regular cycles relative to the first three regular cycles were produced by in-pile particle failures and/or FG leakage from Capsule 1. This can be seen clearly by comparison between measured and the AGR-model predicted (assuming no in-pile failures) R/B values (Figure 28).

Cycles 162B–164B (the first three regular cycles): The agreement between AGR model predictions and measured R/Bs was similar for all capsules. The model underpredicts R/B for Capsule 5 during the first two cycles when the fuel temperature was relatively low, but the prediction improves during the third cycle, as the temperature increases. The model consistently overpredicts R/B for the high-temperature Capsule 3, where no EK defects are likely. For Capsule 1, measured R/Bs increased from less-than-predicted values—for the first two cycles—to above predicted values during the third cycle (Cycle 164B). A possible explanation for this behavior is an underprediction of Capsule 1 fuel temperature, as described in Section 2.2.1. However, the AGR model based on Kr-85m performed well for Capsule 1 during the first three cycles (Figure 28). The AGR model performed best for Capsule 2 for all four isotopes during these first three regular cycles. The consistency between measured and calculated R/Bs over time suggested no in-pile particles failures occurred during these cycles, in agreement with the conclusions based on the GG counts.

Cycles 166A–168A (the last three regular cycles): The Capsule 1 gas line problem started during Cycle 164B and apparent in-pile failures in that capsule by the end of Cycle 166A led to unstable R/Bs in Capsule 1 during and an absence of data during Cycles 166B and 168A. These events in Capsule 1 led to FG leakage from Capsule 1 through the leadout system into the other capsule gas lines, which resulted in increase of R/Bs in other capsules. Evidence of the leakage effect is seen in the comparison of relative increases in R/B of longer versus shorter-lived isotopes. A substantial increase in R/B of the long-lived Kr-85m occurred in Capsules 2–5 during the last three regular cycles (Figure 28). Increases in the R/B of the two shorter-lived isotopes (Kr-89 and Xe-137), however, were substantially less, especially for the top two capsules (Capsules 4 and 5) located furthest from Capsule 1. This apparent decrease with increasing distance from Capsule 1 suggests decay during transport. This FG leakage from Capsule 1 complicated in-pile failure estimation based on measured R/B data.

Therefore, an in-pile particle failure assessment was accomplished by considering both the evidence from GG data and an AGR model predictions for short-lived FG isotopes (i.e., Kr-89 and Xe-137) that are expected to be least impacted by contamination from Capsule 1.

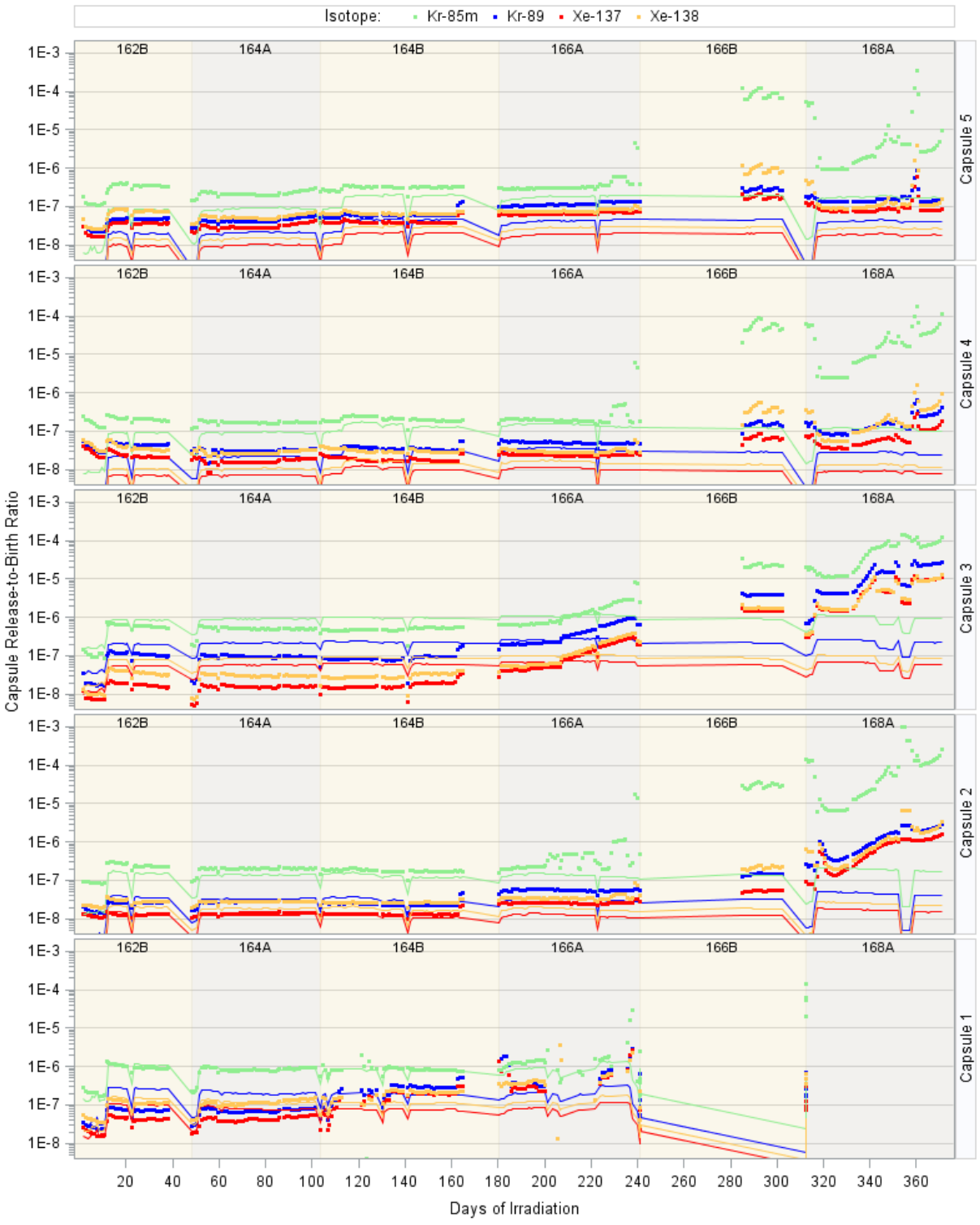

Figure 28. Measured (dots) and predicted (assuming no in-pile failures) capsule R/B for Kr-85m, Kr-89, Xe-137, and Xe-138 isotopes, for all regular cycles.

4.3 In-Pile Particle Failures Assessment

In this section, R/B values for the short-lived isotopes Kr-89 and Xe-137 are used to estimate the number of in-pile particle failures in each capsule. These isotopes were selected because the R/B data for isotopes with much shorter half-lives (<3 minutes) are not stable and have a high measurement uncertainty, and the R/B data for much longer-lived isotopes were likely impacted to a greater extent by the leakage of FG from Capsule 1.

4.3.1 Number of In-pile Particle Failures Prediction and Uncertainty

At the start of the experiment, when no in-pile particle failures had occurred, FG releases stemmed from the EK defects and the DU in the fuel. As the experiment progressed, increases in FG release rates relative to those resulting from EK defects and DU may have been the result of in-pile particle failures if the amount of FG leakage can be deemed insignificant. Given that the R/B per-exposed-kernel (R_p) can be calculated using the AGR-3/4 R/B model (Eq. 5), the number of in-pile particle failures ($N_{failures}$) in each capsule can be expressed as:

$$N_{failures} = \frac{R/B * N_{particles}}{R_p} - N_{EKequivalent} \quad (16)$$

Uncertainty of the estimated number of in-pile failures is associated with uncertainties of the measured R/Bs, number of equivalent EKs, and predicted R/B per-exposed-kernel. The measurement uncertainties of the first two terms were assigned from the FPMS analysis (Table 4 and Table 7). Uncertainty of the predicted R/B per-exposed-kernel is harder to quantify due – in part - to uncertainties in assumptions. For example, particle failures were assumed to occur at maximum temperature locations within the capsule, but the actual location (and thus temperature) was not known.

The AGR model predicting the release from the as-fabricated equivalent EKs has substantial uncertainties associated with the both the initial amount of equivalent EKs (Table 7) and their temperatures (Table 3). To illustrate the sensitivity of the model to these uncertainties, we provide uncertainty bands of model predictions due to one standard deviation for both parameters (Figure 29).

For Capsules 2–4, the upper bound of one standard deviation of EK defects is approximately one, producing a large upper bound on the uncertainty band for R/B, relative to the R/B prediction for the mean number of defects (zero). R/B uncertainty bounds based on one standard deviation of fuel temperature are largest for Capsule 1 because of the large temperature variation in the compacts in that capsule. In general, fuel temperature uncertainty is the dominant factor for Capsule 1 while in other capsules that effect is comparable to that due to the number equivalent EKs. The uncertainty for Capsules 1 and 5 is similar to the others, although they appear narrower due to the larger R/B plotting range.

Because measured R/Bs in Capsule 3 were much lower than the lower bound for predicted R/B based on one standard deviation for equivalent EKs, it is likely that no EK defects existed in Capsule 3. In contrast, since measured R/Bs in Capsules 2 and 4 lie well above the prediction line but within the upper uncertainty bound, it is less likely that zero EK defects existed in Capsules 2 and 4, even though the EK defect fraction in these three capsules (2, 3, and 4) was the same.

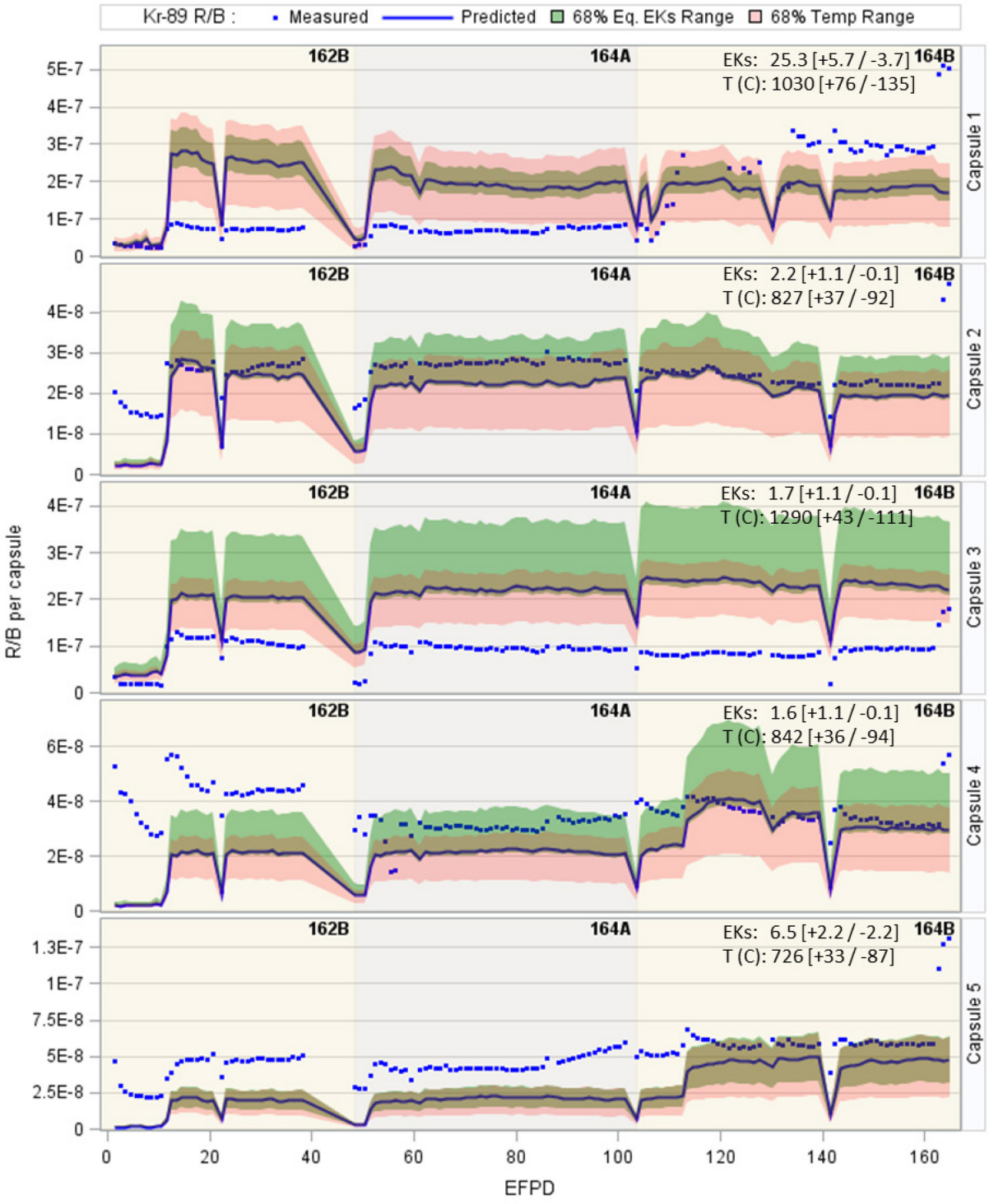

Figure 29. Measured (dots) and predicted (lines) capsule R/B for Kr-89 for three early cycles, to illustrate model sensitivity to uncertainties: Green shaded areas represent uncertainty band of model predictions due to 68% confidence limits for EKF and DUF; Red shaded areas represent uncertainty bands due to 68% confidence limits for EKs' temperature due to unknown location of the EKs.

4.3.2 In-pile Particle Failure Consideration

To estimate the number of failures based on comparison of predicted R/B to measured R/B, we assumed that all failures occurred at the peak fuel temperature location within a capsule. Model overprediction of R/B per-exposed-kernel (R_p in Eq. 16) will result in a negative value for the predicted in-pile failures for a case where no in-pile failure occurred, instead of the expected zero. The estimated number of in-pile failures and as-fabricated equivalent EKs are presented in Figure 30. However, even for short-lived isotopes, FG leakage from Capsule 1 can be significant for the capsules located closest to it. Therefore, the number of in-pile particle failures was based on both GG failure evidence and R/B-based estimates, as discussed below:

- Capsule 1 R/B data suggested that 180–440 failures had occurred near the end of Cycle 166A (Figure 30). The final number of failures in Capsule 1 cannot be determined due to lack of FG release and GG data after Cycle 166A.
- Capsule 2 is estimated to have had approximately four particle failures based on the following observations and analyses:
    - No apparent particle failures occurred up through Cycle 166B — the number of predicted in-pile failures was low and stable (Figure 30), consistent with the absence of GG spikes during these cycles (Figure 26).
    - During Cycle 168A, the number of predicted failures, based on changes in R/B of Xe-137, increased until it reached a maximum of 130 by the end of that cycle (Figure 30). However, most of the increase in FG releases could be attributed to FG leakage from neighboring Capsule 1. For that reason, our estimate of in-pile failures is based on the analysis of the GG data which indicated only four failures. These failures appeared to occur during two distinct periods, before (Figure 31) and after (Figure 32) the unplanned outage that occurred in June 2020:
        - Period “A” (Figure 31): Four GG spikes indicated possible particle failures. However, only the GG spike on May 20, 2020 corresponded to a clear spike in Xe-133 activity, the primary isotope that contributes to the “spike” in the GG system (Scates, 2021). Thus, in this time period, the data indicate one particle failure with good confidence, and potentially three additional failures.
        - Period “B” (Figure 32): GG spikes were not associated with any clear and consistent spikes in measured isotope activities. In addition, all the GG spikes were perfectly synchronized with spikes in Capsules 3 (Figure 34) and 4 (Figure 35), so these spikes are attributed to FG leakage from Capsule 1. Thus, no particle failures are inferred to have occurred during this time.
- Capsule 3 is estimated to have had at least approximately 15 particle failures based on the following observations and analysis:
    - No in-pile failures were apparent through the end of Cycle 166B (Figure 30). R/B-based evidence of failures prior to Cycle 168A are attributed to FG leakage from Capsule 1 because R/B levels dropped back down at the beginning of Cycle 168A. In addition, no GG spikes indicating particle failures were apparent during this time (Figure 26).
    - Like Capsule 2 during Cycle 168A, the number of predicted failures, based on changes in R/B, increased until it reached maximum of approximately 150, by the end of that cycle (Figure 30). However, most of the increase in FG release through Cycle 168A in Capsule 3 is attributed to FG leakage from Capsule 1 and only roughly 15 failures were inferred from spikes in GG counts and/or isotope activities data during Cycle 168A. GG in Capsule 3 behaved differently in two periods in Cycle 168A (before and after the unplanned outage):

- Period “A” (Figure 33): 15 particle failures were associated with GG spikes during the period between May 15 and June 2, 2020. These apparent failures were also evidenced by spikes in isotope activities (bottom plots).
- Period “B” (Figure 34): Multiple GG spikes in Capsule 3 are attributed to the same FG leakage events from Capsule 1 because they did not correspond with clear and consistent spikes in measured activities for all isotopes (bottom plots). As a result, no clear evidence of particle failures was likely to have occurred during this time, based on GG data.

- Capsule 4 is likely to have had zero in-pile failures. The small and unstable increases in predicted failures, during short periods in Cycle 166B and Cycle 168A (Figure 30) are attributed to FG leakage from Capsule 1 because no coincident GG spikes occurred. A few GG spikes during Period “B” of Cycle 168A (Figure 35) are perfectly synchronized with spikes in Capsules 2 (Figure 32) and 3 (Figure 34), suggesting, again, leakage from Capsule 1.
- Capsule 5 is also likely to have had zero in-pile failures. R/B-based estimates of the number of particle failures were roughly constant for all cycles including Cycle 168A (Figure 30). Capsule 5 exhibited the least evidence of FG leakage from Capsule 1, as only a few scattered data points suggested a larger release source during Cycle 166B and 168A when FG leakage from Capsule 1 was substantial. GG spikes typical of particle failures were not observed in Capsule 5 during the entire irradiation, even during Cycle 166B and Cycle 168A (Figure 36), when R/B values suggested a slightly larger source.

A summary of the estimated number of in-pile failures in the AGR-5/6/7 capsules is provided in Table 10. By the end of Cycle 166A, a significant number of in-pile failures appear to have occurred in Capsule 1, causing a substantial increase in FG activity and saturation of the FPMS HPGe detector and an increased activity in the 1A primary cubicle that was picked up by the GG NaI(Tl) detectors. However, the final number of particle failures in Capsule 1 is unknown due to the absence of measured activities. Approximately 15 particle failures are assessed to have occurred in Capsule 3 and between one and four failures in Capsule 2 based on spikes of GG counts and measured activities at the FPMS detectors during the last cycle, Cycle 168A. In contrast, no in-pile failures in Capsules 4 and 5 were indicated, based on GG counts and on the lack of distinct increases in isotope activities relative to that predicted using the AGR R/B model. Post-irradiation examination of Capsules 2 – 5 may help to further refine the particle failure estimate in a manner similar to that used for the AGR-2 experiment (Stempien et al., 2021).

Table 10. Estimated number of in-pile failures in the AGR-5/6/7 capsules.

Capsule 1	180–440 prior to the end of 166A; unknown after 166A
Capsule 2	1–4
Capsule 3	~15
Capsule 4	0
Capsule 5	0

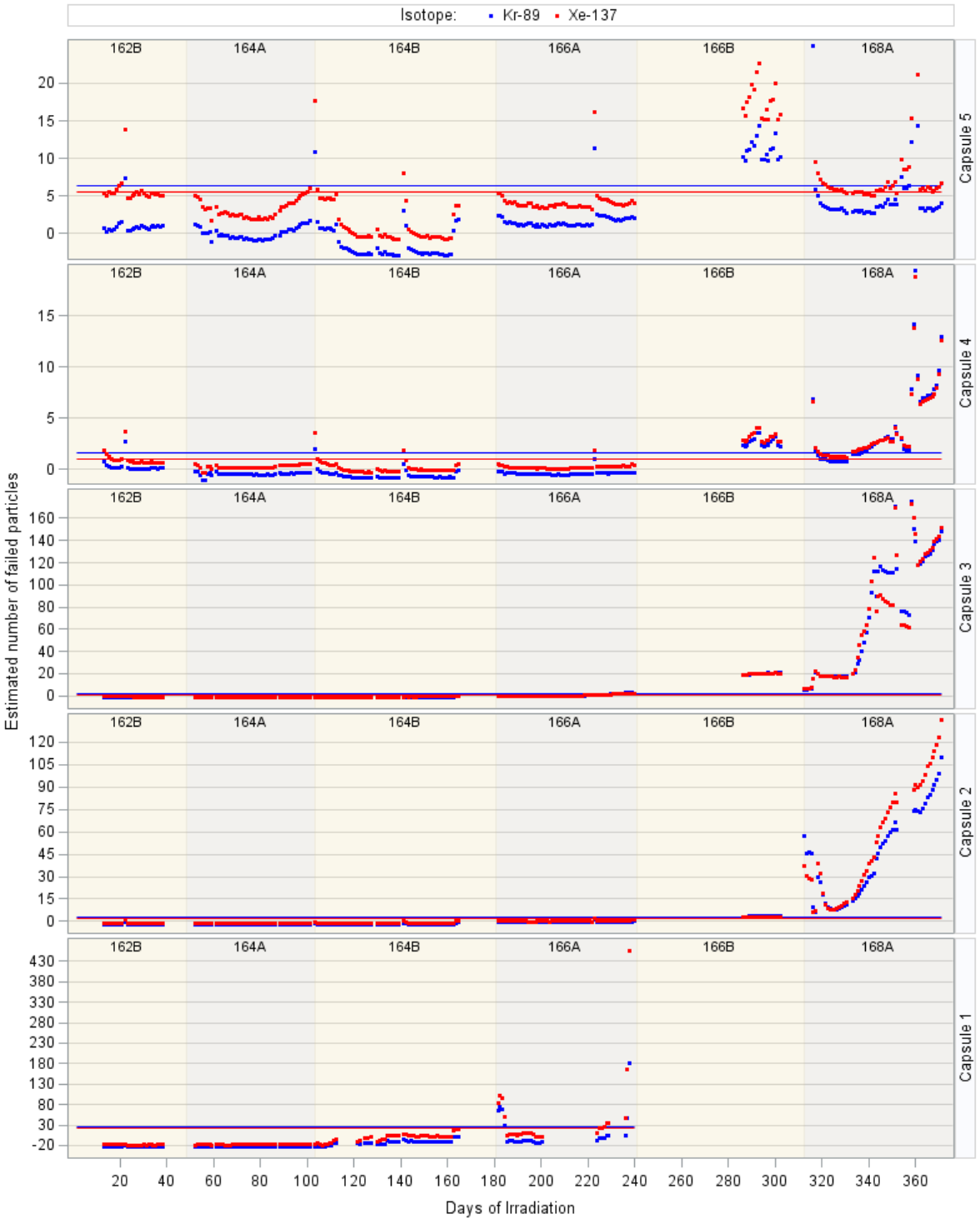

Figure 30. Estimated number of particle failures for AGR-5/6/7 capsules based on Kr-89 (blue color) and Xe-137 (red color): lines are as-fabricated equivalent EKs, and dots are in-pile failures.

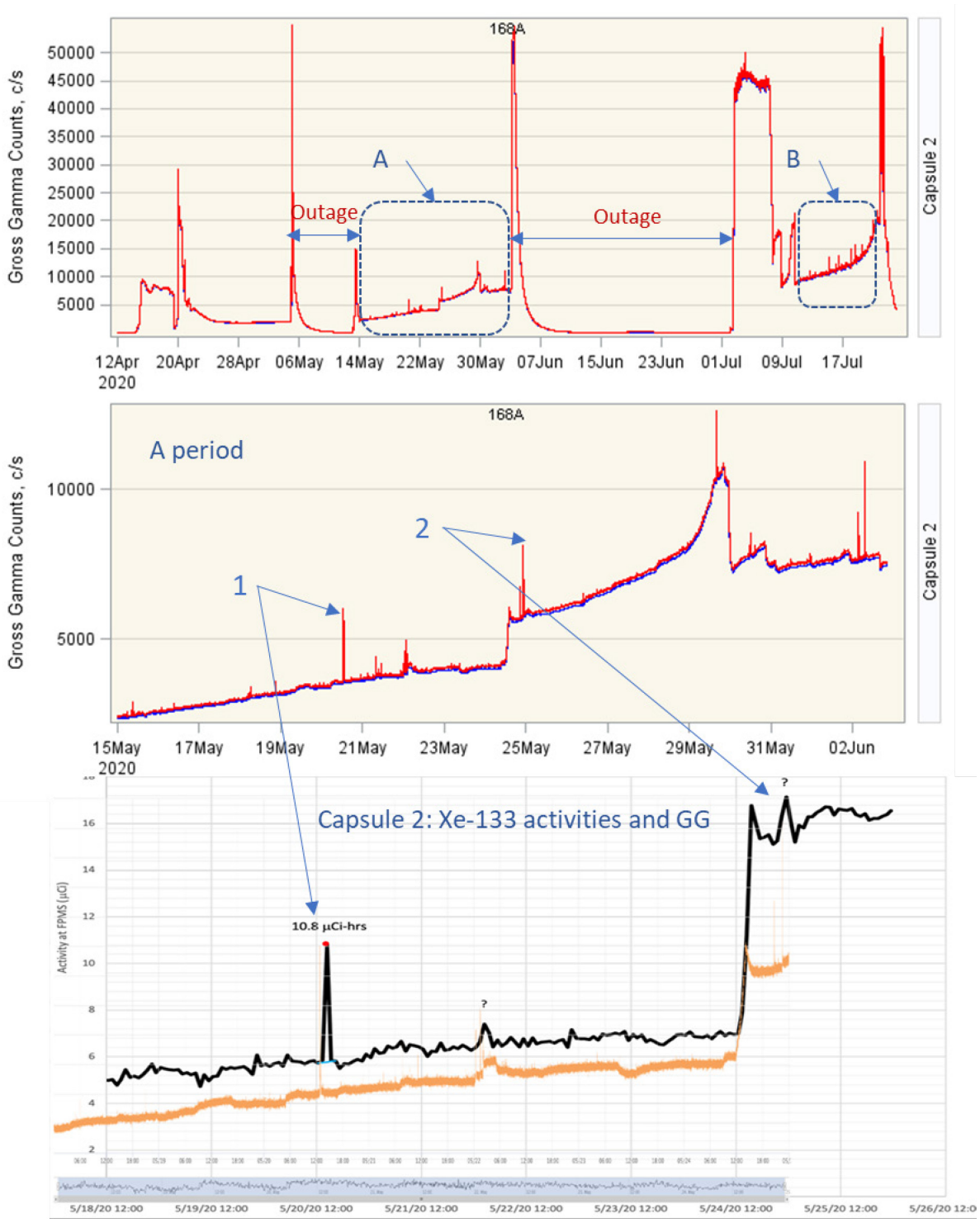

Figure 31. Capsule 2 ATR Cycle 168A – "A" period: 2–4 particle failures were likely. Top – average (blue line) and peak (red line) GG for full cycle, middle – average and peak GG for "A" period, and bottom – for Xe-133 activity (black) overlayed GG data (orange) for "A" period.

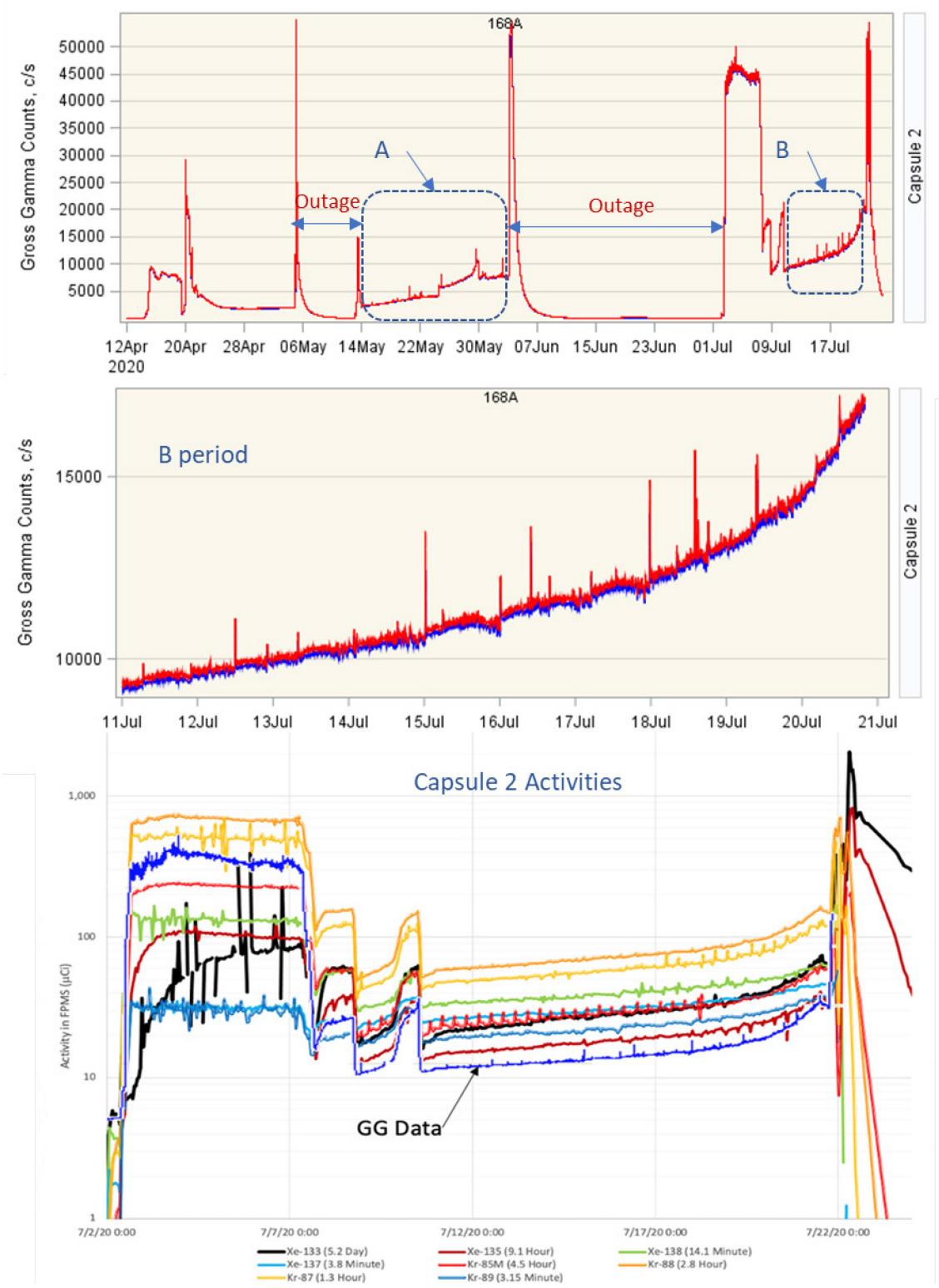

Figure 32. Capsule 2 ATR Cycle 168A – "B" period: No particle failures were likely. Top – full cycle average (blue line) and peak (red line) GG, middle – 'B' period average and peak GG, and bottom – isotopes' activities overlayed with average and peak GG data.

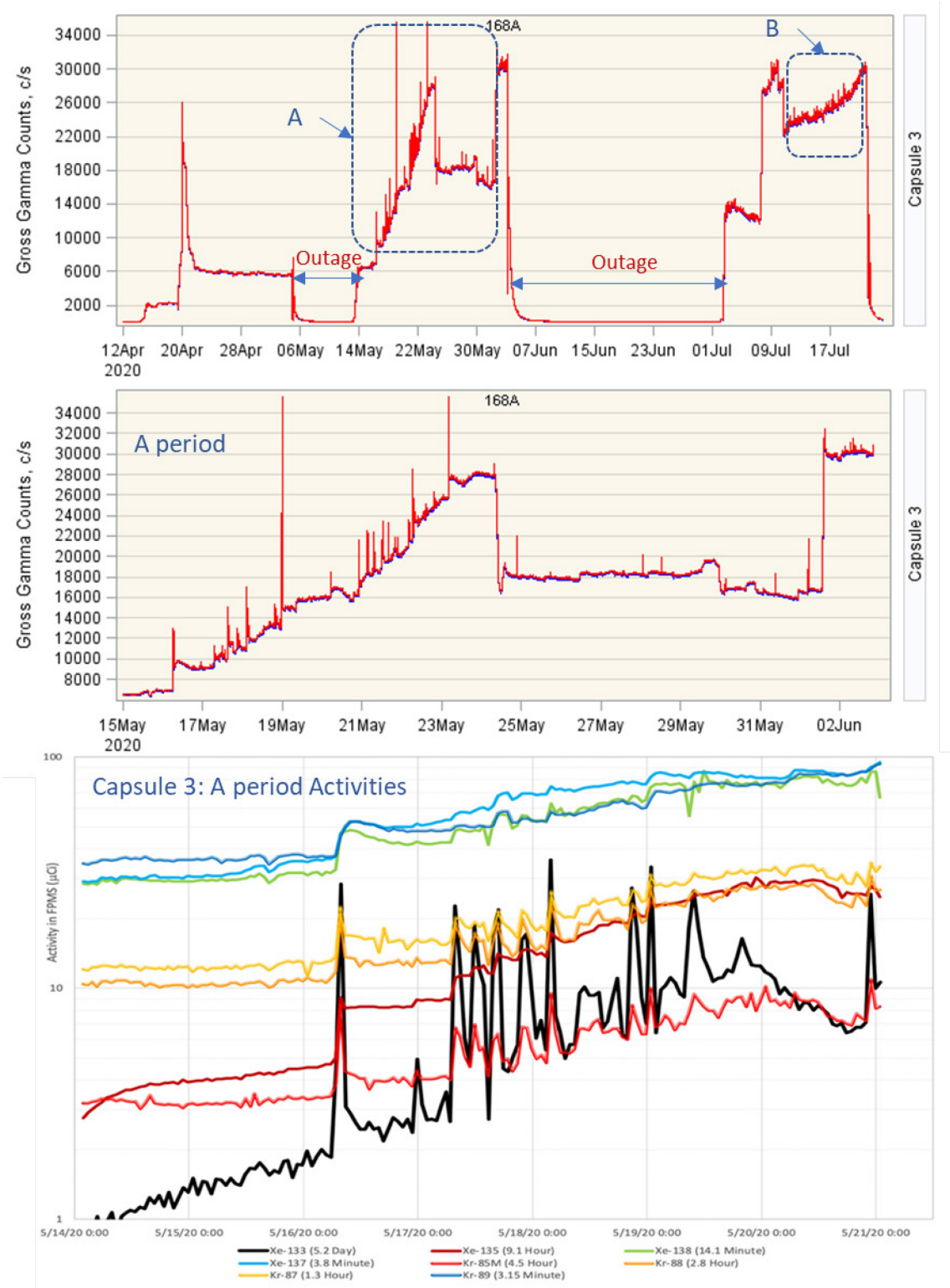

Figure 33. Capsule 3 ATR Cycle 168A – "A" period: up to 15 particle failures were likely due to both GG and isotope activity spikes. Top – average (blue line) and peak (red line) GG for full cycle, middle – GG for "A" period, and bottom – isotopes' activities for "A" period.

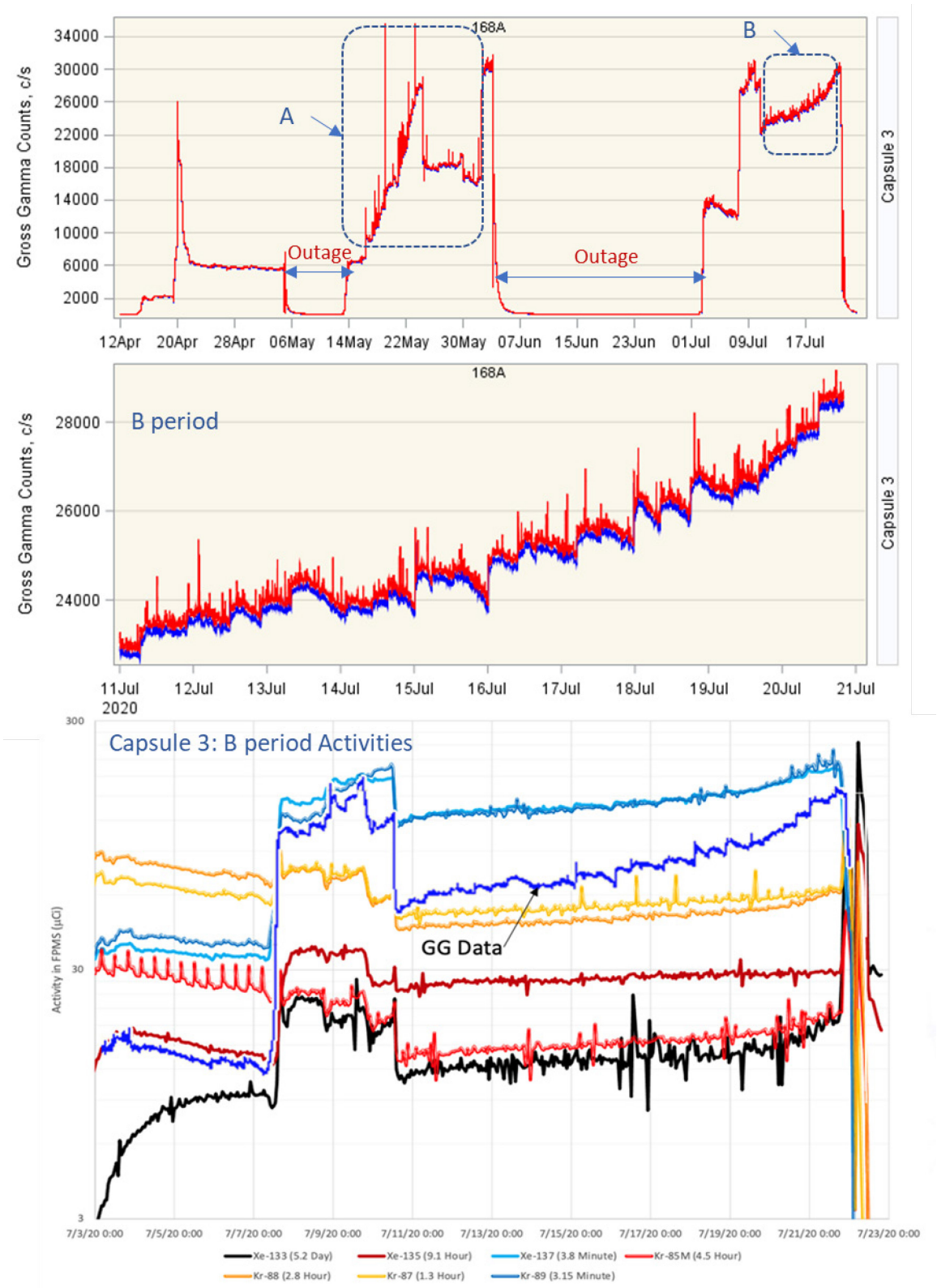

Figure 34. Capsule 3 ATR Cycle 168A – "B" period: No particle failures were likely because GG spikes and isotopes' spikes are random. Top – full cycle average (blue line) and peak (red line) GG, middle – "B" period GG, and bottom – isotopes' activities overlayed with GG data.

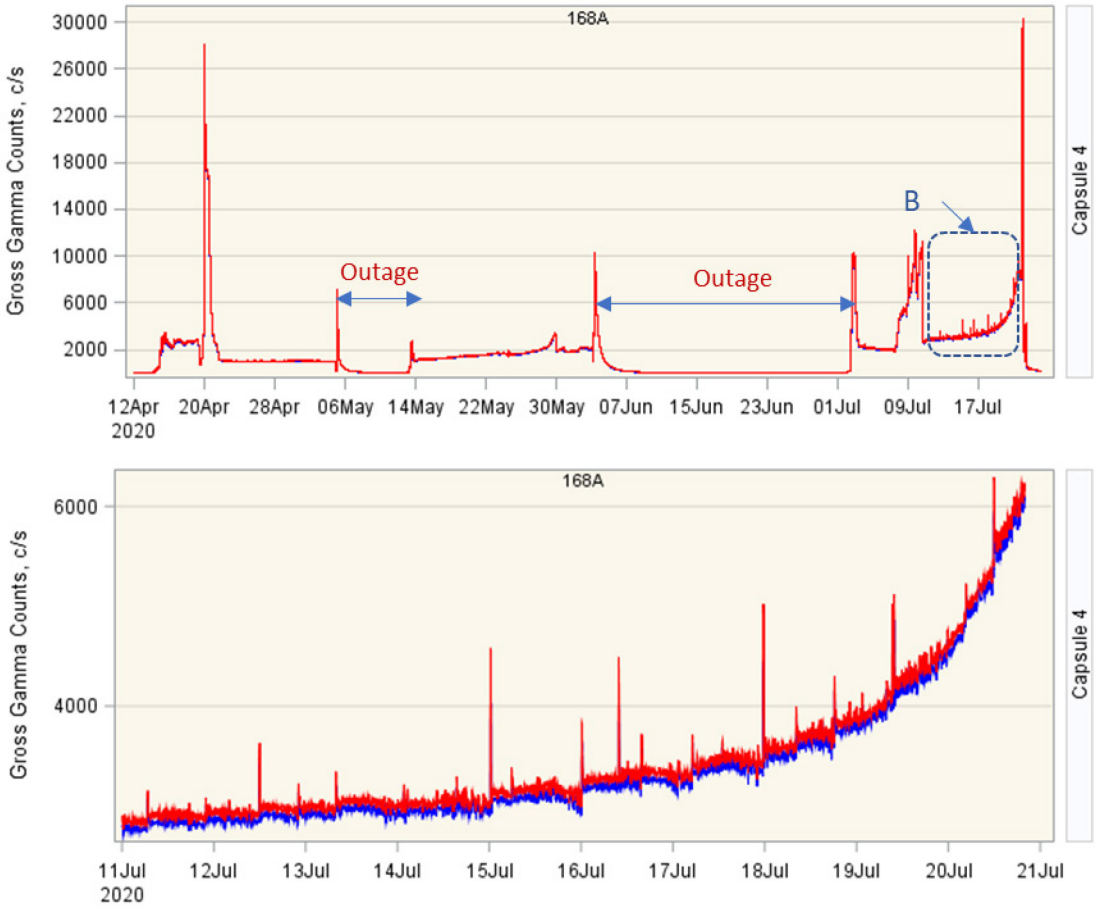

Figure 35. Capsule 4 average (blue line) and peak (red line) GG counts during ATR Cycle 168A: Top – for all cycle and bottom – for "B" period, GG spikes are more likely caused by FG leakage from Capsule 1 because they occurred at the same time of spikes in other capsules, Capsules 2 and 3.

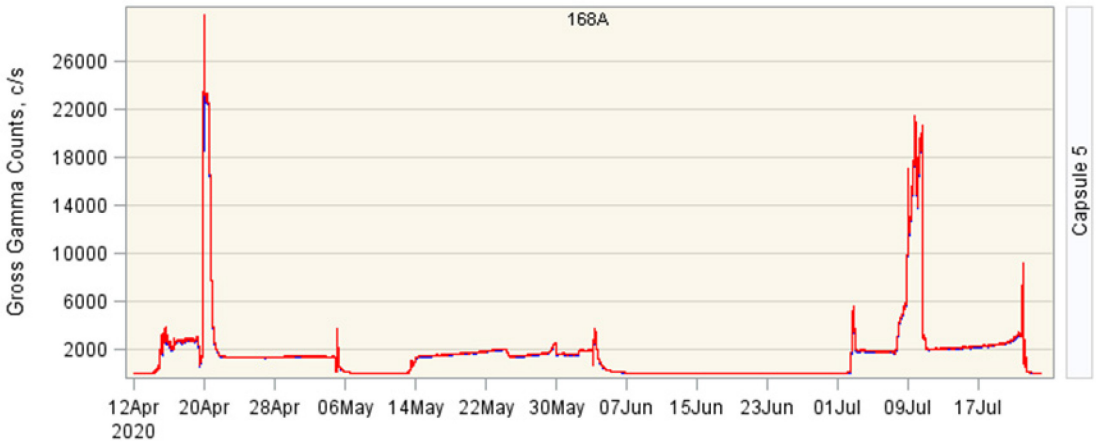

Figure 36. Capsule 5 average (blue line) and peak (red line) GG counts during ATR Cycle 168A: No GG spikes were observable.

5. CONCLUSION

For AGR-5/6/7, fuel compacts were fabricated near commercial scale at BWX Technologies, Inc., and have higher fractions of EK defects and DU contamination relative to compacts used in the previous AGR experiments. In addition, significantly more particles (a total of approximately 570,000) were used in the five AGR-5/6/7 capsules, with Capsule 1 containing 307,625 particles.

This report considered release data for all twelve isotopes but only used R/B data with measurement uncertainty less than 50% and standard 8-hour sampling durations for analysis. Consequently, useable isotopes have a half-life that is sufficiently short to reach equilibrium in the capsule, but long enough to provide a measurable signal in the FPMS detector. Thus, data of the longest half-life isotope, Xe-131m, and two shortest half-life isotopes, Kr-90 and Xe-139, were excluded because of high measurement uncertainty.

Measured R/B values are constant during the first five cycles (i.e., 162B, 163A, 164A, 164B, and 165A), which is consistent with the GG count data that indicated that no in-pile particle failures occurred during that period. Therefore, R/B data during these cycles demonstrates similarity in term of FG release between fuels from AGR-5/6/7 and previous AGR experiments (AGR-1, -2, and -3/4). The following conclusions were drawn based on the analysis:

1. Since the EKF suggests that less than one EK defect would exist in Capsules 2–4, R/B for those capsules should be relatively sensitive to an in-pile particle failure. Since more than 20 equivalent EK defects were estimated Capsule 1, the sensitivity of R/B to a single particle failure is considerably lower, so it would be more difficult to detect small numbers of in-pile failures based on R/B from this capsule.
2. Measured R/B per capsule was substantially higher for AGR-5/6/7 than for AGR-1, which contained fuel manufactured at a laboratory scale. This is consistent with pre-irradiation measurements indicating that the commercially manufactured AGR-5/6/7 fuel had higher as-fabricated EKF and DUF.
3. The German fission-gas release model, incorporated into the PARFUME code (referred as PARFUME-German model), slightly under-predicts R/B in Capsules 2 and 4 and over-predicts R/B in Capsules 1, 3, and 5. The fuel in Capsules 3 and 4 have the same low EKF that suggests that number of EK defects is close to zero. Comparison of model predictions to measured R/B for those two capsules suggests that the assumption of no EK defects is more plausible for Capsule 3 than for Capsule 4.
4. The AGR fission-gas release model provides a good estimate of R/B for Capsules 1, 2 and 4, but over-predicts R/B in Capsule 3 and slightly under-predicts R/B in Capsule 5.
5. The PARFUME-German model DU release factors are notably lower than the AGR-1/AGR-3/4 based DU release factors.
6. The large uncertainty in EKF measurement has significant impact on model prediction uncertainty of R/B per capsule while small uncertainty in DUF measurement has a negligible effect on model prediction uncertainty.
7. The R/B correlation with isotopic decay constant is characterized by *n*, which represents a slope between natural logarithms of R/B per-exposed-kernel and the reciprocal half-life ($\ln R_p$ and $\ln \frac{1}{\lambda}$) for isotopes of each FG (e.g., krypton or xenon). For coated fuel particles, *n* values are in the range of [0.1–0.5]. The daily *n* values calculated for AGR-5/6/7 are approximately 0.3 on average, which were comparable with data from the previous AGR experiments.
8. R/B per-exposed-kernel for the AGR-5/6/7 fuel, which had a kernel diameter of approximately 425 μm, are slightly lower than the values for the AGR-3/4 fuel, which had smaller kernels. The direction

of that difference is consistent with the kernel size dependence of the diffusivity term in the German model.

9. Comparable with AGR-3/4, R/B per-exposed-kernel values for AGR-5/6/7 are lower than predictions by the commonly used Richards and German models. However, they displayed largely similar slopes with respect to reciprocal temperature, which indicates comparable temperature influence on FG releases.
10. Wide variation in measured release rates at a given fuel temperature suggests that factors other than decay constant and temperature are important. Such effects are not captured by the simple transport models described here.

During the last four irradiation cycles (166A – 168A), the FG release in all capsules started to increase when a large number of particles in Capsule 1 combined with damage to the Capsule 1 gas line caused significant FG leakage at various degrees into the other four capsules. In addition, Capsule 1 gas line isolation during the last three cycles prevented measurement of its FG release. Thus, R/Bs in all capsules from Cycle 166A are uncertain because of undefined amount of leakage from Capsule 1, especially for long-lived isotopes.

A few hundred in-pile particle failures were estimated for Capsule 1 by the end of Cycle 166A, but the total number of failures is unknown due to the lack of FG release data in the later cycles. During the last cycle (168A), it is estimated that approximately 15 particles failed in Capsule 3 and as many as four particles failed in Capsule 2 based mainly on evidence from the GG counts. In-pile failures in Capsule 3 were anticipated because the capsule was designed to operate beyond the HTGR normal operating temperature range. In contrast, no in-pile failures were identified in the top two capsules (4 and 5) based on the absence of the typical spikes in gross gamma counts despite low failure estimates using the AGR R/B model for short-lived isotopes (Kr-89 and Xe-137), since small leakage from Capsule 1 was still possible.

6. REFERENCES

Collin B.P., 2018. "AGR-5/6/7 Irradiation Experiment Test Plan." INL/MIS-17-43095, Rev. 1, Idaho National Laboratory. https://www.osti.gov/biblio/1511042-agr-irradiation-experiment-test-plan.

Demkowicz, P.A., Hunn, J.D., Morris, Rooyen, I.V., R.N., Gerczak, T.J., Harp, J.M., and Ploger, S.A., 2015, "AGR-1 Post-Irradiation Examination Final Report," INL/EXT-15-36407, Idaho National Laboratory.

DOE, 1995, *Fuel Capsule HRB 21 Post Irradiation Examination Data Report*, DOE HTGR 100229/ORNL 6836, April 1995.

Hawkes, G.L., 2021. "AGR-5/6/7 Daily As-Run Thermal Analyses." ECAR-5633, Rev. 0, August 2021.

EPRI, 2003, "A Review of Radionuclide Release from HTGR Cores During Normal Operation," EPRI, Palo Alto, CA: 2003. 1009382.

General Atomics, 1987, "Capsule HRB-17/18 Data File," GA 1485, Rev. 4.

General Atomics, 2009, *Technical Basis for NGNP Fuel Performance and Quality Requirements*, GA Project 30302, Rev. 0.

IAEA, 1997, *Fuel performance and fission product behaviour in gas cooled reactors*, IAEA TECDOC 978, November 1997, http://www pub.iaea.org/MTCD/Publications/PDF/te_978_prn.pdf.

INL, 2010, *NGNP Fuel Qualification White Paper, Idaho National Laboratory*, INL/EXT-10-17686, July 2010.

INL, 2018, *PARFUME Theory and Model Basis Report, Idaho National Laboratory*, INL/EXT-08-14497, Rev. 1, September 2018.

Martin, R. G., 1993, *Compilation of Fuel Performance and Fission Product Transport Models and Database for MHTGR Design*, ORNL/NPR 91/6, October 1993.

Marshall D.W., 2017. "AGR-5/6/7 Fuel Specification." INL/MIS-11-21423, Rev. 8, Idaho National Laboratory. https://www.osti.gov/biblio/1529089-agr-fuel-specification.

Marshall D.W., 2019. "AGR-5/6/7 Fuel Fabrication Report." INL/EXT-19-53720, Rev. 1, Idaho National Laboratory. https://doi.org/10.2172/1512795.

Mitchell, T. R., 2020. "Technical Program Plan for INL Advanced Reactor Technologies Advanced Gas Reactor Fuel Development and Qualification Program." PLN-3636, Rev. 9, Idaho National Laboratory. https://www.osti.gov/biblio/1776792-technical-program-plan-inl-advanced-reactor-technologies-advanced-gas-reactor-fuel-development-qualification-program.

Nickel, H., H. Nabielek, G. Pott, A.W. Mehner, "Long time experience with the development of HTR fuel elements in Germany," Nucl. Eng. Des., Vol. 217, 2002, pp. 141–151.

ORNL, 1994, *The Operation of Experiment HFR B1 in the Petten High Flux Reactor*, ORNL/TM-12740, September 1994.

Petti, D. A., J. Buongiorno, J. T. Maki, R. R. Hobbins, and G. K. Miller, 2003, "Key differences in the fabrication, irradiation and high-temperature accident testing of U.S. and German TRISO-coated particle fuel, and their implications on fuel performance," *Nucl. Eng. Des.*, Vol. 222, pp. 281–297.

Pham B.T. and D.M. Scates., 2019. "AGR-5/6/7 Release-to-Birth Ratio Data Analysis for Cycles 162B, 163A, 164A, and 164B." INL/EXT-19-54457, Rev. 2, Idaho National Laboratory. https://www.osti.gov/biblio/1542583-agr-release-birth-ratio-data-analysis-cycles

Pham, B.T., J.J. Einerson, D.M. Scates, J.T. Maki, and D.A. Petti., 2019. "AGR-1, AGR-2 and AGR-3/4 Release-to-Birth Ratio Data Analysis." INL/EXT-14-32970, Rev. 2, Idaho National Laboratory. https://doi.org/10.2172/1599785.

Pham, B.T., Palmer, J.J, Marshall, D.W., Sterbentz, J.W., Hawkes, G.L., and Scates, D.M., 2021, "AGR 5/6/7 Irradiation Test Final As-Run Report," INL/EXT-21-64221, Idaho National Laboratory.

Richards, M. B., 1994, *FG Release from UCO Microspheres: A Theoretical Model for Fractional Release for Non hydrolyzed Fuel with Model Parameters Derived for Capsule HFR B1*, General Atomics, January 1994.

Scates, D. M., 2010, "Fission Product Monitoring and Release Data for the Advanced Gas Reactor 1 Experiment," *Proceedings HTR 2010, Prague, Czech Republic, October 18–20, 2010*, Paper 52.

Scates, D.M., 2021. "Release-to-Birth Ratios for AGR-5/6/7 Operating Cycles 162B through 168A." ECAR-5352, Rev. 0, Idaho National Laboratory.

Stempien, J.D., Hunn, J.D., Morris, R.N., Gerczak, T.J., and Demkowicz, P.A., 2021, "AGR-2 TRISO Fuel Post-Irradiation Examination Final Report," INL/EXT-21-64279, Idaho National Laboratory.

Sterbentz, J.W., 2020. "JMOCUP Physics Depletion Calculation for the As-Run AGR-5/6/7 TRISO Particle Experiment in ATR Northeast Flux Trap," ECAR-5321, Rev. 0, Idaho National Laboratory. https://www.osti.gov/biblio/1774808-jmocup-physics-depletion-calculations-run-agr-triso-particle-experiment-atr-northeast-flux-trap.